

Scales of Fermion Mass Generation and Electroweak Symmetry Breaking

DUANE A. DICUS[†] and HONG-JIAN HE[‡]

Center for Particle Physics and Department of Physics,
University of Texas at Austin, Texas 78712, USA

(September, 2004)

Abstract

The scale of mass generation for fermions (including neutrinos) and the scale for electroweak symmetry breaking (EWSB) can be bounded from above by the unitarity of scattering involving longitudinal weak gauge bosons or their corresponding would-be Goldstone bosons. Including the exact n -body phase space we analyze the $2 \rightarrow n$ ($n \geq 2$) processes for the fermion-(anti)fermion scattering into multiple gauge boson final states. Contrary to naïve energy power counting, we demonstrate that as n becomes large, the competition between an increasing energy factor and a phase-space suppression leads to a *strong new upper bound* on the scale of fermion mass generation at a finite value $n = n_s$, which is *independent of the EWSB scale*, $v = (\sqrt{2}G_F)^{-\frac{1}{2}}$. For quarks, leptons and Majorana neutrinos, the strongest $2 \rightarrow n$ limits range from about 3 TeV to 130 – 170 TeV (with $2 \lesssim n_s \lesssim 24$), depending on the measured fermion masses. Strikingly, given the tiny neutrino masses as constrained by the neutrino oscillations, neutrinoless double-beta decays and astrophysical observations, the unitarity violation of $\nu_L \nu_L \rightarrow n W_L^a$ scattering actually occurs at a scale no higher than ~ 170 TeV. Implications for various mechanisms of neutrino mass generation are analyzed. On the other hand, for the $2 \rightarrow n$ pure Goldstone-boson scattering, we find that the decreasing phase space factor always dominates over the growing overall energy factor when n becomes large, so that the best unitarity bound on the scale of EWSB remains at $n = 2$.

PACS number(s): 12.15.Ff, 14.60.Pq, 11.80.-m, 12.60.-i [Phys. Rev. D **71** (2005) 093009]

[†]Electronic address: dicus@physics.utexas.edu

[‡]Electronic address: hjhe@physics.utexas.edu

CONTENTS

Page#

1. Introduction	3
2. Scales of Mass Generation vs. Unitarity Bounds	7
2.1. Defining the Scale for Mass Generation	7
2.2. High Energy Scattering and Power Counting of Energy	9
2.3. General Unitarity Condition and the Customary $2 \rightarrow 2$ Limits	13
2.3.1. General $2 \rightarrow n$ Unitarity Condition	13
2.3.2. Customary Limits from $2 \rightarrow 2$ Scattering	16
3. Challenge from $2 \rightarrow n$ Inelastic Scattering	19
3.1. Puzzle: Energy Power Counting vs. Kinematic Condition	19
3.2. Resolution: Increasing Power of Energy vs. Phase Space Suppression	20
4. Scales of Mass Generation for Quarks and Leptons	26
4.1. Unitarity Bounds on the Mass Generation Scales from $f\bar{f} \rightarrow n\pi^a$	26
4.2. Model-Dependent Effects from the EWSB Sector	30
5. Scale of Mass Generation for Majorana Neutrinos	38
5.1. Majorana Masses and Neutrino-Neutrino Scattering	38
5.2. Unitarity Violation vs. Mechanisms for Majorana Mass Generation	42
5.2.1. Unitarity Violation vs. Seesaw and Radiative Mechanisms	43
5.2.2. Scale of Mass Generation for Majorana Neutrinos in Supersymmetric Theories	46
5.2.2A. Scale of Mass Generation for Majorana Neutrinos via MSSM Seesaw	46
5.2.2B. Unitarity Violation Scale vs. SUSY Breaking Induced Neutrino Masses	49
6. On the Scale of Electroweak Symmetry Breaking	51
7. Conclusions	55
Acknowledgments	58
Appendix A: Derivation of n-Body Phase Space	59
Appendix B: Refined Unitarity Conditions	60
References	62

1. Introduction

Despite the astonishing success of the standard model [1, 2] for electroweak and strong interactions over the past thirty years, the origin and scales of mass generation remain, perhaps, the greatest mystery. The standard model (SM) contains nineteen free input parameters in total, among which twelve can be expressed in terms of *unpredicted* mass-eigenvalues (two weak gauge boson masses, one Higgs mass, six quark masses and three lepton masses) with one good equality¹ $\frac{m_t}{v/\sqrt{2}} \simeq 1$ and a huge hierarchy $\frac{m_e}{m_t} \simeq 3 \times 10^{-6}$ as fixed by experimental data. There are four additional inputs (three mixing angles and one CP-phase) in the Cabibbo-Kobayashi-Maskawa (CKM) matrix [3] coming from diagonalizing the quark mass matrices, so that sixteen out of the nineteen free parameters² are due to our lack of knowledge about the origin of mass generation. The recent exciting neutrino oscillation experiments [4, 5, 6, 7, 8] further point to three extra neutrino masses³ at the scale of ~ 0.05 eV,⁴ giving another huge hierarchy: $\frac{m_\nu}{m_t} \sim 3 \times 10^{-13}$. In the SM, a single hypothetical Higgs boson [18] is assumed to generate masses for all gauge bosons, quarks and leptons, which, however, leaves all mass scales and their hierarchies fixed by empirical inputs, without real explanation. Furthermore, such a Higgs boson cannot generate neutrino masses without losing renormalizability (given the observed SM particle spectrum) [19] or adding extra new particles (to retain the renormalizability) [20, 21]. Various interesting extensions of the SM have been sought, ranging from compositeness [22, 23, 24], low or high scale supersymmetry [25, 26], grand unification [27], to extra dimensions and deconstructions [28, 29], and string/M theories [30]. Each of them overcomes some unsatisfactory aspects of the SM while adding many new unknowns. Among so many kinds of possible new physics, there is no doubt that understanding the mass generation holds the greatest promise to unravel immediate new clues beyond the SM. Fortunately, on-going and upcoming high energy experiments will actively explore the scales of mass generation (and the associated mixings) for weak gauge bosons, quarks, leptons and neutrinos, either directly or indirectly, in this decade.

While we still seem a long way from finding an imagined theory of everything with only a single

¹Here $v = (\sqrt{2}G_F)^{-\frac{1}{2}} \simeq 246$ GeV is determined by the Fermi constant G_F .

²The remaining three parameters are two gauge couplings (α_s, α_{em}) and one strong CP phase.

³For Majorana neutrinos there are three mixing angles [9] and three CP phases in the leptonic sector [10]. The global analysis [11] of all the current oscillation data strongly disfavors an extra singlet sterile neutrino. The upcoming Fermilab MiniBooNE experiment [12] will resolve the controversy with LSND [13].

⁴The recent astrophysics analyses of the WMAP (Wilkinson Microwave Anisotropy Probe) data [14], in conjunction with the 2dF Galaxy Redshift Survey [15], give an impressive 95% C.L. upper bound, $\sum_j m_{\nu j} \leq 1.01$ eV [16]. Combining the WMAP, SDSS (Sloan Digital Sky Survey) and Lyman- α Forest data results in a better limit of $\sum_j m_{\nu j} \leq 0.65$ eV (95% C.L.) [17].

input parameter to explain the world, we wish to ask a much more modest “bottom-up” question: How do we use high energy scattering processes as a fundamental means to probe the scales of mass generation in a *model-independent way*? What is the energy scale at which the new physics underlying the relevant mass generation has to show up? In particular, fermion mass generation can be independent of the electroweak symmetry breaking (EWSB) that generates the gauge boson masses of the W^\pm and Z^0 ; since the fermion and gauge boson masses need not originate from the vacuum expectation value (VEV) of the same Higgs doublet (as assumed in the SM)⁵, we would hope to probe the scales for fermion mass generation without any *ad hoc* theory assumption. The SM gauge symmetry forbids all bare mass terms for gauge bosons and fermions. If any observed particle mass *is put in by hand* in the SM Lagrangian, the theory is no longer renormalizable and we expect the high energy scattering amplitudes involving this particle to grow with energy and violate unitarity at a certain scale above which the new physics has to show up. In this way the unitarity of the S -matrix puts a *universal upper bound* on the scale of the corresponding mass generation.

In the standard model EWSB sector for generating the W/Z masses, once the neutral physical Higgs boson is removed, the $2 \rightarrow 2$ quasi-elastic scattering amplitudes of longitudinally polarized W/Z 's exhibit the worst high energy behavior [34, 35, 36], proportional to the square of the c.m. energy \sqrt{s} , leading to partial wave unitarity violation at a scale

$$E_W^* \simeq \sqrt{8\pi}v \simeq 1.2 \text{ TeV}, \quad (1.1)$$

similar to the classic analyses of the upper bound on the mass of the Higgs boson [35, 37, 38] where tree-unitarity is violated at a critical Higgs mass $M_H^{\text{crit}} \simeq \sqrt{\frac{16\pi}{3}}v \simeq 1 \text{ TeV}$ ⁶. Eq. (1.1) puts a model-independent upper limit on the scale of EWSB and justifies TeV energy scale for the Large Hadron Collider (LHC) at CERN. Appelquist and Chanowitz derived an analogous upper bound on the scale of fermion mass generation by considering the $2 \rightarrow 2$ inelastic channels of fermion-antifermion scattering $f_\pm \bar{f}_\pm \rightarrow V_L^{a_1} V_L^{a_2}$ ($V^a = W^\pm, Z^0$) [43],

$$E_f^* \simeq \frac{8\pi v^2}{\sqrt{N_c} m_f}, \quad (1.2)$$

where $N_c = 3(1)$ for quarks (leptons). This bound indicates that the upper limit on the scale of fermion mass generation is proportional to the inverse power of the fermion mass itself and is thus

⁵For instance, in the Top-color models [31, 22], the top-condensate Higgs (which gives the observed large top-quark mass) only changes the EWSB vacuum expectation value ($v \simeq 246 \text{ GeV}$) by a few percent and thus has little to do with the EWSB. In the traditional dynamical models, the EWSB is caused by technicolor (TC) gauge interactions [32, 22], while the fermion masses are generated by technifermion condensates via additional extended technicolor (ETC) [33, 22], independent of EWSB.

⁶Subsequent studies and applications may be found, for instance, in Refs. [39, 40, 41, 42] and references therein.

an independent bound from the customary unitarity bound on the EWSB scale in Eq. (1.1). Also, for all the SM fermions (except the top quark), the bound (1.2) is much weaker than Eq. (1.1). However, this traditional wisdom was recently challenged by an interesting study [44], where it was noted that for inelastic scattering with a multi-gauge-boson final state, $f\bar{f} \rightarrow nV_L^a$ ($n > 2$), the n -body phase space integration contributes a nontrivial energy factor s^{n-2} to further enhance the cross section (in addition to the energy dependence of s^1 from the squared amplitude), so that the unitarity bound goes like

$$E_f^* \sim v \left(\frac{v}{m_f} \right)^{\frac{1}{n-1}} \longrightarrow v, \quad (\text{for } n \rightarrow \text{large}), \quad (1.3)$$

which could be pushed arbitrarily close to the weak scale v and thus become independent of the fermion mass m_f for *large enough* n . From this, Ref. [44] deduced that *the fermion-antifermion scattering into weak bosons does not reveal an independent new scale for fermion mass generation*. This is very counter-intuitive since the following *kinematic condition* must hold for any $2 \rightarrow n$ scattering with n weak gauge bosons in the final state,

$$\sqrt{s} > nM_{W(Z)} \simeq \frac{n}{3}v, \quad \implies \quad \frac{E^*}{v} > \frac{n}{3}. \quad (1.4)$$

This shows that as n becomes large, the required c.m. energy \sqrt{s} has to be arbitrarily above the weak scale v , so that the unitarity violation scale, $\sqrt{s} = E^*$, has to *grow at least linearly with* n , instead of decreasing to v , contrary to the power counting argument in Eq. (1.3).

The observation in (1.4) is completely general, valid for any $2 \rightarrow n$ process including both $f\bar{f} \rightarrow nV_L^a$ and $V_L^{a1}V_L^{a2} \rightarrow nV_L^a$. Thus, a similar contradiction may possibly occur for the $V_LV_L \rightarrow nV_L$ scattering. We note that the n -body phase space is the same as before but the squared amplitude now behaves as s^2/v^{2n} , so by naïve power-counting the inelastic unitarity bound goes as,

$$E_W^* \sim v(C_0)^{\frac{1}{2n}} \longrightarrow v, \quad (\text{for } n \rightarrow \text{large}), \quad (1.5)$$

where $C_0 > 1$ is a dimensionless constant determined by the phase-space and the square of the S -matrix element. For $n = 2$, we know from Eq. (1.1) that $C_0 \simeq (\sqrt{8\pi})^4 \simeq 632$. Hence, as n becomes large, we would naively expect E_W^* to approach $v \simeq 246$ GeV, significantly below the traditional $2 \rightarrow 2$ bound $E_W^* \simeq 1.2$ TeV in Eq. (1.1). If this argument holds, we would deduce the new physics scale associated with EWSB to be less than ~ 250 GeV, which could manifest itself as a light Higgs boson or something similar and might already be partly accessible at the on-going Tevatron Run-2.

It is the above general observation based upon the kinematic condition (1.4) that leads us to believe that the energy power counting arguments in Eqs. (1.3) and (1.5) cannot be true and a new resolution must be sought. Therefore, in this study, we systematically and quantitatively analyze the $2 \rightarrow n$ inelastic channels, with $n > 2$, for both $f\bar{f} \rightarrow nV_L$ and $V_L V_L \rightarrow nV_L$ scattering. Our findings show that the exact n -body phase space contributes a non-trivial *dimensionless* factor which *sufficiently suppresses* the effect of the energy growth given by Eqs. (1.3) and (1.5). As a consequence, the kinematic condition (1.4) is satisfied for any large n value, and the scale for fermion mass-generation is proven to be independent of the EWSB scale.

Section 2 establishes the necessary concepts and formalism, and reviews the customary unitarity bounds from $2 \rightarrow 2$ scattering. We first define the scale of mass generation in connection with the unitarity violation scale. We then discuss the equivalence theorem, give a general power counting formula and apply it to count the energy dependence of the relevant scattering amplitudes for our later analyses. We present a systematical derivation of the general unitarity condition for $2 \rightarrow n$ scattering, extending that of Ref. [44]. We then summarize the customary unitarity limits from $2 \rightarrow 2$ scattering for the scale of EWSB and the scales of mass generation for Dirac fermions and Majorana neutrinos.

In Sec. 3 we return to the new puzzle presented around Eqs. (1.3)-(1.4) and resolve it by using an exact expression for the n -body phase space. With estimated amplitudes for the $2 \rightarrow n$ scattering, we analyze the unitarity violation scales for the scatterings $\xi_1 \xi_2 \rightarrow n V_L^a$ where the ξ denotes quarks, leptons, Majorana neutrinos, or longitudinal weak bosons.

In Sec. 4, 5, and 6 we further quantify the estimates in Sec. 3 for quarks and leptons, for Majorana neutrinos, and for EWSB, respectively. In Sec. 4 we first compute the scattering amplitude for $f\bar{f} \rightarrow nV_L^a (n\pi^a)$ from the universal contact interaction. This gives slightly weakened limits for the unitarity violation, i.e., the estimates of Sec. 3 are relaxed by a factor of 2 or so. We then examine the effect of including model-dependent EWSB contributions and note that the effects decrease with the increase of n , and, in particular, we explicitly show that for a SM (or SM-like) EWSB sector the effect on $2 \rightarrow 3$ scattering is to enhance the bounds slightly. Thus, we find that for all light SM fermions (except possibly the top quark) the $2 \rightarrow n$ unitarity limits on the scale of fermion mass generation become the strongest at a value $n = n_s > 2$ and are substantially tighter than the classic Appelquist-Chanowitz bound [43].

In Sec. 5, we present a quantitative calculation of the scattering amplitude for Majorana neutrinos $\nu_L \nu_L \rightarrow nV_L^a$. This relaxes the estimate in Sec. 3 by a factor of about 1.3 – 1.6. Thus

we demonstrate that, without assuming⁷ *a priori* that the same SM Higgs doublet used for EWSB participates in neutrino mass generation, the unitarity of the scattering $\nu_L \nu_L \rightarrow n V_L^a$ puts an upper bound on the Majorana neutrino mass generation at a scale substantially below M_{GUT} ,⁸ around 130 – 170 TeV, with $n_s \approx 20 - 24$. We also discuss the implications of such low-scale unitarity violation for various mechanisms of Majorana neutrino mass generation.

Finally, in Sec.6, we explicitly analyze the scattering $V_L^{a_1} V_L^{a_2} \rightarrow n V_L^a$ ($\pi^{a_1} \pi^{a_2} \rightarrow n \pi^a$), with $n \leq 4$, and show that as n increases the upper bound on the EWSB scale is not driven towards the scale $v \simeq 246$ GeV [cf. Eq. (1.5)], rather, it becomes weaker so that the best constraint still occurs at $n_s = 2$, in agreement with Sec.3. Including our earlier general estimates from Sec.3 for large n values, we conjecture that this feature holds for any value of $n \geq 2$.

We conclude in Sec.7 and derive the expression for n-body phase space in Appendix A. For completeness, in Appendix B we also refine the unitarity conditions of Sec.2.3.1.

2. Scales of Mass Generation vs. Unitarity Bounds

In this section, we start by introducing necessary concepts and formalism for the gauge and fermion mass terms and for the $2 \rightarrow n$ ($n \geq 2$) unitarity limit. Then we briefly review the traditional $2 \rightarrow 2$ unitarity bounds derived for EWSB and fermion (neutrino) mass generation.

2.1. Defining the Scale for Mass Generation

It turns out that the SM Lagrangian, with the physical Higgs boson removed (often called the Higgsless SM) and with all observed particle masses put in by hand, exhibits a nonlinearly realized gauge symmetry [47, 48, 49], under which the three would-be Goldstone bosons $\{\pi^a\}$ [50] can be formulated as

$$U = \exp [i\pi^a \tau^a / v] \tag{2.6}$$

which transforms, under the SM gauge group $\mathcal{G} = SU(2)_L \otimes U(1)_Y$ as,

$$U \rightarrow U' = g_L U g_Y^\dagger, \tag{2.7}$$

⁷For models where neutrino mass generation is independent of the EWSB sector, see, *e.g.*, Refs. [45, 46].

⁸ M_{GUT} stands for the energy scale of the grand unification (GUT) [27].

where $g_L = \exp[-i\theta_L^a \tau^a/2]$ and $g_Y = \exp[-i\theta_Y \tau^3/2]$. Thus the weak gauge boson mass terms, $M_W^2 W^{+\mu} W_\mu^- + \frac{1}{2} M_Z^2 Z^\mu Z_\mu$, are given by the dimension-2 nonlinear operator,

$$\mathcal{L}_V = \frac{v^2}{4} \text{Tr} \left[(D_\mu U) (D^\mu U)^\dagger \right], \quad (2.8)$$

where $D_\mu U = \partial_\mu U + i\frac{g}{2} W_\mu^a \tau^a U - i\frac{g'}{2} U B_\mu \tau^3$.

Now consider a pair of generic SM fermions (f, f') which form a left-handed $SU(2)_L$ weak doublet $F_L = (f_L, f'_L)^T$ (with hypercharge Y_L) and two right-handed weak singlets f_R and f'_R (with hypercharges Y_R and Y'_R). The electric charges of (f, f') are given by $Q_f = \frac{1}{2} + Y_L = Y_R$ and $Q_{f'} = -\frac{1}{2} + Y_L = Y'_R$, respectively. We can write down the following gauge-invariant nonlinear operator of dimension-3,

$$\mathcal{L}_f = -m_f \overline{F_L} U \begin{pmatrix} 1 \\ 0 \end{pmatrix} f_R - m_{f'} \overline{F_L} U \begin{pmatrix} 0 \\ 1 \end{pmatrix} f'_R + \text{H.c.}, \quad (2.9)$$

which contains the fermion bare mass-terms $-m_f \overline{f} f - m_{f'} \overline{f'} f'$.

The SM has no (light) right-handed singlet neutrino ν_R , so that the tiny masses for the active neutrinos (ν_L) indicated by the neutrino oscillations can be naturally of Majorana-type, i.e., $-\frac{1}{2} m_\nu^{ij} \nu_{Li}^T \widehat{C} \nu_{Lj} + \text{H.c.}$, which can be formulated in a gauge-invariant manner,

$$\begin{aligned} \mathcal{L}_\nu &= -\frac{\mathcal{C}_{ij}}{\Lambda} L_i^{\alpha T} \widehat{C} L_j^\beta \Phi^{\alpha'} \Phi^{\beta'} \epsilon^{\alpha\alpha'} \epsilon^{\beta\beta'} + \text{H.c.} \\ &= -\frac{1}{2} \mathcal{C}_{ij} \frac{v^2}{\Lambda} L_i^{\alpha T} \widehat{C} L_j^\beta \overline{\Phi}^{\alpha'} \overline{\Phi}^{\beta'} \epsilon^{\alpha\alpha'} \epsilon^{\beta\beta'} + \text{H.c.} \end{aligned} \quad (2.10)$$

where we choose $F_{Lj} = L_j$ ($j = 1, 2, 3$) as the left-handed lepton doublet, $\widehat{C} = i\gamma^2 \gamma^0$ is the charge-conjugation operator, and $\Phi = U \begin{pmatrix} 0 \\ v/\sqrt{2} \end{pmatrix}^T \equiv \frac{v}{\sqrt{2}} \overline{\Phi}$. Thus, the tiny neutrino Majorana masses are given by

$$m_\nu^{ij} = \mathcal{C}_{ij} \frac{v^2}{\Lambda} \quad (2.11)$$

and naturally suppressed by $v^2/\Lambda \lll v$ in the seesaw mechanism [20] or by the loop-induced factor $\mathcal{C}_{ij} \lll 1$ (which also includes small ratios of lepton masses to the TeV scale) in the radiative mechanism [21]. If Φ is replaced by the linear SM-Higgs-doublet H , Eq. (2.10) recovers the traditional dimension-5 operator of Weinberg [19], implying the *assumption* that the Higgs doublet H (responsible for the EWSB) already participates in the neutrino mass generation. However, like other SM fermions, the mass generation for neutrinos needs *not* originate from the *same* Higgs doublet as EWSB [45, 46], so we will not make the *ad hoc* assumption of $\Phi = H$. Instead, we

will systematically investigate the most generic neutrino mass operator (2.10) which, in the unitary gauge, is just the bare Majorana mass term $-\frac{1}{2}\nu_L^T m_\nu \widehat{C}\nu_L + \text{H.c.}$

We see that despite the fact that the SM gauge symmetry forbids all bare mass terms for the weak gauge bosons and fermions, they can nonetheless be formulated in a gauge-invariant way via the nonlinear realization and thus are necessarily *nonrenormalizable*. Hence, the S -matrix elements of the high energy scattering involving these massive particles will unavoidably violate unitarity at a certain energy scale at which the new physics responsible for the mass generation has to recover the proper unitarization. Generically, we can define the scale Λ_x for generating a mass m_x to be *the minimal energy above which the bare mass term for m_x has to be replaced by a renormalizable interaction* (adding at least one new physical degree of freedom to the experimentally observed particle spectrum). The unitarity violation scale E^* provides an *upper bound* on such a scale Λ_x , i.e.,

$$\Lambda_x \leq E^*, \quad (2.12)$$

and is thus a *conservative and model-independent* estimate of the mass generation scale Λ_x .

Generally speaking, the scale for EWSB and mass generation of W^\pm/Z^0 is naturally around $\mathcal{O}(v)$ [cf. eq. (1.1)], but the mass generation scales for the SM fermions are expected to be much higher (except, perhaps, for the top quark). To study the unitarity bound on the fermion mass we can classify the theories into two types, depending on the nature of EWSB: (i) EWSB is generated in a weakly coupled scenario with a fundamental Higgs boson(s); (ii) EWSB is induced by dynamical symmetry breaking (with a composite Higgs scalar(s) or no Higgs boson). In either case, we can study the scale of the fermion mass generation by examining how the (nonrenormalizable) bare fermion mass term leads to unitarity violation in high energy scattering. For type-(i), without assuming the EWSB Higgs boson(s) to also couple to the fermions, we can derive the unitarity violation bounds from the scattering $f\bar{f} \rightarrow nV_L^a$ (which is well-defined above $\mathcal{O}(1)$ TeV and below the unitarity violation scale). For type-(ii), due to the dynamical EWSB, the longitudinal gauge boson V_L^a and its Goldstone boson π^a are composite and cannot be treated as local fields at energy scales $\gg \mathcal{O}(1)$ TeV. Thus, the scattering $f\bar{f} \rightarrow nV_L^a$ no longer provides a reliable, model-independent bound on the scales of fermion mass generation. Instead, we may consider the scattering $f\bar{f} \rightarrow (f\bar{f})^n$ from effective higher dimensional multi-fermion operators.

2.2. High Energy Scattering and Power Counting of Energy

According to the systematic power counting analysis for electroweak gauge theories [51, 52], high energy scattering of longitudinally polarized weak gauge bosons V_L^a exhibits the worst high energy behavior and thus is expected to provide the strongest unitarity bounds. This is easy to understand intuitively by noting that in the S -matrix element each external fermion field contributes an energy factor of $E^{\frac{1}{2}}$ while an external scalar field gives no additional energy enhancement. However, for scattering involving longitudinally polarized weak bosons, each external field V_L^a gives rise to a factor of E^1 due to its longitudinal polarization vector

$$\epsilon_L^\mu(k) = \frac{1}{M_a} \left(|\vec{k}|, k^0 \vec{k}/|\vec{k}| \right) = \frac{k^\mu}{M_a} + v^\mu(k), \quad v^\mu(k) = \mathcal{O}\left(\frac{M_a}{E}\right), \quad (2.13)$$

where $M_a = M_{W,Z}$ and the term $\mathcal{O}(M_a/E)$ is suppressed in the high energy regime $E \gg M_a$. The term k^μ/M_a leads to a potentially bad high energy behavior for the scattering amplitude and is thus the most sensitive to the unitarity violation. But, the actual energy-dependence of the V_L -amplitude is much more involved due to the various intricate energy cancellations. Consider, for instance, $V_L V_L \rightarrow V_L V_L$ scattering at tree-level. Naïve power counting shows that its amplitude has both $\mathcal{O}(E^4)$ and $\mathcal{O}(E^2)$ individual terms, but the $\mathcal{O}(E^4)$ terms always cancel out due to the generic Yang-Mills gauge structure and the $\mathcal{O}(E^2)$ terms can further cancel down to $\mathcal{O}(E^0)$ if a physical Higgs boson h^0 is present.⁹ Without such a Higgs scalar h^0 , the (W^\pm, Z^0) mass terms may be formulated as the nonlinear dimension-2 operator (2.8) which is nonrenormalizable and gives rise to *non-canceled* $\mathcal{O}(E^2)$ terms without respecting to unitarity. This puts an upper bound on the EWSB scale [35, 37, 39, 41, 42].

The key for carrying out a faithful energy power counting for a scattering amplitude with V_L^a 's is to note [51, 52] that the actual E -dependence is given by in the corresponding amplitude involving would-be Goldstone boson π^a 's. These two scattering amplitudes are quantitatively connected via the Electroweak Equivalence Theorem (ET)¹⁰ [36, 37, 39, 56, 57, 58, 59, 60],

$$\begin{aligned} \mathcal{T} [V_L^{a_1}, \dots, V_L^{a_n}; \Phi_{\text{phys}}] &= C_{\text{mod}} \mathcal{T} [-i\pi^{a_1}, \dots, -i\pi^{a_n}; \Phi_{\text{phys}}] + B, \\ B &\equiv \sum_{\ell=1}^n [C^{\alpha_{\ell+1}} \dots C^{\alpha_n} \mathcal{T} [v^{\alpha_1}, \dots, v^{\alpha_n}, -i\pi^{\alpha_{\ell+1}}, \dots, -i\pi^{\alpha_n}; \Phi_{\text{phys}}] + \text{permutations}] \\ &= \mathcal{O}(M_W/E_j) - \text{suppressed}, \end{aligned} \quad (2.14)$$

⁹It was shown recently [53, 54, 55] that in the compactified (or deconstructed) higher dimensional Higgsless Yang-Mills theories, such $\mathcal{O}(E^2)$ terms are canceled (or suppressed) due to the presence of spin-1 Kaluza-Klein (KK) gauge bosons from a geometric Higgs mechanism.

¹⁰A KK equivalence theorem (KK-ET) [53, 54] has recently been constructed for the geometric Higgs mechanism in compactified higher dimensional Yang-Mills theories on general 5D-backgrounds (including warped space). This is valid independent of whether the zero-mode gauge bosons are massless or not.

where $v^a \equiv v^\mu V_\mu^a$ and Φ_{phys} denotes possible amputated external physical fields [58, 51]¹¹. The B -term on the RHS of the first equation is suppressed by $\mathcal{O}(M_W/E_j)$ relative to the leading term and its precise form [58, 51] is given by the second equation in (2.14). The constant modification factor $C_{\text{mod}} = C^{a_1} \cdots C^{a_n} = 1 + \mathcal{O}(\text{loop})$ is generated from radiative corrections and can be exactly simplified to unity under realistic renormalization schemes [57, 58, 59], but will not affect the power counting analysis. Since the Goldstone fields π^a have no extra polarization vector like (2.13), there is no non-trivial E -cancellation in the π^a -amplitude [the right-hand side of Eq.(2.14)] so that the E -power counting can directly apply.¹² It is shown [51, 52] that such a power counting method can be systematically constructed (à la Weinberg [48]) for any given scattering amplitude \mathcal{T} and its E -power dependence \mathcal{D}_E is, for $E \gg M_{W,Z}, m_f$,

$$\mathcal{D}_E = 2 + 2L - \sum_j \mathcal{V}_j \left(2 - d_j - \frac{1}{2} f_j \right) - e_v, \quad (2.15)$$

where \mathcal{V}_j is the number of vertices of type j which contain $d_j (\geq 0)$ derivatives and $f_j (\geq 0)$ fermionic lines, L is the number of loops, and $e_v (\geq 0)$ is the number of external gauge fields $v^a = V_\mu^a v^\mu$ appeared in an S -matrix element [cf. (2.13) for definition of v^μ]. From (2.15), it can be proven [51, 52] that, for any $n \geq 2$,

$$\mathcal{D}_E \leq 2 + 2L, \quad (2.16)$$

where the equality holds when the amplitude contains only Goldstone boson vertices.

In the following sections, we will systematically analyze unitarity for the $2 \rightarrow n$ ($n > 2$) scattering amplitudes $f\bar{f}, \nu_L \nu_L \rightarrow n V_L^a$ and $V_L^{a_1} V_L^{a_2} \rightarrow n V_L^a$. According to the ET discussed above, to extract the leading energy behavior, we can analyze the corresponding Goldstone boson amplitudes $f\bar{f}, \nu_L \nu_L \rightarrow n \pi^a$ and $\pi^{a_1} \pi^{a_2} \rightarrow n \pi^a$, where the energy power counting can be safely carried out [cf. Eq.(2.15)]. At the tree level ($L = 0$), using the rule (2.15), and the interactions (2.9) (which shows that the coupling of two fermions to any number of π^a has no derivatives) and (2.8) (which shows that the self-coupling of π^a 's always has two derivatives), we can thus deduce,

¹¹This ET relation is deeply rooted in the underlying Higgs mechanism with spontaneous gauge symmetry breaking, even if a fundamental Higgs boson does not exist. As explicitly shown in the second paper of Ref. [57] [cf. its Eqs.(88)-(95)] and in Ref. [52], the ET (2.14) is derived from an amputated Slavnov-Taylor identity $\mathcal{T}[V_S^{a_1} + iC^{a_1} \pi^{a_1}, \dots, V_S^{a_n} + iC^{a_n} \pi^{a_n}, \Phi_{\text{phys}}] = 0$, which directly reflects the fact that *the would-be Goldstone boson π^a and the unphysical scalar component of the vector field $V_S^a = \epsilon_S^\mu V_\mu^a$ ($\epsilon_S^\mu = k^\mu/M_a$, $M_a = M_{W,Z}$) are "confined" together so that no net effect from them can be observed in the physical S -matrix elements – a quantitative formulation of the general Higgs mechanism at the S -matrix level (independent of whether a Higgs boson actually exists).*

¹²In the case that the graviton or its Kaluza-Klein states interact with the longitudinal V_L^a 's via the energy-momentum tensor [61], the E -cancellation associated with the V_L^a -polarizations again manifests in the corresponding amplitude involving the Goldstone boson π^a 's due to the ET (2.14).

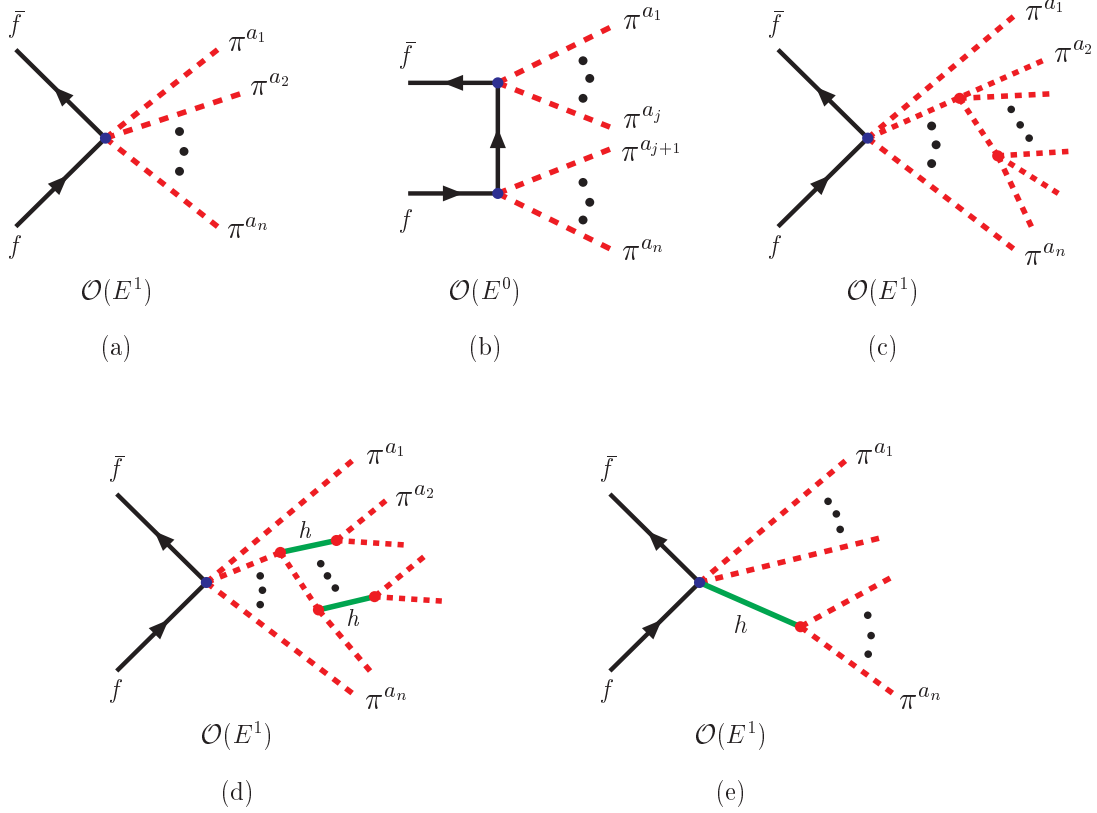


Figure 1: Typical contributions to $f\bar{f} \rightarrow n\pi^a$ scattering: (a) the leading “contact” diagram of $\mathcal{O}(E^1)$; (b) the sub-leading “ $t(u)$ -channel” type diagrams of $\mathcal{O}(E^0)$ which can be ignored for the unitarity analysis; (c) the “hybrid” contact diagrams ($n \geq 3$) including Goldstone self-interactions from the EWSB sector; (d) the “hybrid” contact diagrams ($n \geq 3$) including Goldstone interactions with the EWSB quanta (illustrated here by the SM Higgs boson h^0 as the simplest example of EWSB); (e) the “hybrid” contact diagrams due to the *assumption* of Yukawa interactions between the fermions and the SM Higgs boson h^0 , as the simplest example of fermion mass generation.

for $E \gg M_{W,Z}, m_f$,

$$\begin{aligned}
\mathcal{T}[f\bar{f}, \nu_L \nu_L \rightarrow n V_L^a] &\simeq \mathcal{T}[f\bar{f}, \nu_L \nu_L \rightarrow n \pi^a] = \mathcal{O}(1) \frac{m_{f,\nu}}{v^n} E, \\
\mathcal{T}[V_L^{a_1} V_L^{a_2} \rightarrow n V_L^a] &\simeq \mathcal{T}[\pi^{a_1} \pi^{a_2} \rightarrow n \pi^a] = \mathcal{O}(1) \frac{E^2}{v^n},
\end{aligned} \tag{2.17}$$

where the dimensionality of \mathcal{T} is always given by $\mathcal{D}_{\mathcal{T}} = 4 - (2 + n) = 2 - n$ and is independent of whether the external fields are bosonic or fermionic. [It will be shown from the exact calculation in Sec. 6 that the leading contribution to the second amplitude in Eq.(2.17) is nonvanishing only for $n(\text{even}) = 2, 4, 6, \dots$] Eq.(2.17) shows that the E -power dependence of \mathcal{T} is actually independent of the number of particles in the final state. Therefore, we note that any conceptual change from

including n -body final state reactions ($n > 2$) has to arise from the n -body *phase space integration* which will be systematically analyzed in the following sections.

In Fig. 1, we illustrate the relevant contributions to the scattering $f\bar{f} \rightarrow n\pi^a$. Fig. 1(a) is the leading contribution of $\mathcal{O}(E^1)$ from the contact fermion-Goldstone-boson interaction, solely reflecting the nonzero bare fermion mass term in the unitary gauge. Fig. 1(b) is the sub-leading t/u -channel type of contributions of $\mathcal{O}(E^0)$, and can be ignored for deriving the unitarity bound. Figs. 1(c-e) denote the “hybrid” contact graphs due to the presence of Goldstone self-interactions from Eq. (2.8) and the exchange of associated EWSB quanta (such as the SM Higgs). The EWSB sector is unitarized at the lower scale of $\mathcal{O}(1)$ TeV, but such contributions in Fig. 1(c) and Fig. 1(d-e) can be at most of $\mathcal{O}(E^1)$ in general, as we counted above in Eq. (2.17). Unlike the model-independent leading “contact” contributions in Fig. 1(a), the additions in Fig. 1(c-e) rely on the details of EWSB and are thus highly *model-dependent*. But, this does not affect our general estimate in Sec. 3 which only makes use of the above generic power counting results in Eq. (2.17). For a more precise analysis, we will first estimate the unitarity bounds by quantitatively computing the universal model-independent contribution of Fig. 1(a) in Sec. 4.1. Then, in Sec. 4.2, we further examine the effect of including the type of contributions in Figs. 1(c-e) by specifying an EWSB sector. We will show that such model-dependent contributions only affect the unitarity bound by factors of $\mathcal{O}(1)$, so that our unitarity limits on the scales of fermion mass generation are robust.

2.3. General Unitarity Condition and the Customary $2 \rightarrow 2$ Limits

For the convenience of later analysis and discussion, we give a unified derivation of the unitarity condition on elastic and inelastic scattering including general spins for the particles and a consistent treatment of identical particles in the final state, which extends the derivation of Ref. [44]. Then we briefly review the customary unitarity limits for various elastic and inelastic $2 \rightarrow 2$ scattering processes.

2.3.1. General $2 \rightarrow n$ Unitarity Condition

The unitarity bound originates from the unitarity condition of the S -matrix, $S^\dagger S = 1$, which, with the definition $S = 1 + i\mathcal{T}$, can be expressed as, $\mathcal{T}^\dagger \mathcal{T} = 2\Im \mathcal{T}$. Taking the matrix element of both sides of this relation between identical 2-body states and inserting a complete set of intermediate states into its left-hand side, one arrives at

$$\int_{\text{PS}_2} |\mathcal{T}_{\text{el}}[2 \rightarrow 2]|^2 + \sum_n \int_{\text{PS}_n} |\mathcal{T}_{\text{inel}}[2 \rightarrow n]|^2 = 2\Im \mathcal{T}_{\text{el}}[2 \rightarrow 2], \quad (2.18)$$

where on the left-hand side \int_{PS_n} denotes the n -body phase space integration (including the symmetric factors from the possible identical particles in the final state) and, in the second term, the summation is over all inelastic channels ($n \geq 2$). The right-hand-side is evaluated in the forward direction. For the $2 \rightarrow 2$ elastic channel, we make the partial wave expansion for the scattering amplitude

$$\begin{aligned}\mathcal{T}_{\text{el}}[2 \rightarrow 2] &= 16\pi e^{i(\nu-\nu')\varphi} \sum_j (2j+1) d_{\nu'\nu}^j(\cos\theta) a_j^{\text{el}}, \\ a_j^{\text{el}} &= \frac{1}{32\pi} e^{i(\nu'-\nu)\varphi} \int_{-1}^1 d\cos\theta d_{\nu'\nu}^j(\cos\theta) \mathcal{T}_{\text{el}}[2 \rightarrow 2],\end{aligned}\tag{2.19}$$

where θ and φ are the scattering angles, and $(\nu, \nu') = (\nu_1 - \nu_2, \nu_3 - \nu_4)$ with (ν_1, ν_2) and (ν_3, ν_4) the helicity indices of the incoming and outgoing particles, respectively. The d -functions satisfy the orthonormal condition, $\int_{-1}^1 dx d_{\nu'\nu}^j(x) d_{\nu''\nu}^j(x) = \frac{2\delta_{jj'}}{2j+1}$, and for the special case of $\nu = \nu' = 0$, we have $d_{00}^j(x) = P_j(x)$, with $P_j(x)$ the Legendre polynomials. So, for the incoming and outgoing particles of the same helicities, $\nu_1 = \nu_2$ and $\nu_3 = \nu_4$, (2.19) reduces to

$$\begin{aligned}\mathcal{T}_{\text{el}}[2 \rightarrow 2] &= 16\pi \sum_j (2j+1) P_j(\cos\theta) a_j^{\text{el}}, \\ a_j^{\text{el}} &= \frac{1}{32\pi} \int_{-1}^1 d\cos\theta P_j(\cos\theta) \mathcal{T}_{\text{el}}[2 \rightarrow 2].\end{aligned}\tag{2.20}$$

With (2.19), it is straightforward to compute

$$\int_{\text{PS}_2} |\mathcal{T}_{\text{el}}[2 \rightarrow 2]|^2 = \frac{32\pi}{\varrho_e} \sum_j (2j+1) |a_j^{\text{el}}|^2,\tag{2.21}$$

where the symmetry factor ϱ_e equals $1!(2!)$ if the 2-body final state consists of non-identical (identical) particles¹³. In (2.21) and the rest of this paper, we consider the mass of any initial/final state particle to be much smaller than the c.m. energy, $m_j^2 \ll s$, which is justified for the scattering processes to be analyzed in Sec. 3-6.¹⁴ Using Eqs. (2.19) and (2.21), the unitarity condition (2.18) becomes

$$\sum_j (2j+1) \frac{1}{\varrho_e} \left[\frac{\varrho_e^2}{4} - \left(\Re a_j^{\text{el}} \right)^2 - \left(\Im a_j^{\text{el}} - \frac{\varrho_e}{2} \right)^2 \right] = \frac{1}{32\pi} \sum_n \int_{\text{PS}_n} |\mathcal{T}_{\text{inel}}[2 \rightarrow n]|^2 \geq 0,\tag{2.22}$$

Because the right-hand side of (2.22) is non-negative, we find a consistent solution, for each j ,

$$\left(\Re a_j^{\text{el}} \right)^2 + \left(\Im a_j^{\text{el}} - \frac{\varrho_e}{2} \right)^2 \leq \frac{\varrho_e^2}{4},\tag{2.23}$$

¹³Throughout our derivation the factors due to the proper counting of final state identical particles will solely originate from the *phase space integration of the n -body final state* in the total cross section.

¹⁴For completeness, in Appendix B we give the precise formula of $\int_{\text{PS}_2} |\mathcal{T}_{\text{el}}[2 \rightarrow 2]|^2$ and the refined unitarity conditions by including the possible masses of initial/final state.

which results in

$$\begin{aligned} \left| \Re a_j^{\text{el}} \right| &\leq \frac{\varrho_e}{2}, \\ \left| a_j^{\text{el}} \right| &\leq \varrho_e. \end{aligned} \tag{2.24}$$

When the 2-body final state consists of non-identical particles ($\varrho_e = 1$), these conditions reduce to the familiar form, $|\Re a_j^{\text{el}}| \leq \frac{1}{2}$ and $|a_j^{\text{el}}| \leq 1$. With (2.24) and defining the elastic cross section $\sigma_{\text{el}} \equiv \sum_j \sigma_j^{\text{el}}$, we deduce a bound on σ_{el} in its j -th partial wave, from Eq. (2.21),

$$\sigma_j^{\text{el}}[2 \rightarrow 2] \leq \frac{16\pi(2j+1)\varrho_e}{s}, \tag{2.25}$$

which, for $\varrho_e = 1$, agrees with Eq. (38.47) of Ref. [62]. Finally, by assuming the dominance of $j = 0$ contribution to the elastic channel, an upper bound on the inelastic cross section $\sigma_{\text{inel}}[2 \rightarrow n]$ ($n \geq 2$) can be derived from Eq. (2.22),

$$\sigma_{\text{inel}}[2 \rightarrow n] \leq \frac{4\pi\varrho_e}{s}. \tag{2.26}$$

Here the identical particle factor ϱ_e is determined by the final state of the *elastic* channel (which has the same initial state as the inelastic channel) as indicated by the subscript of ϱ_e . For a given initial state of the inelastic channel, as long as we can find at least one elastic channel (with the same initial state) in which the final state particles are non-identical¹⁵, we can then set $\varrho_e = 1$ in the above *inelastic* bound (2.26) to get the optimal constraint. This mild requirement is satisfied for all the inelastic channels of $f\bar{f}, f\bar{f}' \rightarrow nV_L^a$. Before concluding this subsection, let us derive a partial wave unitarity condition for the $2 \rightarrow 2$ *inelastic* channel [parallel to (2.24)]. Using the same partial wave expansion formula (2.20) for the inelastic amplitude, we can compute

$$\int_{\text{PS}_2} |\mathcal{T}_{\text{inel}}[2 \rightarrow 2]|^2 = \frac{32\pi}{\varrho_i} \sum_j (2j+1) |a_j^{\text{inel}}|^2, \tag{2.27}$$

where $\varrho_i = 1!(2!)$ for an inelastic final state being non-identical (identical) particles. Substituting this back into the RHS of (2.22), we deduce

$$\sum_j (2j+1) \left\{ \frac{\varrho_e}{4} - \frac{1}{\varrho_e} \left[\left(\Re a_j^{\text{el}} \right)^2 + \left(\Im a_j^{\text{el}} - \frac{\varrho_e}{2} \right)^2 \right] \right\} > \sum_j (2j+1) \frac{1}{\varrho_i} |a_j^{\text{inel}}|^2, \tag{2.28}$$

so that, for each j ,

$$|a_j^{\text{inel}}| < \frac{\sqrt{\varrho_i \varrho_e}}{2}. \tag{2.29}$$

¹⁵For some types of initial states in a given model, the final state with identical particles may be automatically forbidden due to the particular charge of this initial state or the absence of certain couplings.

Interestingly, the optimal bound for a given $2 \rightarrow 2$ inelastic channel is realized when we can set $\varrho_e = 1$ for a corresponding elastic channel (which shares the same initial state), i.e., $|a_j^{\text{inel}}| < \sqrt{\varrho_1}/2$. We see that this or (2.29) takes a *different* form from the elastic partial wave condition (2.24) when final state consists of identical particles or when $\Im m a_j \neq 0$.

2.3.2 Customary Limits from $2 \rightarrow 2$ Scattering

2.3.2A. $2 \rightarrow 2$ Unitarity Bound for the EWSB Scale

The unitarity violation from the quasi-elastic scattering $V_L^{a_1} V_L^{a_2} \rightarrow V_L^{a_3} V_L^{a_4}$ was originally studied by Dicus-Mathur/Lee-Quigg-Thacker (DM/LQT) [35, 37] for constraining the Higgs boson mass in the SM. According to the ET, its leading high energy behavior is represented by the corresponding Goldstone boson scattering $\pi^{a_1} \pi^{a_2} \rightarrow \pi^{a_3} \pi^{a_4}$, and can be directly computed from the Higgsless nonlinear Lagrangian (2.8) as

$$\begin{aligned} \mathcal{T}[\pi^0 \pi^0 \rightarrow \pi^0 \pi^0] &= 0, & \mathcal{T}[\pi^0 \pi^0 \rightarrow \pi^+ \pi^-] &= \frac{s}{v^2}, & \mathcal{T}[\pi^+ \pi^- \rightarrow \pi^0 \pi^0] &= \frac{s}{v^2}, \\ \mathcal{T}[\pi^0 \pi^\pm \rightarrow \pi^0 \pi^\pm] &= \frac{t}{v^2}, & \mathcal{T}[\pi^\pm \pi^\pm \rightarrow \pi^\pm \pi^\pm] &= -\frac{s}{v^2}, & \mathcal{T}[\pi^+ \pi^- \rightarrow \pi^+ \pi^-] &= -\frac{u}{v^2}, \end{aligned} \quad (2.30)$$

where $t \simeq -\frac{1}{2}s(1 - \cos\theta)$ and $u \simeq -\frac{1}{2}s(1 + \cos\theta)$. This is usually called the low energy theorem [63] and may be reexpressed in terms of isospin amplitudes $\mathcal{T}[I]$ [64],

$$\begin{aligned} \mathcal{T}[0] &= 3\mathcal{A}(s, t, u) + \mathcal{A}(t, s, u) + \mathcal{A}(u, t, s) = \frac{3s + t + u}{v^2}, \\ \mathcal{T}[1] &= \mathcal{A}(t, s, u) - \mathcal{A}(u, t, s) = \frac{t - u}{v^2}, \\ \mathcal{T}[2] &= \mathcal{A}(t, s, u) + \mathcal{A}(u, t, s) = -\frac{t + u}{v^2}, \end{aligned} \quad (2.31)$$

where $\mathcal{A}(s, t, u) = \frac{s}{v^2}$, and the relevant identical particle factors are not included. Considering the isospin-singlet channel and including the identical particle factor $\varrho_e = 2!$ in the first inequality of Eq. (2.24), we see that the unitarity condition $|\Re a_0^0| \leq \frac{\varrho_e}{2}$ leads to an optimal limit, $\sqrt{s} \leq E_W^*$ with $E_W^* = \sqrt{8\pi} v \simeq 1.2 \text{ TeV}$. Another derivation is to define the normalized isospin-singlet state (including identical particle factors), $|0\rangle = \frac{1}{\sqrt{6}} [2|\pi^+ \pi^-\rangle + |\pi^0 \pi^0\rangle]$, and compute the scattering amplitude in the singlet-channel,

$$\mathcal{T}[0] = \frac{1}{6} [4\mathcal{T}[+-, +-] + 4\mathcal{T}[+-, 00] + \mathcal{T}[00, 00]] = \frac{2(s - u)}{3v^2}. \quad (2.32)$$

Thus, from (2.32) the usual unitarity condition of the s -wave amplitude ($|\Re a_0^0| \leq 1/2$) imposes an optimal bound for the isospin singlet-channel,

$$E_W^* = \sqrt{8\pi} v \simeq 1.2 \text{ TeV}. \quad (2.33)$$

which we mentioned earlier in Eq. (1.1).

2.3.2B. $2 \rightarrow 2$ Unitarity Bound on the Scale of Fermion Mass Generation

Appelquist and Chanowitz (AC) [43] considered the scattering $f_{\pm}\bar{f}_{\pm} \rightarrow V_L^{a_1}V_L^{a_2}$ [65] with fermion bare mass terms¹⁶, and derived the asymptotic amplitude,

$$\mathcal{T}[f_{\pm}\bar{f}_{\pm} \rightarrow W_L^+W_L^-] = \pm \frac{m_f}{v^2}\sqrt{s}, \quad (2.34)$$

where the subscripts for $f_{\pm}\bar{f}_{\pm}$ indicate the fermion helicity $\pm\frac{1}{2}$. For the color-singlet initial state, this gives the s -wave unitarity limit $\sqrt{s} \leq E^* \simeq \frac{8\pi v^2}{\sqrt{N_c}m_f}$, as we mentioned earlier in Eq. (1.2).

Defining the spin-singlet combination for the initial state fermions, $\frac{1}{\sqrt{2}}[|f_+\bar{f}_+\rangle - |f_-\bar{f}_-\rangle]$, we may make this bound slightly tighter,

$$E_f^* \simeq \frac{8\pi v^2}{\sqrt{2N_c}m_f}. \quad (2.35)$$

One can further define a normalized isospin-singlet state for the out-going gauge bosons with the combination [41] $\frac{1}{\sqrt{6}}[2|W_L^+W_L^-\rangle + |Z_L^0Z_L^0\rangle]$, and thus slightly reduce the bound (2.35) by an additional factor of $\sqrt{\frac{2}{3}} \simeq 1/1.22$, i.e.,¹⁷ $E_f^* \simeq \frac{8\pi v^2}{\sqrt{3N_c}m_f}$.

2.3.2C. $2 \rightarrow 2$ Unitarity Bound on the Scale of Majorana Neutrino Mass Generation

The Majorana neutrino scattering $\nu_{L\pm}\nu_{L\pm} \rightarrow V_L^{a_1}V_L^{a_2}$ was considered recently by Maltoni-Niczyporuk-Willenbrock (MNW) [44, 66] who derived an upper bound on the scale of the neutrino mass generation by using the Weinberg dimension-5 operator [19] with the usual SM Higgs doublet. For the inelastic scattering $\frac{1}{\sqrt{2}}[|\nu_{L+}\nu_{L+}\rangle - |\nu_{L-}\nu_{L-}\rangle] \rightarrow \frac{1}{\sqrt{2}}|Z_LZ_L\rangle$ or $\frac{1}{\sqrt{2}}|hh\rangle$, one obtains, from the condition (2.29) ($\varrho_e = 2$),¹⁸

$$E_{\nu}^* \simeq \frac{4\sqrt{2}\pi v^2}{m_{\nu}}, \quad (2.36)$$

¹⁶Their equivalent gauge-invariant nonlinear formulation is given in Eq. (2.9).

¹⁷For clarity of the following analyses with a multiple V_L^a (π^a) final state, we will ignore such minor improvements and thus will use (2.35) for comparison.

¹⁸In this paper we will not add extra identical particle normalization factors for the *initial* state as they are irrelevant to the calculation of the cross section and unitarity bound (cf. Sec. 2.3.1). For convenience, we may do so in the amplitude calculation only for final state identical particles as far as the total cross section and unitarity bound are concerned (which also means that in the condition (2.29) we will accordingly remove the final state identical particle factor ϱ_i and still retain ϱ_e), but we keep in mind that this is inappropriate when computing the differential cross section.

which can be improved to $E_\nu^* \simeq \frac{4\pi v^2}{m_\nu}$ by using a mixed final state $\frac{1}{2}|Z_L Z_L + hh\rangle$ [44].

In our analysis, the bare neutrino Majorana mass term arises from the nonlinear operator (2.10) *without* assuming the participation of the SM Higgs boson. With this, the scattering processes $\frac{1}{\sqrt{2}}[|\nu_{L+}\nu_{L+}\rangle - |\nu_{L-}\nu_{L-}\rangle] \rightarrow |W_L^+ W_L^-\rangle$, $\frac{1}{\sqrt{2}}|Z_L Z_L\rangle$ and $\frac{1}{\sqrt{2}}[|\nu_{L+}\nu_{L+}\rangle - |\nu_{L-}\nu_{L-}\rangle] \rightarrow |\pi^+\pi^-\rangle$, $\frac{1}{\sqrt{2}}|\pi^0\pi^0\rangle$ can be computed. The helicity amplitudes are

$$\begin{aligned} \mathcal{T}[\nu_{L\pm}\nu_{L\pm} \rightarrow W_L^+ W_L^-] &\simeq -\mathcal{T}[\nu_{L\pm}\nu_{L\pm} \rightarrow \pi^+\pi^-] \simeq \pm \frac{2m_\nu}{v^2} \sqrt{s}, \\ \mathcal{T}[\nu_{L\pm}\nu_{L\pm} \rightarrow \frac{1}{\sqrt{2}}Z_L Z_L] &\simeq -\mathcal{T}[\nu_{L\pm}\nu_{L\pm} \rightarrow \frac{1}{\sqrt{2}}\pi^0\pi^0] \simeq \pm \frac{2\sqrt{2}m_\nu}{v^2} \sqrt{s}. \end{aligned} \quad (2.37)$$

Thus, for a spin-singlet initial state, the scattering $\frac{1}{\sqrt{2}}[|\nu_{L+}\nu_{L+}\rangle - |\nu_{L-}\nu_{L-}\rangle] \rightarrow \frac{1}{\sqrt{2}}|Z_L Z_L\rangle$ leads to a unitarity violation limit

$$E_\nu^* \simeq \frac{2\sqrt{2}\pi v^2}{m_\nu}. \quad (2.38)$$

The reason that this limit is stronger than (2.36) by a factor of 2 is the absence of the SM Higgs boson in our nonlinear operator (2.10). This is due to the fact that the s -channel SM-Higgs exchange arising from the usual dimension-5 Weinberg operator will partially cancel with the gauge amplitude in the unitary gauge and push the unitarity violation to a slightly higher scale. We also note that with the isospin-singlet combination for the final state gauge bosons, $\frac{1}{\sqrt{6}}[2|W_L^+ W_L^-\rangle + |Z_L^0 Z_L^0\rangle]$, the bound (2.38) may be further improved by factor of $\frac{\sqrt{3}}{2} \simeq 1/1.15$. With the typical neutrino mass $m_\nu \sim 0.05$ eV, the limit (2.38) [or (2.36)] gives, $E_\nu^* \sim 10^{16}$ GeV, which is right at the grand unification (GUT) scale.

3. Challenge from $2 \rightarrow n$ Inelastic Scattering

3.1. Puzzle: Energy Power Counting vs. Kinematic Condition

According to the power counting result Eq. (2.17), the E -power dependence of the scattering amplitudes for $f\bar{f}, \nu_L \nu_L \rightarrow nV_L^a$ and $V_L^{a_1} V_L^{a_2} \rightarrow nV_L^a$ ($n \geq 2$) is independent of the number of V_L^a 's in the final state. This means that any conceptual change for $n > 2$ has to come from the n -body phase space. Indeed, it is straightforward to count the E -power dependence from the n -body phase space integration,

$$\begin{aligned} \frac{1}{\mathcal{J}_{\text{in}}} \int_{\text{PS}_n} &= \frac{1}{\varrho \mathcal{J}_{\text{in}}} \int \frac{d^3 k_1 \cdots d^3 k_n}{2E_1 \cdots 2E_n} (2\pi)^{4-3n} \delta^{(4)} \left(p_1 + p_2 - \sum_{j=1}^n k_j \right) \\ &\sim s^{n-3} = E^{2(n-3)}, \end{aligned} \quad (3.39)$$

where $\mathcal{J}_{\text{in}} = 4 [(p_1 \cdot p_2)^2 - (m_1 m_2)^2]^{\frac{1}{2}} \simeq 2s$ is the flux factor of the initial state, ϱ is the symmetry factor from possible identical particles in the final state, and we define $E \equiv \sqrt{s}$. Eq. (3.39) shows that the phase space contributes a nontrivial energy power factor to the cross section which grows with n .

Combining the powers of energy for the scattering amplitude in Eq. (2.17) and for the n -body phase space integration in Eq. (3.39), we arrive at the following naïve power counting estimate, including all *dimensionful* parameters in the cross section,

$$\sigma[2 \rightarrow n] \propto \frac{1}{s} \left(\frac{m_f}{v} \right)^{2(2-\delta)} \left(\frac{s}{v^2} \right)^{n-2+\delta}, \quad (n \geq 2), \quad (3.40)$$

where $\delta = 1$ for $f\bar{f}, \nu_L \nu_L \rightarrow nV_L^a$ (as considered in [44]) and $\delta = 2$ for $V_L^{a_1} V_L^{a_2} \rightarrow nV_L^a$. For simplicity, we have used m_f to denote the mass of either a Dirac fermion f or a Majorana neutrino ν_L . With the general condition (2.26) the naïve estimate (3.40) results in the unitarity limit,

$$\tilde{E}^* \sim v \left[C_0 \left(\frac{v}{m_f} \right)^{2(2-\delta)} \right]^{\frac{1}{2(n-2+\delta)}} \rightarrow v, \quad (\text{for } n \rightarrow \text{large}), \quad (3.41)$$

where C_0 is a dimensionless constant undetermined by the power counting. From (3.41), we see that for $\delta = 1$, it gives the bound (1.3) (which is the conclusion of Ref. [44]), while for $\delta = 2$, it results in the bound (1.5). It is clear that if the above naïve power counting estimate could really hold, then one is led to a striking conclusion that all unitarity bounds from multiple V_L -production would approach the same scale $v \simeq 246 \text{ GeV}$ for arbitrarily large n , and thus such scattering processes

would reveal *no new scale* (other than v) for the mass generation. As we have observed, even for the EWSB scale, this would imply a significant reduction of the customary $2 \rightarrow 2$ limit (1.1) [or (2.33)].

The puzzle is sharpened when we consider the general kinematic condition for all multiple V_L -production processes,

$$\sqrt{s} > nM_{W(Z)} \simeq \frac{n}{3}v, \quad \longrightarrow \quad E^* > v\frac{n}{3}, \quad (3.42)$$

which must hold for all these processes as we advertized in the Introduction. When n becomes large, this condition requires the unitarity violation scale $\sqrt{s} = E^*$ to *grow at least linearly with n* , rather than arbitrarily approaching the scale v . This unavoidably contradicts to the conclusion drawn from the naïve power counting estimate (3.41). It is this observation that leads us to believe that the condition (3.41) cannot really hold and a deeper resolution must exist.

3.2. Resolution: Increasing Power of Energy vs. Phase Space Suppression

At this point it appears clear that in order to be consistent with the kinematic condition (3.42) there must be additional n -dependent *dimensionless* factors in the *exact* n -body phase space integration that sufficiently suppress the E -power enhancement in Eq. (3.39).

When the possible angular dependence is ignored in the squared amplitude, $|\mathcal{T}|^2$, the cross section factorizes into the squared amplitude times the phase space, so the n -body phase space integration can be done exactly (cf. Appendix A) and is given by

$$\begin{aligned} \frac{1}{\mathcal{J}_{\text{in}}} \int_{\text{PS}_n} &= \frac{1}{\varrho \mathcal{J}_{\text{in}}} \int \frac{d^3k_1 \cdots d^3k_n}{2E_1 \cdots 2E_n} (2\pi)^{4-3n} \delta^{(4)} \left(p_1 + p_2 - \sum_{j=1}^n k_j \right) \\ &= \frac{s^{n-3}}{2^{4(n-1)} \pi^{2n-3} (n-1)! (n-2)! \varrho}. \end{aligned} \quad (3.43)$$

For the processes $f\bar{f}, \nu_L \nu_L \rightarrow nV_L^a$ and $V_L^{a_1} V_L^{a_2} \rightarrow nV_L^a$, using Eq. (2.17) we can generically write the form of the squared amplitudes as,

$$|\mathcal{T}|^2 = c_0(\theta_j) (2N_c)^{2-\delta} \frac{m_f^{2(2-\delta)} s^\delta}{v^{2n}}, \quad (3.44)$$

where δ is defined below Eq. (3.40) and $c_0(\theta_j)$ is a process-dependent, dimensionless coefficient with possible dependence on the scattering angles (θ_j) ¹⁹. Here, the factor $2N_c$ comes from the color-singlet channel of the initial state fermion pair with a proper helicity combination [cf. Eq. (4.58)],

¹⁹It turns out that for the scattering $f\bar{f}, \nu_L \nu_L \rightarrow nV_L^a$, the universal leading contributions are given by the ‘‘contact’’ Feynman diagrams represented in Fig. 1(a) where the c_0 has no angular dependence.

and $N_c = 3(1)$ for quarks (leptons or neutrinos). Thus, we can have a *realistic estimate* for the scattering cross section,

$$\sigma = \frac{C_0 (2N_c)^{2-\delta}}{2^{4(n-1)} \pi^{2n-3} (n-1)!(n-2)!} \frac{1}{s} \left(\frac{\sqrt{s}}{v} \right)^{2(n-2+\delta)} \left(\frac{m_f}{v} \right)^{2(2-\delta)}, \quad (3.45)$$

where $C_0 \equiv \bar{c}_0/\varrho$ and \bar{c}_0 is a constant factor originating from the coefficient c_0 in the squared amplitude (3.44) and includes the possible modification to the n -body phase space integration (3.43) (if c_0 has nontrivial angular dependence). Substituting (3.45) into the general condition (2.26), we thus arrive at the following *improved estimate* of the unitarity bound,

$$E^* = v \left[C_0 2^{4n-2} \pi^{2(n-1)} (n-1)!(n-2)! (2N_c)^{\delta-2} \left(\frac{v}{m_f} \right)^{2(2-\delta)} \right]^{\frac{1}{2(n-2+\delta)}}, \quad (3.46)$$

where the process-dependent constant C_0 will be evaluated by an exact calculation (cf. Sec.4-5). For the current estimate it is reasonable to assume $C_0 = \mathcal{O}(1)$ or, in a more precise form,

$$C_0^{\frac{1}{2(n-2+\delta)}} \sim 1, \quad (3.47)$$

which becomes increasingly more accurate as n gets larger. In fact, Eq. (3.46) may be regarded as an exact bound (with the constant C_0 to be derived from the precise calculation), and thus the formula (3.47) may actually represent *all our approximations* made in the current estimate of the unitarity bound: **(i)**. ignore the dimensionless coefficient $c_0(\theta_j)$ in the amplitude-square (3.44) including its possible angular dependence [that may lead to an $\mathcal{O}(1)$ correction to the n -body phase space integration (3.43)]; **(ii)**. ignore the symmetry factor $1/\varrho$ arising from possible identical particles in a given final state.

The crucial observation from Eq. (3.46) is to note that the n -dependent dimensionless factor $[(n-1)!(n-2)!]^{\frac{1}{2(n-2+\delta)}}$ does not approach unity as n becomes large, rather, it increases almost linearly with n . This can be understood from Stirling's formula²⁰, $n! \simeq n^n e^{-n} \sqrt{2\pi n}$, from which we can estimate, for large n ,

$$[(n-1)!(n-2)!]^{\frac{1}{2(n-2+\delta)}} \simeq (n!)^{\frac{1}{n}} \simeq \frac{n}{e} > \frac{n}{3}, \quad (\text{for } n \gg 1), \quad (3.48)$$

where the constant $e = 2.7182818\dots$. It is this feature that makes our bound (3.46) fully consistent with the kinematic condition (3.42)! For the processes $f\bar{f}, \nu_L \nu_L \rightarrow n V_L^a$ ($\delta = 1$) with light quarks (leptons) or neutrinos, i.e., $v^2/m_f^2 \gg 1$, we observe that there is a *competition* in the unitarity bound (3.46) between the quickly decreasing factor $(v/m_f)^{\frac{1}{n-1}}$ and the almost linearly

²⁰The relative error of this formula is less than 4% for $n \geq 2$.

increasing factor $[(n-1)!(n-2)!]^{\frac{1}{2(n-2+\delta)}}$ when n becomes large. As a consequence we expect the strongest unitarity bound to occur at a value $n = n_s > 2$ and, after n exceeds n_s , the factor $[(n-1)!(n-2)!]^{\frac{1}{2(n-2+\delta)}}$ will become dominant and eventually force the bound (3.46) to grow almost linearly with n . Only for the heaviest SM fermion, the top quark (where $v^2/m_t^2 \simeq 2 \not\gg 1$), can the value of n_s be equal (or very close) to 2. On the other hand, for the process $V_L^{a1} V_L^{a2} \rightarrow n V_L^a$ ($\delta = 2$), when n increases, the only possible *decreasing* factor on the right-hand side of Eq. (3.46) is $(\sqrt{C_0}/(2\pi))^{\frac{1}{n}}$, provided $\sqrt{C_0} > 2\pi$. But our current estimate under the approximation (3.47) implies the setting $C_0 \sim 1$. So it seems that we will have $n_s = 2$ for the EWSB scale which corresponds to the customary $2 \rightarrow 2$ unitarity limit discussed in Sec. 2.3.2 [cf. Eq. (2.33)]. Since the current estimate does not precisely fix the value of C_0 , a reliable determination of C_0 and thus n_s should be given by a quantitative calculation, which will indeed support $n_s = 2$ (cf. Sec. 6).

Considering the region $n \gg 1$ and thus $\mathcal{O}(1)^{\frac{1}{2(n-2+\delta)}} \sim \mathcal{O}(1)^{\frac{1}{2n}} \sim 1$, we can further derive a complete asymptotic formula for Eq. (3.46),

$$\begin{aligned}
E^* &\approx v \left(\frac{v}{m_f} \right)^{\frac{2-\delta}{n}} \frac{4\pi}{e} n, & (\text{for } n \gg 1) \\
&\approx \frac{4\pi v}{e} \left[n + (2-\delta) \ln \left(\frac{v}{m_f} \right) + \mathcal{O} \left(\frac{(2-\delta)^2}{n} \right) \right].
\end{aligned} \tag{3.49}$$

From this, we deduce that for each asymptotic value of n , the leading difference between the unitarity bounds of two types of fermions with masses m_{f_1} and m_{f_2} is given by²¹

$$E_{f_1}^* - E_{f_2}^* \approx \frac{4\pi v}{e} \left[\ln \left(\frac{m_{f_2}}{m_{f_1}} \right) + \mathcal{O} \left(\frac{1}{n} \right) \right], \tag{3.50}$$

which is independent of the value of n . Similarly, the difference between the unitarity limit E_f^* for the fermion f and the limit E_W^* for the scale of EWSB behaves as

$$E_f^* - E_W^* \approx \frac{4\pi v}{e} \left[\ln \left(\frac{v}{m_f} \right) + \mathcal{O} \left(\frac{1}{n} \right) \right], \tag{3.51}$$

and is again independent of n in its asymptotic region.

Finally, in Fig. 2, we numerically plot out the bound (3.46) under the approximation (3.47), for a number of typical processes including $V_L^{a1} V_L^{a2}$, $t\bar{t}$, $b\bar{b}$, $\tau^-\tau^+$, e^-e^+ , $\nu_L \nu_L \rightarrow n V_L^a$, where we have

²¹For the analysis in the current section, f denotes either a quark, a charged lepton, or a Majorana neutrino.

input the following central values for the SM fermion masses [62],²²

$$\begin{aligned} (m_t, m_b, m_c, m_s, m_u, m_d) &= (178.0, 4.85, 1.65, 0.105, 0.003, 0.006) \text{ GeV}, \\ (m_\tau, m_\mu, m_e) &= (1.777, 0.1057, 0.000511) \text{ GeV}. \end{aligned} \quad (3.52)$$

For leptons and heavy quarks (c, b, t) the pole-masses are used, while for light quarks (u, d, s) the current-quark masses under $\overline{\text{MS}}$ [62] are chosen as the light quark pole-masses are hard to directly extract. Our $2 \rightarrow n$ analysis shows that for light fermions the minimum $n = n_s$ is sizable and the unitarity limit is insensitive to the fermion masses, so a small difference between the pole-mass and $\overline{\text{MS}}$ mass for light fermions does not cause a visible effect in Fig. 2. The absolute scale for neutrino masses will be further determined by various experiments. As mentioned earlier, the recent WMAP data [14], in conjunction with the 2dF Galaxy Redshift Survey [15] put a 95% C.L. upper limit $\sum_j m_{\nu j} \leq 1.01 \text{ eV}$ [16]. From the WMAP, SDSS and Lyman- α Forest data, a stronger bound [17], $\sum_j m_{\nu j} \leq 0.65 \text{ eV}$ (95% C.L.), may be derived. Neutrino oscillations measure the difference of squared mass-eigenvalues and the atmospheric data require the larger mass gap bounded by [4, 10],

$$0.04 \text{ eV} \leq \Delta_{\text{atm}}^{\frac{1}{2}} \leq 0.06 \text{ eV}, \quad (99\% \text{ C.L.}), \quad (3.53)$$

where $\Delta_{\text{atm}} = |m_{\nu_{1,2}}^2 - m_{\nu_3}^2|$. This requires the neutrino mass scale to be bounded from below, i.e., $m_\nu \gtrsim \Delta_{\text{atm}}^{\frac{1}{2}} \sim 0.05 \text{ eV}$, and when the neutrino mass spectrum exhibits a hierarchical structure, the quantity $\Delta_{\text{atm}}^{\frac{1}{2}}$ actually sets the mass scale for one or two of the active neutrinos [10, 69]. The upcoming laboratory experiments on neutrinoless double β -decay [70, 71] are indispensable to further pin down the neutrino mass scale. Without losing generality, we choose a sample neutrino mass value $m_\nu \simeq 0.05 \text{ eV}$ for the analyses in Fig. 2 (and in the Table 1 below).

Fig. 2 shows that the scattering processes $f\bar{f}, \nu_L \nu_L \rightarrow n V_L^a$ indeed put new unitarity limits on the scale of fermion mass generation, *independent of the scale v* , and in agreement with the original motivation of Appelquist and Chanowitz [43]. However, strikingly, our analysis further reveals that for the light fermions including neutrinos, leptons and quarks, the strongest bounds generally occur at a value $n = n_s > 2$. The current improved estimates of (n_s, E_{min}^*) are summarized in Table 1. Note that these bounds easily satisfy the kinematic constraint Eq. (1.4).

Another feature of Fig. 2 is that the curves for the quarks and charged leptons become almost parallel in the asymptotic region $n \gtrsim 15$, and the upper curve (for neutrinos) also becomes parallel when $n \gtrsim 35$. This fact can be understood from the asymptotic formula, Eqs. (3.50) and (3.51).

²²Recently both D0 and CDF announced their updated analyses of the Run-I data for top quark mass measurements [67]. The resulting world average for the top quark pole-mass is $m_t = 178.0 \pm 4.3 \text{ GeV}$ [68].

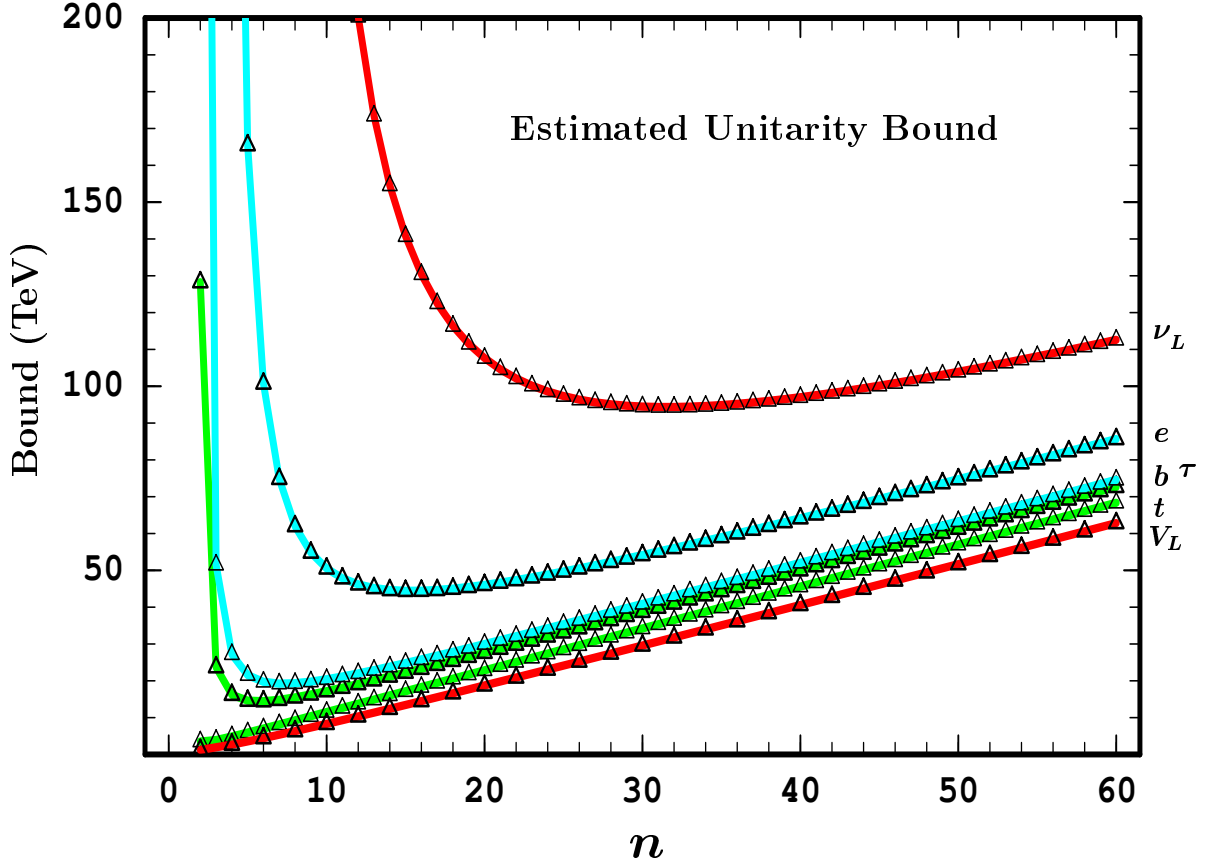


Figure 2: Realistic estimate of the unitarity bound E^* , based upon Eq. (3.46) with the approximation (3.47), for the scattering processes $V_L^{a1}V_L^{a2}$, $t\bar{t}$, $b\bar{b}$, $\tau^-\tau^+$, e^-e^+ , $\nu_L\nu_L \rightarrow nV_L^a$ (curves from bottom to top), as a function of $n (\geq 2)$. Only those points corresponding to integer n have physical meaning, and on the lowest curve n is restricted to the even integers.

Fig. 2 further shows that for the scattering $t\bar{t} \rightarrow nV_L^a$ the unitarity bounds are very close for $n = 2, 3, 4$, and it is easy to check that the minimum of the bound can shift to $n_s = 4$ if we just average over the spin and color for the $t\bar{t}$ pair instead of composing a spin-0 and color-singlet initial state. The precise calculations in Sections 4, 5, and 6 below will quantitatively improve the above estimated numbers but, as we will see, all the qualitative features in Fig. 2 and Table 1 remain. Finally, it is very useful to compare these estimated bounds (Table 1) with the customary $2 \rightarrow 2$ limits (2.33), (2.35) and (2.36) [cf. Sec. 2.3.2] whose predictions are summarized in Table 2. Comparing Table 1 and 2, we see that for the scales of EWSB and top mass generation, our estimates in Table 1 agree with the customary limits in Table 2; however, for all the light fermions and for the Majorana neutrinos, our bounds are substantially stronger than the AC [43] and MNW [44, 66]

limits by *many orders of magnitude*.

Table 1: The estimated *lowest* unitarity bound E_{\min}^* [derived from the Eqs. (3.46) and (3.47)] for the scattering process $\xi_1\xi_2 \rightarrow nV_L^a$ and the corresponding number of final state particles $n = n_s$, where $\xi_{1,2} = V_L, f, \nu_L$ or their anti-particles.

$\xi_1\xi_2$	$V_L^{a_1}V_L^{a_2}$	$t\bar{t}$	$b\bar{b}$	$c\bar{c}$	$s\bar{s}$	$d\bar{d}$	$u\bar{u}$	$\tau^-\tau^+$	$\mu^-\mu^+$	e^-e^+	$\nu_L\nu_L$
n_s	2	2	6	7	10	12	13	7	10	15	32
E_{\min}^* (TeV)	1.2	3.5	14	18	26	35	37	19	28	44	95

Table 2: Predictions of the customary unitarity limits for the scattering process $\xi_1\xi_2 \rightarrow V_L^{a_1}V_L^{a_2}$, based upon Eqs. (2.33), (2.35) and (2.38).

$\xi_1\xi_2$	$V_L^{a_1}V_L^{a_2}$	$t\bar{t}$	$b\bar{b}$	$c\bar{c}$	$s\bar{s}$	$d\bar{d}$	$u\bar{u}$	$\tau^-\tau^+$	$\mu^-\mu^+$	e^-e^+	$\nu_L\nu_L$
$E_{2 \rightarrow 2}^*$ (TeV)	1.2	3.5	128	377	6×10^3	10^5	2×10^5	606	10^4	2×10^6	1.1×10^{13}

4. Scales of Mass Generation for Quarks and Leptons

In this section we will attempt to improve on our new limits on the scales of fermion mass generation by computing the matrix elements more precisely. A parallel treatment of Majorana neutrinos will be given in Sec. 5. In Sec. 4.1, we first systematically derive the precise unitarity limits for various $f\bar{f} \rightarrow n\pi^a$ (nV_L^a) scatterings with quarks/leptons in the initial state, which result in optimal upper bounds on the scales of the fermion mass generation. Then, we compare these quantitative limits with our estimates given in the previous section (Table 1 and Fig. 2). In Sec. 4.2 we include EWSB effects among the π^a [cf. Fig. 1(c-d)]. We also comment on fermion mass generation with dynamical EWSB, where the V_L^a and its would-be Goldstone boson π^a are composite fields.

4.1. Unitarity Bound on the Mass Generation Scale from $f\bar{f} \rightarrow n\pi^a$

From the nonlinear fermion mass term (2.9), we deduce the following fermion-Goldstone interaction Lagrangian,

$$\mathcal{L}_f^{\text{int}} = - \sum_{n=1}^{\infty} \frac{i^n}{v^n n!} \begin{cases} |\vec{\pi}|^n \left(m_f \bar{f} f + m_{f'} \bar{f}' f' \right), & (n = \text{even}), \\ |\vec{\pi}|^{n-1} \left[\pi^0 \left(m_f \bar{f} \gamma_5 f - m_{f'} \bar{f}' \gamma_5 f' \right) \right. \\ \left. + \sqrt{2} \pi^- \bar{f}' \left(m_f P_L - m_{f'} P_R \right) f + \text{H.c.} \right], & (n = \text{odd}), \end{cases} \quad (4.54)$$

where $|\vec{\pi}| = [2\pi^+ \pi^- + \pi^0 \pi^0]^{\frac{1}{2}}$ and $P_{L(R)} = \frac{1}{2}(1 \mp \gamma^5)$. This leads to three types of $2 \rightarrow n$ processes, containing the leading contact diagrams shown in Fig. 1(a),

$$\begin{aligned} \text{(a). } & f\bar{f}, f'\bar{f}' \rightarrow (\pi^+)^{\ell} (\pi^-)^{\ell} (\pi^0)^{n-2\ell}, & (n = \text{even}), \\ \text{(b). } & f\bar{f}, f'\bar{f}' \rightarrow (\pi^+)^{\ell} (\pi^-)^{\ell} (\pi^0)^{n-2\ell}, & (n = \text{odd}), \\ \text{(c). } & f\bar{f}' \rightarrow (\pi^+)^{\ell+1} (\pi^-)^{\ell} (\pi^0)^{n-2\ell-1}, & (n = \text{odd}), \end{aligned} \quad (4.55)$$

which may be generically denoted as $f^a \bar{f}^b \rightarrow (\pi^+)^k (\pi^-)^{\ell} (\pi^0)^{n-k-\ell}$, where $f^a, f^b \in (f, f')$ as appropriate. The helicity amplitudes $\mathcal{T}[f_{\pm}^a \bar{f}_{\pm}^b; n, k, \ell]$ are given by

$$\begin{aligned} n = \text{even: } & \mathcal{T}[f_{\pm} \bar{f}_{\pm}; n, \ell, \ell] = \mp i^n \mathcal{C}_1 \frac{m_f \sqrt{s}}{v^n}, & \mathcal{T}[f'_{\pm} \bar{f}'_{\pm}; n, \ell, \ell] = \mp i^n \mathcal{C}_1 \frac{m_{f'} \sqrt{s}}{v^n}; \\ n = \text{odd: } & \mathcal{T}[f_{\pm} \bar{f}_{\pm}; n, \ell, \ell] = -i^n \mathcal{C}_2 \frac{m_f \sqrt{s}}{v^n}, & \mathcal{T}[f'_{\pm} \bar{f}'_{\pm}; n, \ell, \ell] = +i^n \mathcal{C}_2 \frac{m_{f'} \sqrt{s}}{v^n}, \\ & \mathcal{T}[f_{\pm} \bar{f}'_{\pm}; n, \ell + 1, \ell] = -i^n \mathcal{C}_3 \left(\frac{m_f}{m_{f'}} \right) \frac{\sqrt{s}}{v^n}, & \mathcal{T}[f'_{\pm} \bar{f}_{\pm}; n, \ell, \ell + 1] = -i^n \mathcal{C}_3 \left(\frac{m_{f'}}{m_f} \right) \frac{\sqrt{s}}{v^n}; \end{aligned} \quad (4.56)$$

where the coefficients $(\mathcal{C}_1, \mathcal{C}_2, \mathcal{C}_3)$ are defined as

$$\begin{aligned}\mathcal{C}_1 &= \frac{1}{n!} C_{\frac{n}{2}}^\ell 2^\ell (\ell!)^2 (n-2\ell)!, \\ \mathcal{C}_2 &= \frac{1}{n!} C_{\frac{n-1}{2}}^\ell 2^\ell (\ell!)^2 (n-2\ell)!, \\ \mathcal{C}_3 &= \frac{\sqrt{2}}{n!} C_{\frac{n-1}{2}}^\ell 2^\ell \ell! (\ell+1)! (n-2\ell-1)!,\end{aligned}\tag{4.57}$$

and $C_n^\ell \equiv \frac{n!}{\ell!(n-\ell)!}$. Now we define a color-singlet initial state with a proper helicity combination,

$$|\text{in}\rangle = \begin{cases} \frac{1}{\sqrt{2N_c}} \sum_{\beta=1}^{N_c} [|f_+^{a\beta} \bar{f}_+^{a\beta}\rangle \mp |f_-^{a\beta} \bar{f}_-^{a\beta}\rangle], \\ \frac{1}{\sqrt{N_c}} \sum_{\beta=1}^{N_c} |f_+^{a\beta} \bar{f}_+^{b\beta}\rangle, \quad (a \neq b), \end{cases}\tag{4.58}$$

where on the right-hand side $N_c = 3$ (1) for quarks (leptons), and for the first definition the sign $-$ ($+$) between the two helicity states corresponds to the $n = \text{even}$ (odd) case for an initial state $|\text{in}\rangle$ of spin-0(1). With these we compute the cross section for $|\text{in}\rangle \rightarrow (\pi^+)^k (\pi^-)^\ell (\pi^0)^{n-k-\ell}$ as

$$\begin{aligned}\sigma[\text{in}; n, k, \ell] &= \frac{C_{0j}(2^x N_c)}{2^{4(n-1)} \pi^{2n-3} (n-1)!(n-2)!} \frac{1}{s} \left(\frac{\sqrt{s}}{v} \right)^{2(n-1)} \left(\frac{m_{\hat{f}}}{v} \right)^2, \\ C_{0j} &\equiv \frac{\mathcal{C}_j^2}{\varrho} = \frac{\mathcal{C}_j^2}{k! \ell! (n-k-\ell)!},\end{aligned}\tag{4.59}$$

where $\hat{f} \in (f, f')$, and $x = 1$ (0) for the first (second) definition of the initial state in Eq. (4.58). For the three processes in Eq. (4.55), the maximal values of C_{0j} can be derived as

$$C_{01}^{\max} = \frac{2^n \left(\frac{n!}{2}\right)^2}{(n!)^2}, \quad C_{02}^{\max} = \frac{1}{n!}, \quad C_{03}^{\max} = \frac{2^n \left(\frac{n-1}{2}\right)! \left(\frac{n+1}{2}\right)!}{(n!)^2},\tag{4.60}$$

corresponding to $k = \ell = \frac{n}{2}$, $k = \ell = 0$, and $k = \ell + 1 = \frac{n+1}{2}$, respectively. Thus, for each given type of fermion, using the general unitarity condition (2.26), we arrive at the bound $\sqrt{s} \leq E_f^*$ with

$$E_f^* = v \left[\left(\frac{v}{m_{\hat{f}}} \right)^2 \frac{4\pi}{(2^x N_c) \mathcal{R}_j^{\max}} \right]^{\frac{1}{2(n-1)}}.\tag{4.61}$$

\mathcal{R}_j^{\max} is given by

$$\mathcal{R}_j^{\max} = \frac{C_{0j}^{\max}}{2^{4(n-1)} \pi^{2n-3} (n-1)!(n-2)!},\tag{4.62}$$

or, using (4.60),

$$\begin{aligned}
\mathcal{R}_1^{\max} &= \frac{\left(\frac{n!}{2}\right)^2}{2^{3n-4}\pi^{2n-3}(n!)^2(n-1)!(n-2)!}, & (n = \text{even}), \\
\mathcal{R}_2^{\max} &= \frac{1}{2^{4(n-1)}\pi^{2n-3}n!(n-1)!(n-2)!}, & (n = \text{odd}), \\
\mathcal{R}_3^{\max} &= \frac{\left(\frac{n-1}{2}\right)!\left(\frac{n+1}{2}\right)!}{2^{3n-4}\pi^{2n-3}(n!)^2(n-1)!(n-2)!}, & (n = \text{odd}).
\end{aligned} \tag{4.63}$$

where $\mathcal{R}_{1,2,3}^{\max}$ have $x = 1, 1, 0$ and correspond to the processes (a), (b) and (c) in Eq. (4.55), respectively.

Table 3: The precise minimum unitarity bound E_{\min}^* [derived from Eq. (4.61)] for the scattering process $\xi_1\xi_2 \rightarrow n\pi^a(nV_L^a)$ and the corresponding number of final state particles $n = n_s$, where $\xi_{1,2} = f$ or \bar{f} .

$\xi_1\xi_2$	$t\bar{t}$	$b\bar{b}$	$c\bar{c}$	$s\bar{s}$	$d\bar{d}$	$u\bar{u}$	$\tau^-\tau^+$	$\mu^-\mu^+$	e^-e^+
n_s	2	4	6	8	10	10	6	8	12
E_{\min}^* (TeV)	3.49	23.4	30.8	52.1	77.4	83.6	33.9	56.3	107

Finally, using the bound (4.61), we derive the lowest bound for each scattering and the corresponding number of final state particles $n = n_s$, as shown in Table 3. This is to be compared with our estimated bounds in Table 1 and the customary limits in Table 2. We see that the precise bounds agree well with our estimate for the case of a heavy top quark, but significantly improve the estimates in Table 1 for all other light fermions; the limits in Table 3 become about a factor of 1.5 – 2 higher. The shape of each bound as a function of n is shown in Fig. 3 for all SM quarks and leptons, where n_s corresponds to the minimum of each curve. The values of n_s are visibly smaller than those in Table 1 and Fig. 2. Once $n > n_s$, the curves also grow much faster than Fig. 2, but still exhibit very similar slopes for $n \gtrsim 15$. This is because for the large n the power factor $(v/m_f)^{\frac{1}{n-1}}$ is essentially unity and the dimensionless phase-space factor [cf. Eqs. (3.48) and (4.62)] becomes dominant. Using the Stirling formula, we find that the three functions $\mathcal{R}_{1,2,3}^{\max}$ in Eq. (4.62) exhibit the same asymptotic behavior

$$\mathcal{R}_{1,2,3}^{\max} \approx \left[\frac{e^{\frac{3}{2}}}{4\pi n^{\frac{3}{2}}} \right]^{2n}, \quad (\text{for } n \gg 1), \tag{4.64}$$

so that the final unitarity limit (4.61) behaves as

$$(E_f^*)_{\text{asym}} \approx v \left(\frac{v}{m_{\hat{f}}} \right)^{\frac{1}{n-1}} \left[\frac{4\pi}{e^{\frac{3}{2}}} n^{\frac{3}{2}} \right], \quad (\text{for } n \gg 1) \quad (4.65)$$

$$= \frac{4\pi v}{e^{\frac{3}{2}}} \left[n^{\frac{3}{2}} + n^{\frac{1}{2}} \ln \left(\frac{v}{m_{\hat{f}}} \right) + \frac{1}{2} n^{-\frac{1}{2}} \ln^2 \left(\frac{v}{m_{\hat{f}}} \right) + \mathcal{O} \left(n^{-\frac{3}{2}} \right) \right], \quad (4.66)$$

where we approximate $\mathcal{O}(1)^{\frac{1}{2(n-1)}} \approx 1$ for $n \gg 1$. We see that unlike Eq. (3.49), the leading term in the above bound has $n^{\frac{3}{2}}$ (rather than n^1) power dependence. This is why the curves in Fig. 3 grow much faster than those in Fig. 2 in the asymptotic region of n . Furthermore, we note that the second term in the expansion (4.66) depends on both $n^{\frac{1}{2}}$ and $m_{\hat{f}}$, contrary to (3.49). But, the third term in the expansion of (4.66) is only suppressed by $n^{-\frac{1}{2}}$ (not n^{-1}) and thus can be sizable due to the squared logarithm. For instance, comparing the limits for e^-e^+ and $t\bar{t}$ scatterings and using Eq. (4.65), we obtain, numerically,

$$(E_e^* - E_t^*)_{\text{asym}} \approx \begin{cases} 61.1 \text{ TeV}, & (n = 15), \\ 63.4 \text{ TeV}, & (n = 30), \end{cases} \quad (4.67)$$

which explains why in Fig. 3 the curves are almost parallel for the displayed asymptotic region $15 \lesssim n \leq 30$. Finally, the charm quark has a slightly stronger bound than the tau lepton despite $m_c < m_\tau$ (cf. Fig. 3 and Table 3) because the color factor $N_c = 3$ in (4.61) helps to lower the bound for charm.

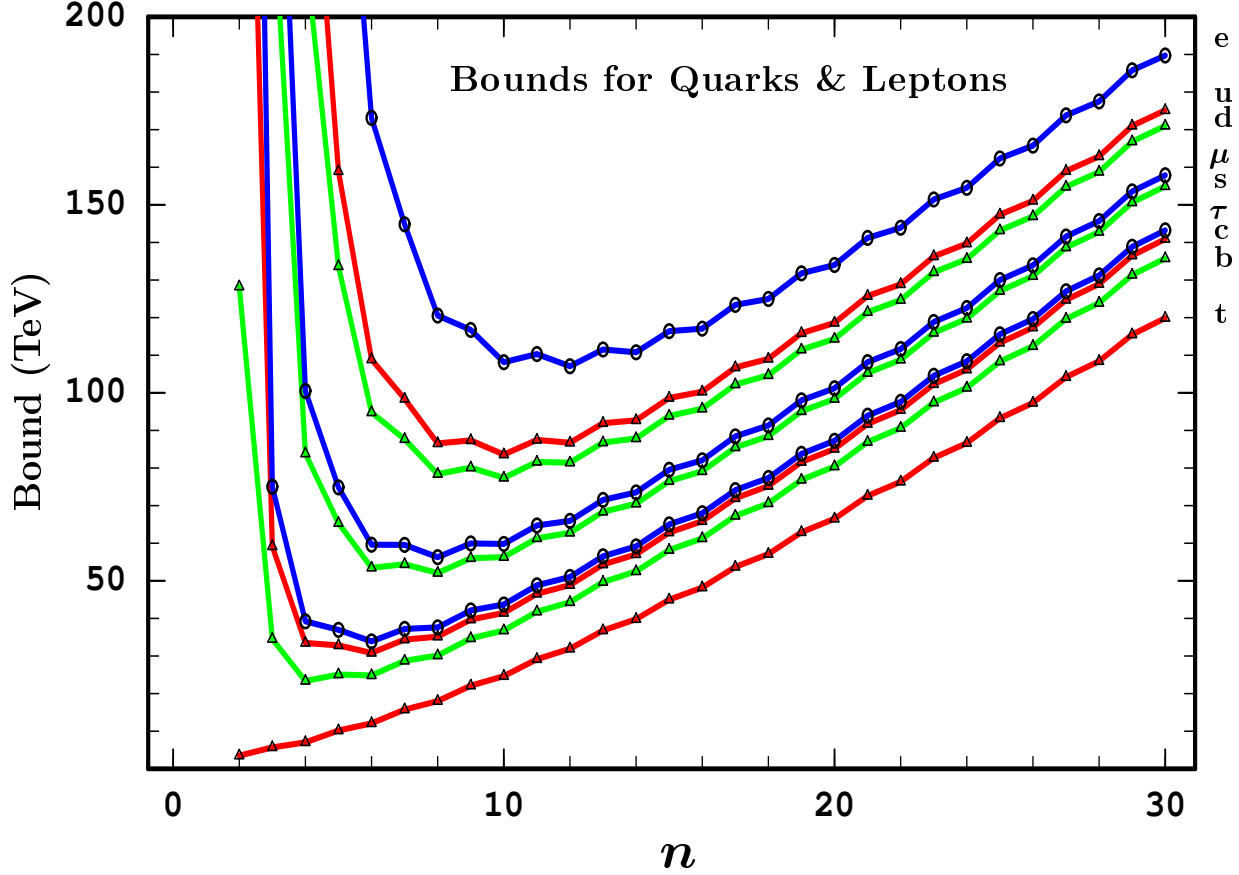


Figure 3: Precise unitarity bound E_f^* based upon Eq.(4.61), for the scattering processes $t\bar{t}, b\bar{b}, c\bar{c}, \tau^-\tau^+, s\bar{s}, \mu^-\mu^+, d\bar{d}, u\bar{u}, e^-e^+ \rightarrow n\pi^a$ (nV_L^a) (curves from bottom to top), as a function of n (≥ 2). For the points with odd n values, the best bounds are actually given by $t_+\bar{b}_+, t_-\bar{b}_-, c_+\bar{s}_+, \tau_+\nu_-, c_-\bar{s}_-, \mu_+\nu_-, u_-\bar{d}_-, u_+\bar{d}_+, e_+\nu_- \rightarrow n\pi^a$ (curves from bottom to top), respectively. Only integer values of n have physical meaning. The curves marked by circles represent bounds for leptons and those marked by triangles are for quarks; also, for clarity, the up-type, down-type quarks and the leptons are plotted in three different colors.

4.2. Model-Dependent Effects from EWSB Sector

As shown in Fig.1(c,d), for $n \geq 3$ the tree-level scattering process $f\bar{f} \rightarrow n\pi^a$ can have additional contributions involving the EWSB sector, i.e., the Goldstone boson self-interaction vertices and the exchange of the new quanta that unitarize the EWSB sector (such as the SM Higgs boson). These contributions depend on the details of the EWSB mechanism and are thus highly model-

dependent. In the following, we will take the simplest EWSB sector of the SM as an explicit example and examine how our universal estimates of the unitarity bounds [based upon the pure contact interactions among fermions and Goldstone bosons in Fig. 1(a)] are affected by the EWSB contributions via Fig. 1(c,d). The diagrams in Fig. 1(a) and (c,d) are of the same $\mathcal{O}(E^1)$ by power counting, so that a contribution of type-(c,d) may affect the amplitude by a factor of $\mathcal{O}(2-3)$ and thus the total cross section by a factor of $[\mathcal{O}(2-3)]^2 \leq \mathcal{O}(10)$. Thus we expect the unitarity bound of Sec. 4.1 to be changed by at most a factor of $[\mathcal{O}(2-3)]^{\frac{1}{(n-1)}}$ ($n \geq 3$) since the n -body phase space integration contributes an energy factor of s^{n-2} (cf. Sec. 3.1-3.2). Numerically the factor $[\mathcal{O}(2-3)]^{\frac{1}{(n-1)}}$ is at most 1.7 (for $n = 3$), and becomes close to unity as n increases above 3. This means that, fortunately, the effect of the EWSB contribution is small for light fermions since their strongest unitarity bounds occur at significantly large n values (cf. Fig. 2-3). The effect for top-quark case is interesting since the analysis based on contact contribution alone shows that the unitarity bound is strongest for $n_s = 2$ and only becomes slightly weaker for $n_s = 3$. Hence, adding the EWSB contribution associated with $t\bar{t} \rightarrow n\pi^a$ ($n \geq 3$) processes could push the location of the minimum unitarity limit up to $n_s = 3$. As explicitly shown below, this is indeed the case, but the improvement in the unitarity bound for all fermions (including the top-quark) is always less than a factor of 2, as expected.

For convenience we first consider the SM with its EWSB sector (Higgs sector) nonlinearly realized. The Higgs-Goldstone fields of the SM can then be formulated as 2×2 matrix,

$$\Phi = (v + h^0)U, \quad U = \exp[i\pi^a \tau^a / v], \quad (4.68)$$

where the physical Higgs field h^0 transforms as a singlet under $SU(2)_L \otimes U(1)_Y$. Correspondingly, the EWSB Lagrangian of the SM takes the form,

$$\mathcal{L}_{\text{EWSB}} = \mathcal{L}_{\Phi}^{\text{kin}} - V(h) = \frac{1}{4} \text{Tr}[(D^\mu \Phi)(D_\mu \Phi)^\dagger] - \frac{\lambda}{4} [(v + h^0)^2 - v^2]^2, \quad (4.69)$$

where $D_\mu \Phi = (\partial_\mu h^0)U + (v + h^0)D_\mu U$ and $D_\mu U$ is defined below Eq. (2.8). The kinematic term $\mathcal{L}_{\Phi}^{\text{kin}}$ can be simplified as

$$\mathcal{L}_{\Phi}^{\text{kin}} = \frac{1}{2}(\partial_\mu h^0)(\partial^\mu h^0) + \frac{1}{4}(v^2 + 2vh^0 + h^{02}) \text{Tr}[(D^\mu U)(D_\mu U)^\dagger]. \quad (4.70)$$

The part $\frac{v^2}{4} \text{Tr}[(D^\mu U)(D_\mu U)^\dagger]$ is the same as Eq. (2.8) and contains the following pure Goldstone

Lagrangian,

$$\begin{aligned}
\mathcal{L}_{\text{GB}} &= \frac{v^2}{4} \text{Tr}[(\partial^\mu U)(\partial_\mu U)^\dagger] \\
&= \frac{1}{2} \partial^\mu \vec{\pi} \cdot \partial_\mu \vec{\pi} + \sum_{n(\text{even})=4}^{\infty} \frac{(-)^{\frac{n}{2}} 2^{n-2}}{n! v^{n-2}} (\vec{\pi} \cdot \vec{\pi})^{\frac{n}{2}-2} \left[(\vec{\pi} \cdot \partial_\mu \vec{\pi})^2 - (\vec{\pi} \cdot \vec{\pi}) (\partial^\mu \vec{\pi} \cdot \partial_\mu \vec{\pi}) \right],
\end{aligned} \tag{4.71}$$

where

$$\begin{aligned}
\vec{\pi} \cdot \vec{\pi} &= 2\pi^+\pi^- + \pi^0\pi^0, \\
(\vec{\pi} \cdot \partial_\mu \vec{\pi})^2 - (\vec{\pi} \cdot \vec{\pi}) (\partial^\mu \vec{\pi} \cdot \partial_\mu \vec{\pi}) \\
&= (\pi^+\partial_\mu \pi^- + \pi^-\partial_\mu \pi^+ + \pi^0\partial_\mu \pi^0)^2 - (2\pi^+\pi^- + \pi^0\pi^0) (2\partial^\mu \pi^+\partial_\mu \pi^- + \partial^\mu \pi^0\partial_\mu \pi^0).
\end{aligned} \tag{4.72}$$

The next crucial step in the SM is to assume that the physical Higgs boson h^0 , in addition to breaking the electroweak gauge symmetry, also couples to the fermions, generating all the fermion masses via the Yukawa interactions, whose strength is given by ratio of the fermion masses $m_{f,f'}$ over the VEV v ,

$$y_f = \sqrt{2} m_f/v, \quad y_{f'} = \sqrt{2} m_{f'}/v. \tag{4.73}$$

Thus the bare fermionic mass-term $-m_f \bar{f}f - m_{f'} \bar{f}'f'$ will be generated from the following gauge-invariant Yukawa Lagrangian of the nonlinearly realized SM,

$$\mathcal{L}_Y^{\text{NL}} = -m_f \left(1 + \frac{h^0}{v}\right) \overline{F_L} U \begin{pmatrix} 1 \\ 0 \end{pmatrix} f_R - m_{f'} \left(1 + \frac{h^0}{v}\right) \overline{F_L} U \begin{pmatrix} 0 \\ 1 \end{pmatrix} f'_R + \text{H.c.} \tag{4.74}$$

The expanded interaction Lagrangian of (4.74) can be directly obtained from Eq. (4.54) by adding an *overall factor* $(1 + h^0/v)$.

The Feynman rules of this nonlinearly realized SM given by Eqs.(4.69) and (4.74) are very different from the usual linearly realized SM. But, as they both share the *same* unitary-gauge Lagrangian, they are actually equivalent and thus both renormalizable. In particular, we note that the above nonlinearly realized Higgs boson couples to the Goldstone fields with two derivatives, similar to the Goldstone self-interaction vertices. This is crucial for maintaining the unitarity of the Goldstone boson scatterings $\pi^{a_1}\pi^{a_2} \rightarrow n\pi^a$ and the fermion-anti-fermion scatterings $f\bar{f} \rightarrow n\pi^a$ in the nonlinear SM. For instance, in the latter case, the energy power counting shows that the contributions of the EWSB sector in Fig.1(c,d) are of the same $\mathcal{O}(E^1)$ as that of the universal contact contributions in Fig.1(a). Hence, the unitarity of the SM will force all $\mathcal{O}(E^1)$ terms in Fig.1(a,c,d) and Fig.1(e) to at least cancel down to $\mathcal{O}(E^0)$, i.e., Fig.1(a) + (c) + (d) + (e) = $\mathcal{O}(E^0)$, or,

$$\text{Fig.1(a) + (c) + (d)} = - \text{Fig.1(e)} + \mathcal{O}(E^0) = \mathcal{O}(E^1). \tag{4.75}$$

Now we will explicitly analyze the unitarity violation for the scattering $f\bar{f}, f\bar{f}' \rightarrow 3\pi^a$ by including the EWSB contributions of the SM [cf. Fig. 1(c+d)], but *without assuming* the Yukawa interactions of the Higgs boson h^0 for fermion mass generation [cf. Fig. 1(e)]. This means that we will only include leading contributions from Fig. 1(a)+(c)+(d) at $\mathcal{O}(E^1)$ [cf. Eq. (4.75)]. Then, we will explicitly show how the contributions from a given type of EWSB mechanism such as that in the SM [cf. Fig. 1(c,d)] could affect the final unitarity bound. We choose the process $f\bar{f}, f\bar{f}' \rightarrow n\pi^a$ with $n = 3$ not only because $n = 3$ is the simplest nontrivial case where the EWSB effect first shows up, but also because the $n = 3$ case is expected to have *the largest EWSB effect* on the unitarity limit, as explained earlier in this subsection.

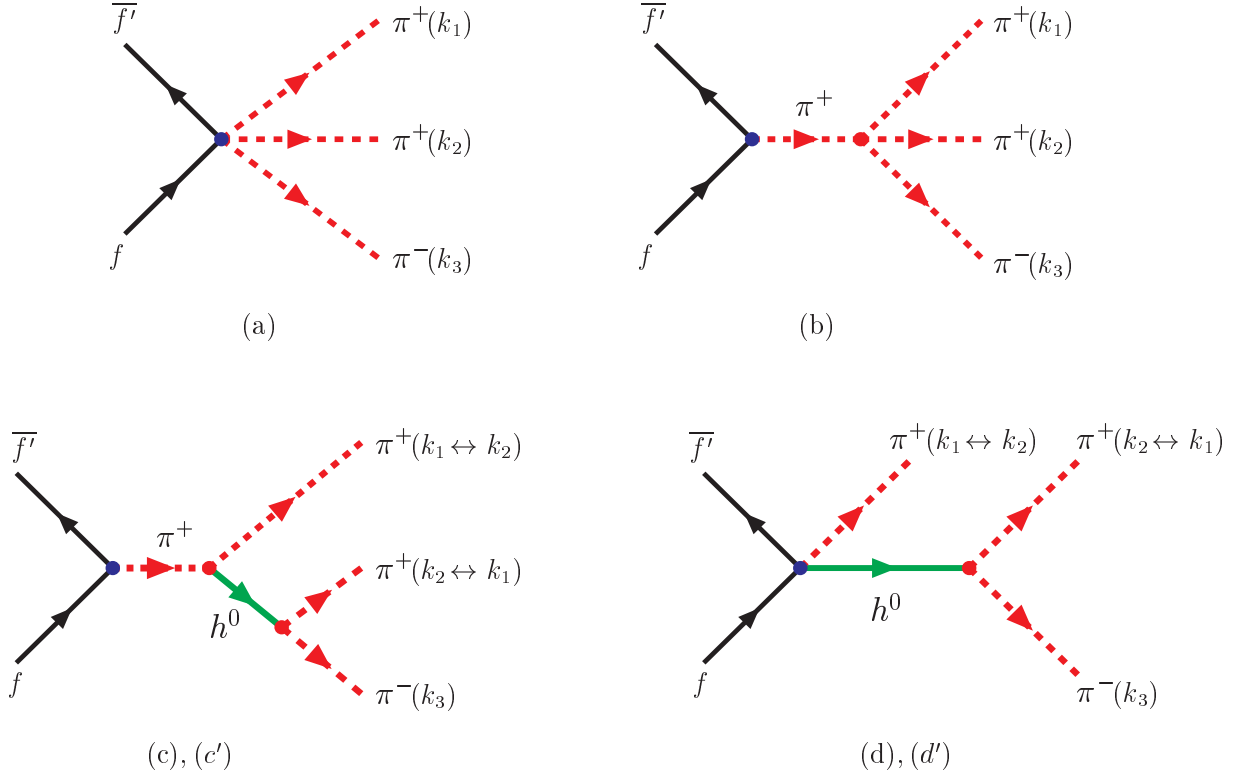


Figure 4: Leading Feynman diagrams of $\mathcal{O}(E^1)$ for the scattering $f\bar{f}' \rightarrow \pi^+\pi^+\pi^-$ in the non-linearly realized SM. (a) Model-independent universal “contact” contribution; (b) s -channel contribution due to the Goldstone boson self-interactions from the SM EWSB sector; (c, c') s -channel contributions due to Higgs-Goldstone boson interactions from the SM EWSB sector; (d, d') Yukawa-type contributions due to the *assumption* that the *same* SM Higgs boson h^0 is responsible for the fermion mass generation.

For the $n = 3$ case, the best unitarity limit comes from the scattering $f\bar{f}' \rightarrow \pi^+\pi^+\pi^-$. The relevant diagrams are explicitly shown in Fig. 4. We see that Fig. 4(a) is the model-independent universal ‘‘contact’’ contribution (studied in Sec. 4.1); Fig. 4(b) is the s -channel contribution from the Goldstone self-interactions in the SM EWSB sector; Fig. 4(c,c') are the s -channel contributions from Higgs-Goldstone interactions in the SM EWSB sector; Fig. 4(d,d') are the Yukawa-type contributions due to the *assumption* that the *same* SM Higgs boson h^0 is responsible for fermion mass generation. We then compute the helicity amplitudes for all the individual contributions in Fig. 4, at the leading $\mathcal{O}(E^1)$,

$$\begin{aligned}
i\mathcal{T} [f_{\pm}\bar{f}'_{\pm} \rightarrow \pi^+\pi^+\pi^-] (a) &= \frac{\sqrt{2}}{v^3} \begin{pmatrix} m_f \\ m_{f'} \end{pmatrix} \left[-\frac{2}{3} \right] \sqrt{s}, \\
i\mathcal{T} [f_{\pm}\bar{f}'_{\pm} \rightarrow \pi^+\pi^+\pi^-] (b) &= \frac{\sqrt{2}}{v^3} \begin{pmatrix} m_f \\ m_{f'} \end{pmatrix} \left[-\frac{1}{3} + \frac{\hat{s}_{12}}{s} \right] \sqrt{s}, \\
i\mathcal{T} [f_{\pm}\bar{f}'_{\pm} \rightarrow \pi^+\pi^+\pi^-] (c + c') &= \frac{\sqrt{2}}{v^3} \begin{pmatrix} m_f \\ m_{f'} \end{pmatrix} \left[\left(\frac{\hat{s}_{23}}{s} - 1 \right) \frac{\hat{s}_{23}}{\hat{s}_{23} - m_H^2} + \left(\frac{\hat{s}_{13}}{s} - 1 \right) \frac{\hat{s}_{13}}{\hat{s}_{13} - m_H^2} \right] \sqrt{s}, \\
i\mathcal{T} [f_{\pm}\bar{f}'_{\pm} \rightarrow \pi^+\pi^+\pi^-] (d + d') &= \frac{\sqrt{2}}{v^3} \begin{pmatrix} m_f \\ m_{f'} \end{pmatrix} \left[\frac{\hat{s}_{23}}{\hat{s}_{23} - m_H^2} + \frac{\hat{s}_{13}}{\hat{s}_{13} - m_H^2} \right] \sqrt{s},
\end{aligned} \tag{4.76}$$

where $\hat{s}_{ij} = (k_i + k_j)^2$ and $s = (k_1 + k_2 + k_3)^2 \simeq \hat{s}_{12} + \hat{s}_{23} + \hat{s}_{13} \gg M_W^2$. Summing up all contributions in (4.76), we arrive at

$$\begin{aligned}
\mathcal{T} [f_{\pm}\bar{f}'_{\pm} \rightarrow \pi^+\pi^+\pi^-]_{\text{SM}} &= (a) + (b) + (c + c') + (d + d') \\
&= -i \frac{\sqrt{2}}{v^3} \begin{pmatrix} m_f \\ m_{f'} \end{pmatrix} \left[\frac{\hat{s}_{23}}{\hat{s}_{23} - m_H^2} + \frac{\hat{s}_{13}}{\hat{s}_{13} - m_H^2} \right] \frac{m_H^2}{\sqrt{s}} = \mathcal{O}\left(\frac{1}{\sqrt{s}}\right),
\end{aligned} \tag{4.77}$$

which means that the corresponding $2 \rightarrow 3$ total cross section will behave as $\mathcal{O}(1/s)$ or smaller. According to the unitarity condition (2.26), the scattering $f_{\pm}\bar{f}'_{\pm} \rightarrow \pi^+\pi^+\pi^-$ is indeed unitary in the SM, as expected. If we *do not assume* the Higgs boson to be responsible for the fermion mass generation, the diagrams in Fig. 4(d)+(d') must be removed, and thus the remaining contributions give

$$\begin{aligned}
\mathcal{T} [f_{\pm}\bar{f}'_{\pm} \rightarrow \pi^+\pi^+\pi^-] &= (a) + (b) + (c + c') \\
&= i \frac{\sqrt{2}}{v^3} \begin{pmatrix} m_f \\ m_{f'} \end{pmatrix} \left[\frac{\hat{s}_{23}}{\hat{s}_{23} - m_H^2} + \frac{\hat{s}_{13}}{\hat{s}_{13} - m_H^2} \right] \sqrt{s} + \mathcal{O}\left(\frac{1}{\sqrt{s}}\right) \\
&= -(d + d').
\end{aligned} \tag{4.78}$$

Finally, we evaluate the total cross section numerically using the leading order amplitude in (4.78) and plot the results in Fig. 5(a)-(d) in comparison with the imposed unitarity condition (2.26).

In this figure, we consider four types of initial helicity states, $f_\lambda \bar{f}'_{\lambda'} \in (t_+ \bar{b}_+, u_+ \bar{d}_+, \tau_-^+ \bar{\nu}_-, e_-^+ \bar{\nu}_-)$, where the corresponding cross sections are proportional to the fermion masses $(m_t^2, m_u^2, m_\tau^2, m_e^2)$, respectively. We have further included the Higgs width in Eq. (4.78) for the actual calculations of Fig. 5, but we see that the effects of the Higgs mass and width are significant only in Fig. 5(a) where the unitarity violation scale occurs around 3 TeV or so; for all other light fermions such effects are almost invisible because the relevant unitarity violation scales are substantially above the largest values of the Higgs boson mass and width. We see that for all cases in Fig. 5 the inclusion of the EWSB contributions makes the cross sections larger for the whole energy range and thus further enhances the unitarity constraints, but the corrections to the bounds are small, around 40 – 50% or so, i.e., always less than about a factor of 2 for the $2 \rightarrow 3$ processes. As explained earlier, with the increasing number $n (> 3)$ of the final state particles, such corrections will become even smaller, approaching unity like $[\mathcal{O}(2 - 3)]^{\frac{1}{n-1}}$. Therefore, we conclude that the estimated unitarity limits based on model-independent, universal “contact” interactions are robust and reliable up to a factor of ~ 2 or much less.

The Fig. 5(a) has another very interesting feature, namely, the inclusion of the EWSB effect pushes the unitarity limit for the scale of the top-quark mass generation down to the region of

$$E^* = 2.8 - 3.3 \text{ TeV}, \quad \text{for } m_H = 115 - 800 \text{ GeV}, \quad (4.79)$$

which is below the best bound derived from the scattering $t\bar{t} \rightarrow 2\pi^a$ in Table 3. So, we see that by including the EWSB contributions (from the minimal SM), the strongest unitarity limit for the scale of the top-quark mass generation occurs at $n = 3$, rather than $n = 2$. Hence, the present unitarity limits from $2 \rightarrow n$ ($n \geq 3$) scattering gives better upper limits on the scale of fermion mass generation than the classic Appelquist-Chanowitz bounds via $2 \rightarrow 2$ scattering, for all known fermions including the top quark!

Finally, we note that in addition to Fig. 4 there are three independent $2 \rightarrow 3$ scattering processes, $f\bar{f} \rightarrow \pi^0 \pi^0 \pi^0$, $\pi^+ \pi^- \pi^0$ and $f\bar{f}' \rightarrow \pi^+ \pi^0 \pi^0$. We have verified the energy cancellation for each of the above amplitudes at $\mathcal{O}(E^1)$ when the complete SM diagrams are included. Furthermore, without assuming the Yukawa interaction of the Higgs boson h^0 for fermion mass generation, we compute

the amplitudes including the contributions from the EWSB sector of the SM. We find, at $\mathcal{O}(E^1)$,

$$\begin{aligned}
\mathcal{T} [f_{\pm} \bar{f}_{\pm} \rightarrow \pi^0 \pi^0 \pi^0] &= i \frac{m_f}{v^3} \left[\frac{\hat{s}_{12}}{\hat{s}_{12} - m_H^2} + \frac{\hat{s}_{23}}{\hat{s}_{23} - m_H^2} + \frac{\hat{s}_{13}}{\hat{s}_{13} - m_H^2} \right] \sqrt{s}, \\
\mathcal{T} [f_{\pm} \bar{f}_{\pm} \rightarrow \pi^+ \pi^- \pi^0] &= i \frac{m_f}{v^3} \left[\frac{\hat{s}_{12}}{\hat{s}_{12} - m_H^2} \right] \sqrt{s}, \\
\mathcal{T} [f_{\pm} \bar{f}'_{\pm} \rightarrow \pi^+ \pi^0 \pi^0] &= i \frac{\sqrt{2}}{v^3} \begin{pmatrix} m_f \\ m_{f'} \end{pmatrix} \left[\frac{\hat{s}_{23}}{\hat{s}_{23} - m_H^2} \right] \sqrt{s}.
\end{aligned} \tag{4.80}$$

Accordingly, we have computed their cross sections numerically and found the unitarity limits for these processes to be always weaker than the limits from $f \bar{f}' \rightarrow \pi^+ \pi^+ \pi^-$.

Before concluding this subsection, we would like to remark that the current analysis only makes the mild restriction that the longitudinal weak boson $V_L^a (= W_L^{\pm}, Z_L^0)$, or its corresponding would-be Goldstone boson $\pi^a (= \pi^{\pm}, \pi^0)$, behaves as a fundamental field below the unitarity violation scale. This includes all supersymmetry (SUSY) or non-SUSY models with fundamental Higgs doublets for the EWSB. There are dynamical models in which V_L^a or π^a is composite but the compositeness scale is very high, around the GUT scale or above. Examples of this kind of theory include the classic minimal top-condensate model [72, 73] and its various viable supersymmetric extensions [74], and more recently the dynamical EWSB models via a neutrino condensate [75]. In these cases the current analysis of the scattering $f \bar{f} \rightarrow n V_L^a (n \pi^a)$ will apply. For the case where V_L^a or π^a is composite at a scale of only a few TeV, we may need other types of processes based on effective higher dimensional fermionic operators (such as $f \bar{f} \rightarrow (f \bar{f})^k$ with $k \geq 1$)²³ for a generic unitarity analysis of the scales of light fermion mass generation.

²³Recent complementary studies [76] analyzed the *low energy* phenomenological constraints on the scale of new physics via generic four-fermion contact interactions involving the leptonic $\tau - \mu$ flavor violation.

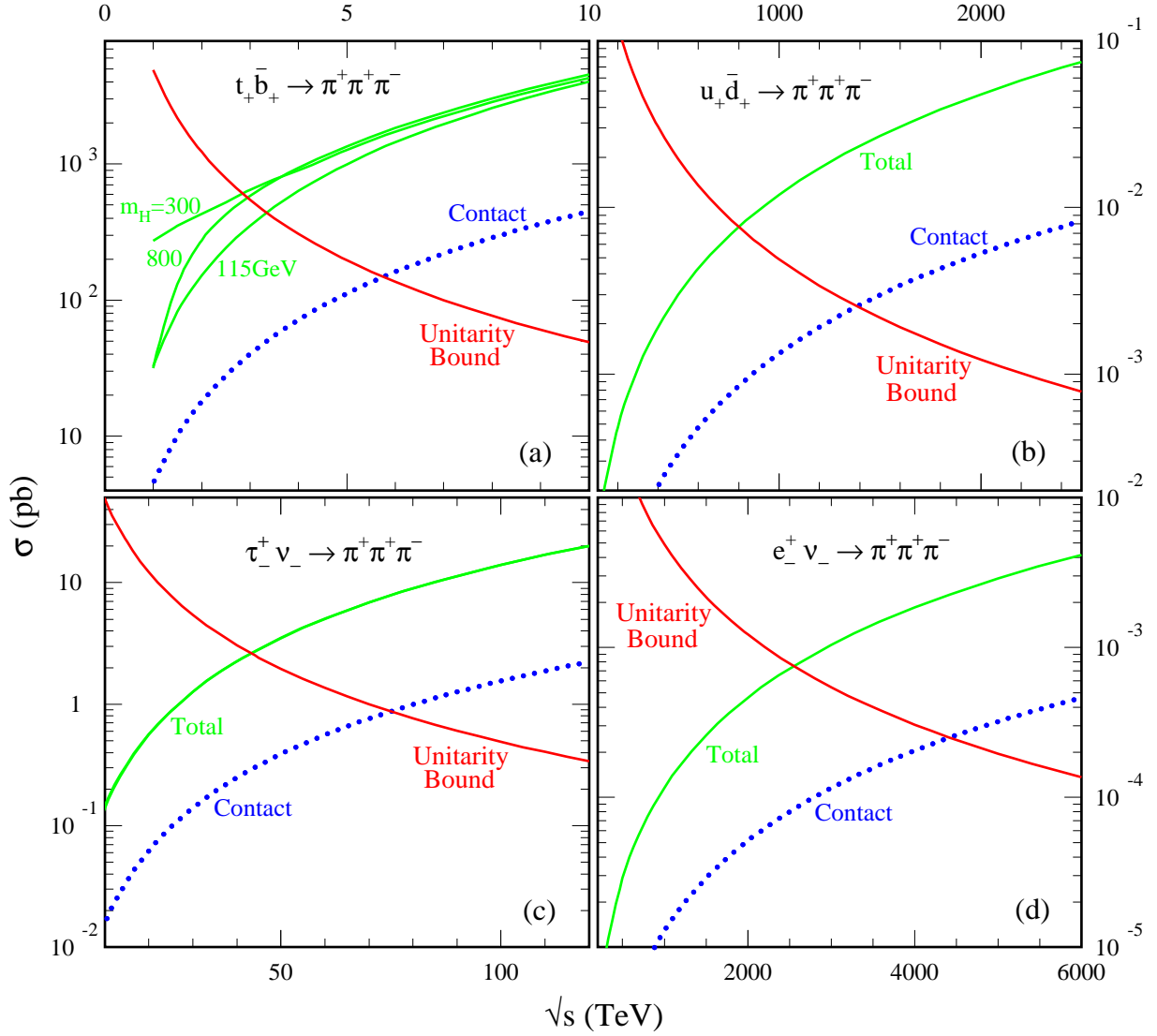


Figure 5: The effect of the SM EWSB sector on the unitarity bound for the scale of fermion mass generation. (a). Same helicity scattering $t_+ \bar{b}_+ \rightarrow \pi^+ \pi^+ \pi^-$: the total cross sections including the contributions from the SM Higgs sector are shown in solid curves, for $m_H = 115, 300, 800$ GeV, respectively. The cross section given by the universal “contact” contribution alone is shown as dotted curve. (b). Same as (a), but for the scattering $u_+ \bar{d}_+ \rightarrow \pi^+ \pi^+ \pi^-$. (c). Same as (a), but for the scattering $\tau_+ \nu_- \rightarrow \pi^+ \pi^+ \pi^-$. (d). Same as (a), but for the scattering $e_+ \nu_- \rightarrow \pi^+ \pi^+ \pi^-$. In all cases, including the contribution of EWSB makes the cross section larger and thus tends to enhance the unitarity limit, but the effect is always less than a factor of two for the current $2 \rightarrow 3$ scattering. Such effects will become even smaller for $2 \rightarrow n$ scattering as n increases above 3.

5. Scale of Mass Generation for Majorana Neutrinos

Parallel to Sec. 4, this section is devoted to a quantitative analysis of the scale of mass generation for Majorana neutrinos. In Sec. 5.1, we will derive the interactions of Majorana neutrinos with weak gauge bosons and Goldstone bosons. Then we systematically analyze the scattering processes $\nu_L \nu_L \rightarrow n\pi^a (nV_L^a)$ and deduce new unitarity limits on the scale of neutrino mass generation. In Sec. 5.2, we discuss the interpretation and implication of our new bounds for the underlying mechanism of neutrino mass generation. Three types of mass mechanisms will be addressed, including the seesaw mechanism [20], the radiative mechanism [21] and the proposal for generating neutrino masses from supersymmetry breaking [77].

5.1. Majorana Masses and Neutrino-Neutrino Scattering

Given the observed particle spectrum of the SM, neutrinos can only have the Majorana mass term, $-\frac{1}{2}m_\nu^{ij}\nu_{Li}^T\widehat{C}\nu_{Lj} + \text{H.c.}$, which violates lepton number by two units. With the nonlinearly realized Goldstone field U [cf. (2.6)], such a dimension-3 bare mass term can be made gauge-invariant but is necessarily nonrenormalizable. As we showed earlier in Eq. (2.10), this uniquely takes the form of the Weinberg operator [19] with the nonlinear field defined as $\Phi = \frac{v}{\sqrt{2}}\overline{\Phi}$ with $\overline{\Phi} = U(0, 1)^T$, i.e.,

$$\mathcal{L}_\nu = -\frac{1}{2}m_\nu^{ij}L_i^{\alpha T}\widehat{C}L_j^\beta\overline{\Phi}^{\alpha'}\overline{\Phi}^{\beta'}\epsilon^{\alpha\alpha'}\epsilon^{\beta\beta'} + \text{H.c.}, \quad (5.81)$$

where $m_\nu^{ij} = \mathcal{C}_{ij}\frac{v^2}{\Lambda}$ is the neutrino Majorana mass derived in Eq. (2.11). The neutrino Majorana mass term allows us to introduce, for convenience, a (real) Majorana neutrino field $\chi (= \chi^c)$ by defining

$$\chi = \frac{1}{\sqrt{2}}(\nu_L + \nu_L^c), \quad (5.82)$$

where $\nu_L = \sqrt{2}P_L\chi$ and $\nu_L^c \equiv (\nu_L)^c = \sqrt{2}P_R\chi$ with $P_{L,R} = \frac{1}{2}(1 \mp \gamma^5)$. Using a properly normalized notation for the lepton doublet $L_j = \left(\frac{1}{\sqrt{2}}\nu_{Lj}, \ell_{Lj}\right)^T$ and the operator (5.81), we arrive at the following kinetic and mass terms for the Majorana neutrino field χ ,

$$\mathcal{L}_\chi^{\text{kin}} = \frac{1}{2}\overline{\chi}_j(i\not{\partial} - m_{\nu j})\chi_j, \quad (5.83)$$

where $m_{\nu j}$ is the j th real mass eigenvalue derived from diagonalizing the symmetric 3×3 mass matrix $\{m_\nu^{ij}\}$. The gauge interactions of χ , which can be deduced from the SM Lagrangian, are

$$\mathcal{L}_\chi^{\text{G}} = -\frac{g}{4c_w}\overline{\chi}_j\gamma^\mu\gamma^5\chi_j Z_\mu^0 - \frac{g}{2\sqrt{2}}\mathbb{V}_{ij}\overline{\ell}_{Li}\gamma^\mu\gamma^5\chi_j W_\mu^- + \text{H.c.}, \quad (5.84)$$

where $c_w = \cos \theta_w$ with θ_w the Weinberg angle, and \mathbb{V}_{ij} is the Maki-Nakagawa-Sakata-Pontecorvo (MNSP) mixing [9] from diagonalizing the lepton and neutrino mass matrices. In this expression, we have used the fact that the Majorana field χ_j has vanishing vector coupling. Despite the difference between the gauge couplings of the Majorana neutrinos and the massless SM-neutrinos, their contributions to the existing physical observables, such as the invisible decay width of Z^0 etc, differ only by a tiny amount of $\mathcal{O}(m_\nu^2/M_Z^2)$. The real test of the Majorana nature of neutrinos has to come from the next generation of neutrinoless double-beta decay experiments.

Comparing the operator (5.81) with the nonlinear Dirac mass term (2.9), we see that (5.81) also appears as dimension-3 but contains two nonlinear U matrices and violates lepton number by two units. Hence, the Feynman rules for the neutrino-Goldstone interactions are different from those in Eq. (2.9) though the relevant vertices always have a contact structure with 2 fermions and n Goldstone fields $\pi^{a_1}\pi^{a_2}\dots\pi^{a_n}$ ($n \geq 1$). It is clear that this does not affect our general power counting for the amplitude $\mathcal{T}[\nu_L\nu_L \rightarrow n\pi^a]$ which takes the same form as $\mathcal{T}[f\bar{f} \rightarrow n\pi^a]$ [cf. Eq. (2.17)]. This is why our estimates in Fig. 2 and Table 1 apply to $\nu_L\nu_L \rightarrow n\pi^a$ scattering as well.

To carry out the quantitative analysis, we deduce from (5.81) the following neutrino-Goldstone interaction Lagrangian, in the neutrino mass-eigenbasis,²⁴

$$\mathcal{L}_{\nu\nu\pi^n}^{\text{Int}} = -\frac{1}{2}m_{\nu j}\bar{\chi}_j[\mathbb{A}(\pi) + i\gamma_5\mathbb{B}(\pi)]\chi_j, \quad (5.85)$$

where $\mathbb{A}(\pi)$ and $\mathbb{B}(\pi)$ are given by

$$\begin{aligned} \mathbb{A}(\pi) &\equiv \Re(U_{22})^2 - 1 = \sum_{n(\text{even})=2}^{\infty} \frac{i^n}{v^n} \left[K_{1,n} 2^{\frac{n}{2}} (\pi^+\pi^-)^{\frac{n}{2}} + \sum_{\ell=0}^{\frac{n}{2}-1} K_{4,n\ell} (\pi^+\pi^-)^\ell (\pi^0)^{n-2\ell} \right], \\ \mathbb{B}(\pi) &\equiv -\Im(U_{22})^2 = \sum_{n(\text{odd})=1}^{\infty} \frac{i^{n-1}}{v^n} K_{2,n} \sum_{\ell=0}^{\frac{n-1}{2}} C_{\frac{n-1}{2}}^\ell 2^\ell (\pi^+\pi^-)^\ell (\pi^0)^{n-2\ell}, \end{aligned} \quad (5.86)$$

and

$$\begin{aligned} K_{1,n} &= \sum_{k=0}^{\frac{n}{2}} \frac{1}{(2k)!(n-2k)!} = \frac{2^{n-1}}{n!}, & (n = \text{even}), \\ K_{2,n} &= \sum_{k=0}^{\frac{n-1}{2}} \frac{n+1}{(2k)!(n-2k-1)!(2k+1)(n-2k)} = \frac{2^n}{n!}, & (n = \text{odd}), \\ K_{3,n} &= \sum_{k=0}^{\frac{n}{2}-1} \frac{1}{(2k)!(n-2k-2)!(2k+1)(n-2k-1)} = \frac{2^{n-1}}{n!}, & (n = \text{even}), \end{aligned} \quad (5.87)$$

²⁴The extension to an initial state like $\ell_i^+\chi_j$ is straightforward.

$$K_{4,n\ell} = 2^\ell \left[K_{1,n} C_{\frac{n}{2}}^\ell + K_{3,n} C_{\frac{n}{2}-1}^\ell \right] = \frac{2^{n+\ell-1}}{n!} \left[C_{\frac{n}{2}}^\ell + C_{\frac{n}{2}-1}^\ell \right], \quad (n = \text{even}),$$

with the notation $C_n^\ell \equiv n! / [\ell! (n - \ell)!]$. Consider the generic scattering process $|\chi_{j\pm} \bar{\chi}_{j\pm}\rangle \rightarrow (\pi^+)^{\ell} (\pi^-)^{\ell} (\pi^0)^{n-2\ell}$ ($\ell = 0, 1, 2, 3, \dots$) for three cases: (a) $n(\text{even}) = 2\ell$; (b) $n(\text{even}) > 2\ell$; (c) $n(\text{odd}) \geq 3$. We compute the helicity amplitudes $\mathcal{T}[\chi_{j\pm} \bar{\chi}_{j\pm}; \ell, \ell, n - 2\ell]$, from the leading contact diagrams [cf. Fig. 1(a)],

$$\begin{aligned} n = \text{even} : \quad \mathcal{T}[\chi_{j\pm} \bar{\chi}_{j\pm}; \frac{n}{2}, \frac{n}{2}, 0] &= \pm i^{n+1} \mathcal{C}_1^\nu \frac{m_{\nu j} \sqrt{s}}{v^n}, \\ \mathcal{T}[\chi_{j\pm} \bar{\chi}_{j\pm}; \ell, \ell, n - 2\ell] &= \pm i^{n+1} \mathcal{C}_2^\nu \frac{m_{\nu j} \sqrt{s}}{v^n}; \\ n = \text{odd} : \quad \mathcal{T}[\chi_{j\pm} \bar{\chi}_{j\pm}; \ell, \ell, n - 2\ell] &= + i^{n+1} \mathcal{C}_3^\nu \frac{m_{\nu j} \sqrt{s}}{v^n}; \end{aligned} \quad (5.88)$$

where the dimensionless coefficients $\mathcal{C}_{1,2,3}^\nu$ are given by

$$\begin{aligned} \mathcal{C}_1^\nu &= 2^{\frac{n}{2}} \left(\frac{n}{2}!\right)^2 K_{1,n}, \\ \mathcal{C}_2^\nu &= 2^\ell (\ell!)^2 (n - 2\ell)! \left[K_{1,n} C_{\frac{n}{2}}^\ell + K_{3,n} C_{\frac{n}{2}-1}^\ell \right], \\ \mathcal{C}_3^\nu &= 2^\ell (\ell!)^2 (n - 2\ell)! C_{\frac{n-1}{2}}^\ell K_{2,n}. \end{aligned} \quad (5.89)$$

We further define the normalized combination for the initial state of Majorana neutrinos with spin-0 (or spin-1),

$$|\text{in}\rangle = \frac{1}{\sqrt{2}} \left[|\chi_{j+} \bar{\chi}_{j+}\rangle \mp |\chi_{j-} \bar{\chi}_{j-}\rangle \right], \quad (5.90)$$

corresponding to the case of $n = \text{even}(\text{odd})$, and find the corresponding S -matrix element

$$\begin{aligned} \mathcal{T}[\text{in}; \ell, \ell, n - 2\ell] &= \frac{1}{\sqrt{2}} \left(\mathcal{T}[\chi_{j+} \bar{\chi}_{j+}; \ell, \ell, n - 2\ell] \mp \mathcal{T}[\chi_{j-} \bar{\chi}_{j-}; \ell, \ell, n - 2\ell] \right) \\ &= \sqrt{2} \mathcal{T}[\chi_{j\pm} \bar{\chi}_{j\pm}; \ell, \ell, n - 2\ell]. \end{aligned} \quad (5.91)$$

This means that the cross section for the initial state $|\text{in}\rangle$ is enhanced by a factor $\sqrt{2}$. Using this we derive the $2 \rightarrow n$ inelastic cross section as

$$\begin{aligned} \sigma[\text{in}; \ell, \ell, n - 2\ell] &= \frac{2C_{0r}^\nu}{2^{4(n-1)} \pi^{2n-3} (n-1)! (n-2)!} \frac{1}{s} \left(\frac{\sqrt{s}}{v} \right)^{2(n-1)} \left(\frac{m_{\nu r}}{v} \right)^2, \\ C_{0r}^\nu &= \frac{(\mathcal{C}_r^\nu)^2}{\varrho} = \frac{(\mathcal{C}_r^\nu)^2}{(\ell!)^2 (n - 2\ell)!}, \quad (r = 1, 2, 3). \end{aligned} \quad (5.92)$$

Finally, with the condition (2.26) and $\varrho_e = 2!$, we derive the inelastic unitarity limit, $\sqrt{s} \leq E_\nu^*$, with

$$E_\nu^* = v \left[\frac{v}{m_{\nu r}} \sqrt{\frac{4\pi}{\mathcal{R}_{\nu r}^{\max}}} \right]^{\frac{1}{n-1}}, \quad (5.93)$$

where $\mathcal{R}_{\nu r}^{\max}$ is given by

$$\begin{aligned}\mathcal{R}_{\nu 1}^{\max} &= \frac{\left(\frac{n!}{2}\right)^2 (K_{1,n})^2}{2^{3n-4} \pi^{2n-3} (n-1)! (n-2)!}, & (n = \text{even}, \ell = \frac{n}{2}), \\ \mathcal{R}_{\nu 2}^{\max} &= \frac{n (K_{1,n} + K_{3,n})^2}{2^{4(n-1)} \pi^{2n-3} (n-2)!}, & (n = \text{even}, \ell < \frac{n}{2}), \\ \mathcal{R}_{\nu 3}^{\max} &= \frac{n (K_{2,n})^2}{2^{4(n-1)} \pi^{2n-3} (n-2)!}, & (n = \text{odd}),\end{aligned}\tag{5.94}$$

and for $n = \text{even}$, the best limits are from $(\mathcal{R}_{\nu 1}^{\max}, \mathcal{R}_{\nu 2}^{\max})_{\max}$. Numerically, we find that the bounds given by $\mathcal{R}_{\nu 1}^{\max}$ and $\mathcal{R}_{\nu 2}^{\max}$ differ very little, always less than 2%.

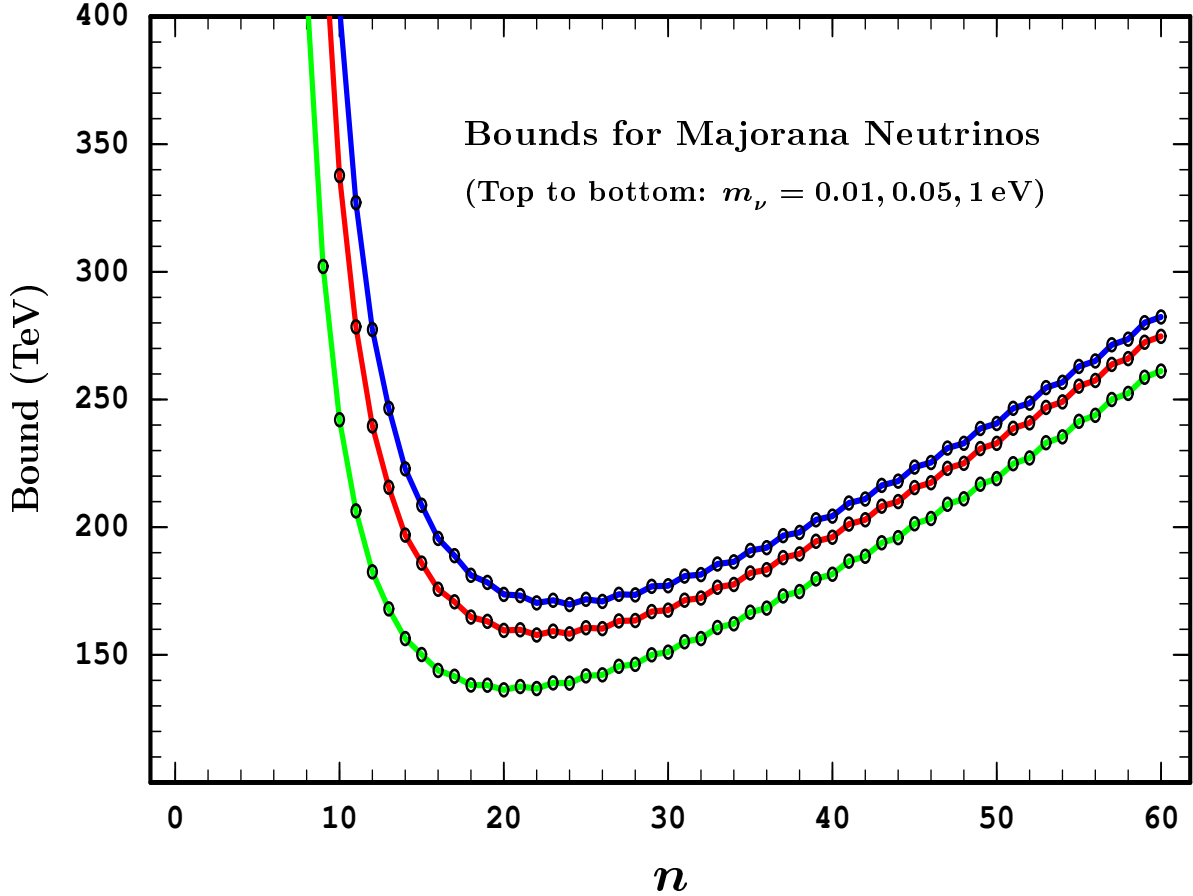


Figure 6: Scales of mass generation for Majorana neutrinos: the precise unitarity bounds E_{ν}^* from Eq. (5.93) are plotted as a function of $n (\geq 2)$, where $m_{\nu j} = 0.01, 0.05, 1 \text{ eV}$ (curves from top to bottom). Only integer values of n have a physical meaning. The minimum point of each curve is given in Eq. (5.95).

With the formulas (5.92)-(5.94), we plot the numerical results of the unitarity limits in Fig. 6 for three typical values of the neutrino masses $m_{\nu j}$. We find that the best unitarity bound in each case to be

$$E_{\min}^* = 136, 158, 170 \text{ TeV}, \quad \text{located at } n = n_s = 20, 22, 24, \quad (5.95)$$

for $m_{\nu j} = 1, 0.05, 0.01 \text{ eV}$, respectively. Under the same input $m_\nu = 0.05 \text{ eV}$, this agrees to our early generic *estimate* (Table 1) within about a factor of 1.7. Comparing Eq. (5.95) with Table 3, it is striking to note that even though the neutrino mass is about ten million times smaller than the electron mass ($m_\nu/m_e \sim 10^{-7}$), the unitarity violation scale associated with its mass generation is only about a factor of 1.3-1.6 higher than that for the electron!²⁵ For neutrinos such an unitarity violation occurs in the multiple $nV_L^a (n\pi^a)$ production with the number $n = n_s = 20 - 24$, while for the electron it appears at $n = n_s = 11$. This leads to an exciting observation that the mass-generation mechanisms for both the electron and neutrinos have to reveal themselves at or below the scale of $\sim 10^2 \text{ TeV}$. The scales for the mass generations of other leptons and light quarks are much lower, as shown in our Table 2 of Section 4. This not only provides an important guideline for model-building, but also indicates where to seek definitive *experimental tests*, such as the relevant astrophysical processes [78].

5.2. Unitarity Violation vs. Mechanisms for Majorana Mass Generation

The unitarity violation scale (2.38) derived from the customary $2 \rightarrow 2$ scattering indicates that the scale of mass generation for Majorana neutrinos could be as high as the GUT scale. At first sight, this sounds quite natural if we note that the traditional seesaw mechanism [23] invokes a heavy right-handed neutrino whose mass is intrinsically tied to the GUT scale. But, knowing there are other low scale mechanisms for neutrino mass generation [21, 77, 79, 80, 81], we then wonder how the unitarity violation limit would just fit into the seesaw mechanism rather than other mechanisms especially since the analysis of unitarity violation is universal, independent of a particular mechanism. Furthermore, now we have shown in Sec. 5.1 that the unitarity violation scale associated with nonzero neutrino mass can be as low as $\mathcal{O}(100) \text{ TeV}$ once we open up the inelastic multiple gauge boson channels for neutrino-neutrino scattering. What is the physics interpretation and implication of our new bounds for the underlying mechanism of neutrino mass generation?

²⁵If we only look at the customary limit from $2 \rightarrow 2$ scattering (cf. Sec. 2.3.2C and Table 2), we would naively expect the mass-generation scale for Majorana neutrinos to be as high as the GUT scale ($\sim 10^{16} \text{ GeV}$). The reason that the scale is substantially lower will be discussed in the following subsection.

We address this issue by analyzing three types of neutrino mass generation mechanisms, including the seesaw mechanism [20], the radiative mechanism [21] and neutrino masses induced from SUSY breaking [77].

5.2.1. Unitarity Violation vs. Seesaw and Radiative Mechanisms

In our unitarity analysis of Majorana neutrinos (cf. Sec. 5.1), we have strictly followed the same logic as for Dirac fermions or weak gauge bosons to define the scale Λ_ν for generating the Majorana mass m_ν , i.e., the scale Λ_ν is the minimal energy at which the *bare Majorana mass term*,

$$\mathcal{L}_\nu^m = -\frac{1}{2}m_\nu^{ij} \nu_{L_i}^T \widehat{C} \nu_{L_j} + \text{H.c.}, \quad (5.96)$$

has to be replaced by a renormalizable interaction [cf. the general definition given above Eq. (2.12)]. A crucial difference between the current study and Refs. [44, 66] for the scale of Majorana neutrino mass generation is that the neutrinos are not assumed to couple to the same Higgs doublet which breaks the electroweak gauge symmetry for their mass generation. We put in the *bare mass terms* by hand for any given type of fermions and derive the corresponding unitarity violation scale as the most general and model-independent limit on their mass generation. For instance, if we replace the nonlinear field Φ in Eq. (2.10) or (5.81) by the usual SM Higgs doublet H , we recover the original Weinberg dimension-5 operator [19] which is *not* a pure mass term even in the unitary gauge and implies the assumption that the SM Higgs doublet actually participates in neutrino mass generation. To see this more clearly consider, for instance, the traditional seesaw mechanism with a heavy singlet Majorana neutrino ν_R [20], which gives the renormalizable Lagrangian²⁶

$$\mathcal{L}_{\text{seesaw}} = -y_j^\nu \bar{L}_j \epsilon H^* \nu_R - \frac{1}{2} M_R \nu_R^T \widehat{C} \nu_R + \text{H.c.}, \quad (5.97)$$

and leads to the dimension-5 Weinberg operator after integrating out the heavy ν_R . Because of the assumption that the SM Higgs doublet H generates the Dirac mass term $-m_{Dj} \bar{\nu}_{Lj} \nu_R$, the resulting dimension-5 Weinberg operator invokes the Higgs H for Majorana neutrino mass generation. But, by our general procedure, we put in this Dirac mass term by hand and replace (5.97) by

$$\mathcal{L}'_{\text{seesaw}} = -m_{Dj} \bar{\nu}_{Lj} \nu_R - \frac{1}{2} M_R \nu_R^T \widehat{C} \nu_R + \text{H.c.}, \quad (5.98)$$

which, after integrating out the heavy ν_R , generates the *bare* Majorana mass term of Eq. (5.96), and can be further made gauge-invariant as in Eq. (5.81) with the nonlinear field $\overline{\Phi}$. Hence, studying the unitarity violation of the scattering $\nu_L \nu_L \rightarrow n\pi^a$ based on a dimension-5 Weinberg operator

²⁶By definition, H has hypercharge $\frac{1}{2}$.

[by integrating out ν_R from (5.97)] *only probes the scale of the singlet mass M_R* which obeys the decoupling theorem [82]²⁷. But the seesaw neutrino mass is really a *combined outcome of both bare mass terms in Eq. (5.98)* which corresponds to the operator (5.81) after integrating out ν_R . Unlike the singlet Majorana mass term for ν_R , the non-singlet Dirac mass term in Eq. (5.98) does not respect the decoupling theorem [82]. Hence, studying the unitarity violation of the scattering $\nu_L\nu_L \rightarrow n\pi^a$ based on (5.81) probes the scale at which the *full* seesaw mechanism (5.98) has to set in. As will be clear below, even though the singlet neutrino ν_R can be still as heavy as Λ_{GUT} , the inelastic $2 \rightarrow n$ unitarity requires the seesaw mechanism to *start* at a scale not much above $\mathcal{O}(\text{TeV})$!

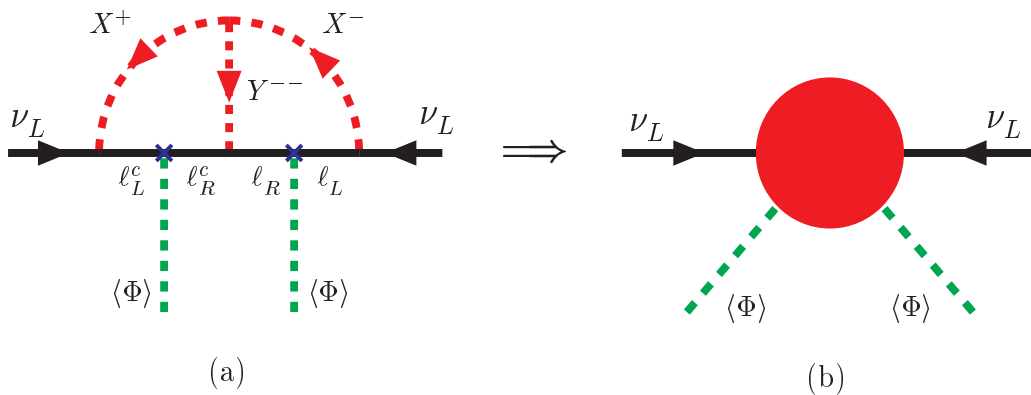


Figure 7: Majorana neutrino masses radiatively generated at a low scale of $\mathcal{O}(\text{TeV}) \lll \Lambda_{\text{GUT}}$. (a) An example of two-loop radiative neutrino mass generation with two extra charged singlet scalars (X^-, Y^{--}). Here the inserted lepton Dirac masses are given by Eq. (2.9). (b) The Majorana neutrino mass contained in the effective mass operator (5.81), after integrating out all heavy scalars (X^-, Y^{--}) from (a).

We further note that the most general operator (5.81) need not necessarily arise from a seesaw mechanism as in Eq. (5.98). It was demonstrated that even without introducing a heavy ν_R , the desired Majorana mass term (5.96) can be generated from a radiative mechanism at the *TeV scale* [21]. An explicit example of a two-loop mechanism [79] for radiative Majorana neutrino mass generation is illustrated in Fig. 7(a). After integrating out the two extra charged singlet scalars (X^-, Y^{--}), this generates an effective Majorana mass term for neutrinos in Fig. 7(b) which is just contained in the operator (5.81). It is very interesting to note that in Fig. 7(a) this two-loop mechanism also connects the Majorana neutrino masses to the lepton Dirac masses given by Eq. (2.9).

²⁷As expected, the resulting unitarity violation scale from the high energy $\frac{1}{2} [|\nu_{L+}\nu_{L+}\rangle - |\nu_{L-}\nu_{L-}\rangle] \rightarrow \frac{1}{2} |Z_L Z_L + hh\rangle$ scattering [44] is, $\frac{4\pi v^2}{m_\nu} \sim 4\pi M_R \sim (10^{15} - 10^{17}) \text{ GeV} \sim \Lambda_{\text{GUT}}$, [cf. Eq. (2.36)], which is 12 – 14 orders of magnitude higher than the weak scale.

The step from Fig. 7(a) to 7(b) of integrating out heavy singlet scalars (X^- , Y^{--}) is fully *parallel to* the derivation of Majorana neutrino masses from the seesaw Lagrangian (5.98) by integrating out the singlet ν_R ! If we consider the special case that the lepton masses are generated by the SM Higgs doublet H , we can replace the two nonlinear Goldstone fields Φ in Fig. 7(a) by H and the corresponding effective neutrino mass operator in Fig. 7(b) is just the original dimension-5 Weinberg operator. Again this is fully parallel to the step of deriving the seesaw neutrino masses from the *renormalizable* Lagrangian (5.97) by integrating out ν_R , which results in the dimension-5 Weinberg operator.

So, once we put in all fermion mass-terms by hand (without making extra model-dependent assumptions about their origins), the Majorana neutrino masses generated either from the seesaw mechanism or from the radiative mechanism can be formulated as the generic effective mass operator (5.81). However, in the seesaw mechanism the new singlet fermion ν_R is known to be as heavy as the GUT scale [20] while the new singlet scalars such as (X^- , Y^{--}) in the radiative mechanism can naturally have masses of $\mathcal{O}(\text{TeV})$ [21]. Then it is intriguing to ask: how does the unitarity violation given by inelastic neutrino scattering $\nu_L \nu_L \rightarrow n\pi^a$ [based on (5.81)] constrain the *new physics scale* for neutrino mass generation? We know that *this limit must be universal, independent of whether the underlying dynamics is a seesaw mechanism or a radiative mechanism*. Starting with the general mass operator (5.81), we thus expect that the optimal bound on the unitarity violation scale should be neither simply fixed by the mass M_R ($\sim \Lambda_{\text{GUT}}$) of ν_R in the seesaw mechanism nor by the masses $M_{X,Y}$ ($\sim \text{TeV}$) of (X^- , Y^{--}) in the radiative mechanism. This is because neither M_R nor $M_{X,Y}$ are the whole story in each mechanism: there has to be additional Dirac mass terms [either the first term in Eq. (5.98) or the lepton mass insertions in Fig. 7(a)] which do not respect the usual decoupling theorem [82]. This non-decoupling feature means either a weak-doublet Higgs or a nonlinear field U has to be invoked to make the Dirac mass term invariant under the SM gauge group, where in the first case the Dirac mass is proportional to the Higgs Yukawa coupling (forbidding the decoupling of the corresponding Higgs scalar), and in the second case the nonlinear U field links the nonrenormalizable Goldstone-fermion coupling to the Dirac mass. In general, such a nondecoupling occurs when we build *any* fermion mass term involving the left-handed $SU(2)_L$ doublet fermion together with (i) a weak singlet fermion (giving a Dirac mass), or, (ii) itself (giving a Majorana mass). Indeed, it is this common non-decoupling feature that forces the unitarity violation scale of Majorana neutrinos to be around $\mathcal{O}(100)$ TeV, substantially below the GUT scale but not much above the scale for electron mass generation despite the fact of $m_\nu/m_e \sim 10^{-7}$.

For the above explicit models of seesaw and radiative neutrino mass generation, this means that

our new limits constrain the new physics scale of the leptonic Higgs Yukawa interaction, which must invoke extra new fields (such as right-handed neutrinos or Zee-scalars or triplet-Higgs) as needed for ensuring renormalizability and generating lepton number violation (although our new bounds do not directly constrain the masses of these new fields themselves which obey the decoupling theorem).

5.2.2. Mass Generation Scale for Majorana Neutrinos in Supersymmetric Theories

Supersymmetry (SUSY) is attractive for stabilizing the weak scale, but does not explain the huge hierarchies in the fermion mass-spectrum or the observed flavor mixings. In fact, it necessarily extends the SM with extra three-family superpartners and thus *adds* new puzzles to the “flavor problem” [83]. Furthermore, similar to the SM, the minimal supersymmetric SM (MSSM) [25] also does not provide nonzero neutrino masses. Therefore, it is important to extend MSSM appropriately to accommodate the massive neutrinos.

5.2.2A. Scale of Mass Generation for Majorana Neutrinos via MSSM Seesaw

A minimal extension of the MSSM, for instance, is to introduce a heavy right-handed singlet neutrino ν_R to form a seesaw mechanism [20]. The MSSM superpotential can thus be generalized to

$$\begin{aligned} W &= W_{\text{MSSM}} + \Delta W \\ &= [H_d L y_e \bar{e} + H_d Q y_d \bar{d} - H_u Q y_u \bar{u} - \mu H_d H_u] + [-H_u L y_\nu \bar{\nu} - \bar{\nu} M_R \bar{\nu}], \end{aligned} \quad (5.99)$$

where $\bar{\nu}$ is a chiral superfield²⁸ containing a right-handed singlet neutrino $\bar{\nu}_R$ and its scalar-partner $\tilde{\nu}_R$, while the other chiral superfields have the same meaning as in MSSM. Integrating out the heavy $\bar{\nu}$ field, we obtain a generic (model-independent) dimension-5 effective operator for the MSSM Lagrangian,

$$\Delta \mathcal{L}_5 = -\frac{m_\nu^{ij}}{v_u^2} L_i^{\alpha T} \hat{C} L_j^\beta H_u^{\alpha'} H_u^{\beta'} \epsilon^{\alpha\alpha'} \epsilon^{\beta\beta'} + \text{H.c.}, \quad (5.100)$$

where $H_u = \left(\phi_u^+, \frac{v_u + \phi_u^0 + ip_u^0}{\sqrt{2}} \right)^T$, $v_u = v \sin \beta$, and $\tan \beta = \langle H_u \rangle / \langle H_d \rangle$. This generates new interactions of the Majorana neutrinos with the Goldstone bosons and Higgs particles,

$$\Delta \mathcal{L}_5^{\nu\nu} = -\frac{m_\nu^{ij}}{2v_u^2} \left(\nu_{Li}^T \hat{C} \nu_{Lj} \right) (H_u)^2 + \text{H.c.} \quad (5.101)$$

²⁸The singlet field $\bar{\nu}$ can expand in flavor space, e.g., one for each family, and the mass M_R then becomes a 3×3 matrix. In fact, the leptogenesis mechanism [84] for explaining the cosmological baryon asymmetry of the universe necessarily requires at least two right-handed neutrinos to ensure the existence of the needed CP-violation phase from the seesaw sector (called minimal neutrino seesaw) [85].

This Lagrangian becomes, in the mass eigenbasis,

$$\Delta\mathcal{L}_5^{\nu\nu} = -\frac{m_{\nu j}}{2}\bar{\chi}_j\chi_j - \frac{m_{\nu j}}{v^2\sin^2\beta}\bar{\chi}_j[\mathbb{C}(H_u) - i\gamma_5\mathbb{D}(H_u)]\chi_j, \quad (5.102)$$

where

$$\begin{aligned} \mathbb{C}(H_u) &= v\sin\beta\phi_u^0 + \frac{1}{2}\left[\phi_u^{02} - p_u^{02}\right], \\ &= vs_\beta(c_\alpha h^0 + s_\alpha H^0) + \frac{1}{2}\left[c_\alpha^2 h^{02} + s_\alpha^2 H^{02} + s_{2\alpha}h^0H^0 - s_\beta^2\pi^{02} - c_\beta^2 A^{02} - s_{2\beta}\pi^0A^0\right], \\ \mathbb{D}(H_u) &= v\sin\beta p_u^0 + \phi_u^0 p_u^0 \\ &= vs_\beta(s_\beta\pi^0 + c_\beta A^0) + [c_\alpha s_\beta\pi^0 h^0 + c_\alpha c_\beta h^0 A^0 + s_\alpha s_\beta\pi^0 H^0 + s_\alpha c_\alpha H^0 A^0], \end{aligned} \quad (5.103)$$

and $(s_\alpha, c_\alpha) \equiv (\sin\alpha, \cos\alpha)$, $(s_\beta, c_\beta) \equiv (\sin\beta, \cos\beta)$ and $(s_{2\alpha}, s_{2\beta}) \equiv (\sin 2\alpha, \sin 2\beta)$. The fields (π^0, π^\pm) and (h^0, A^0, H^0, H^\pm) are would-be Goldstone bosons and physical Higgs scalars, respectively. Here α denotes the usual mixing angle in the neutral Higgs sector of the MSSM [86]. As an important feature of the linearly realized MSSM Higgs sector with fundamental Higgs bosons, we see that the new interactions in (5.102) contain at most two Goldstone/Higgs bosons, involving the neutral (pseudo-)scalars only. This means that the leading amplitudes of high energy Majorana neutrino scattering come from the contact diagrams with a two-body final state, i.e., $n = 2$ [similar to Fig. 1(a)], which are of order E^1 . Hence, the best unitarity limit is expected to be of $O(v^2/m_{\nu j})$, similar to the classic bound derived for the SM case [44]. Also, with (5.102) we immediately deduce the scattering amplitudes

$$\begin{aligned} \mathcal{T}[\chi_{j\pm}\bar{\chi}_{j\pm} \rightarrow W_L^+W_L^-] &= -\mathcal{T}[\chi_{j\pm}\bar{\chi}_{j\pm} \rightarrow \pi^+\pi^-] = 0 + \mathcal{O}(E^0), \\ \mathcal{T}[\chi_{j\pm}\bar{\chi}_{j\pm} \rightarrow H^+H^-] &= 0 + \mathcal{O}(E^0), \end{aligned} \quad (5.104)$$

whose leading order behavior only starts at $\mathcal{O}(E^0)$, and is due to the exchange of t channel charged leptons. Comparing the first amplitudes in (5.104) and (2.37), we note that the reason that $\mathcal{T}[\chi_{j\pm}\bar{\chi}_{j\pm} \rightarrow W_L^+W_L^-]$ vanishes at $\mathcal{O}(E^1)$ in the present case is due to the cancellation from the s -channel Higgs contribution which is absent in (2.37) where we did not assume, *a priori*, the Higgs Yukawa interactions for the neutrino mass generation. In (5.104), the absence of a residual $\mathcal{O}(E^1)$ contribution to the $W_L^+W_L^-$ channel becomes evident by inspecting the corresponding Goldstone amplitude $\mathcal{T}[\chi_{j\pm}\bar{\chi}_{j\pm} \rightarrow \pi^+\pi^-]$ and the interaction Lagrangian (5.102).

For the current analysis of the Majorana neutrino scattering into Higgs/Goldstone boson pairs in the MSSM, it is clear that the relevant scattering energy is at the GUT scale. So it is safe to

ignore all the masses of the final state Higgs bosons, and accordingly the mixing angle α in the neutral Higgs mass matrix. Under this massless limit, we have $\phi_u^0 \simeq h^0$. Also, we will consider the parameter region with moderate to large $\tan\beta \sim 10 - 50$ in the discussion below, which implies $s_\beta \geq 0.995 \simeq 1$ and $c_\beta \leq 10^{-1} \ll 1$ so that $p_u^0 \simeq \pi^0$. Thus, for estimating the optimal unitarity limit, it suffices to set $c_\beta \approx 0$. With these we see that the interactions in (5.102) are greatly simplified and reduce to the case of one Higgs doublet,

$$\Delta\mathcal{L}_{5\text{int}}^{\nu\nu} \simeq -\frac{m_{\nu j}}{v^2} \bar{\chi}_j \left[\left(v h^0 + \frac{1}{2} (h^{02} - \pi^{02}) \right) - i\gamma_5 (v\pi^0 + \pi^0 h^0) \right] \chi_j. \quad (5.105)$$

From this we compute the leading amplitudes,

$$\begin{aligned} \mathcal{T} \left[\chi_{j\pm} \bar{\chi}_{j\pm} \rightarrow \frac{1}{\sqrt{2}} Z_L Z_L \right] &= -\mathcal{T} \left[\chi_{j\pm} \bar{\chi}_{j\pm} \rightarrow \frac{1}{\sqrt{2}} \pi^0 \pi^0 \right] \simeq \pm \frac{\sqrt{2} m_{\nu j}}{v^2} \sqrt{s}, \\ \mathcal{T} \left[\chi_{j\pm} \bar{\chi}_{j\pm} \rightarrow \frac{1}{\sqrt{2}} h^0 h^0 \right] &\simeq \pm \frac{\sqrt{2} m_{\nu j}}{v^2} \sqrt{s}, \\ \mathcal{T} \left[\chi_{j\pm} \bar{\chi}_{j\pm} \rightarrow \frac{1}{\sqrt{2}} Z_L h^0 \right] &= -i \mathcal{T} \left[\chi_{j\pm} \bar{\chi}_{j\pm} \rightarrow \pi^0 h^0 \right] \simeq + \frac{2 m_{\nu j}}{v^2} \sqrt{s}. \end{aligned} \quad (5.106)$$

To derive the optimal unitarity limit, it is desirable to consider the scattering in the spin-singlet channel with a normalized final state, $\frac{1}{\sqrt{2}} [|\chi_{j+} \bar{\chi}_{j+}\rangle - |\chi_{j-} \bar{\chi}_{j-}\rangle] \rightarrow \frac{1}{2} [|Z_L Z_L\rangle + |h^0 h^0\rangle]$. Evaluating the corresponding s -wave unitarity limit gives,

$$E_\nu^* < \frac{4\pi v^2}{m_{\nu j}}, \quad (5.107)$$

which is at the GUT scale, in agreement with the bound mentioned below Eq. (2.36).

It is no surprise that the MSSM unitarity limit (5.107) on the scale of Majorana neutrino mass generation from the Weinberg operator (5.100) is as high as the GUT scale. This is because the nonrenormalizability of the dimension-5 operator (5.100) arises solely from integrating out the heavy right-handed singlet neutrino ν_R which obeys the decoupling theorem. The other part of the neutrino seesaw sector is the Dirac mass term m_D , which is already generated from the renormalizable Yukawa interactions with the fundamental Higgs doublet H_u . As a result, the MSSM Higgs doublet H_u does participate in the neutrino mass generation, and therefore *the minimal scale of the mass generation for Majorana neutrinos in the MSSM is already known and is partly set by the Higgs masses of $\mathcal{O}(v)$, which are extremely low and right at the weak scale!* This is why including a fundamental Higgs doublet in the dimension-5 operator (5.100) causes unitarity violations at the GUT scale which could be saturated only by the heavy right-handed singlet neutrino ν_R . In the next subsection we will provide an interesting counter example showing that invoking the SUSY breaking sector for the

neutrino mass generation would even allow the right-handed neutrino mass M_R to be as low as the weak scale and thereby evade the bound (5.107).

5.2.2B. Unitarity Violation vs. SUSY Breaking Induced Neutrino Masses

In addition to the SUSY flavor problem mentioned earlier, the MSSM further suffers a conceptual μ -problem, namely, the supersymmetric μ parameter in (5.99) is expected to be at the Planck scale (M_{Pl}) which contradicts the original motivation of stabilizing the Higgs mass at the weak scale. A resolution of this is to invoke a global symmetry \mathbb{G} which forbids the vector-like mass term $H_d H_u$ and is broken only by the SUSY breaking sector. In fact, both the supersymmetric μ and M_R terms in Eq. (5.99) are bi-linear and invariant under the SM gauge group, so we wonder why the same suppression mechanism would not simultaneously keep both of them around the weak scale. This motivates the recent proposal of generating small neutrino masses from SUSY breaking [77]. For the current discussion, we will analyze a variation of the model in [77] and effectively generate both a dynamical μ -term and a seesaw mechanism at the weak scale. Consider that the SUSY breaking comes from a hidden sector at an intermediate scale $\mathbf{m}_1 \approx \sqrt{v M_{\text{Pl}}}$ via fields \mathfrak{B} with $\langle \mathfrak{B} \rangle_F = F \approx \mathbf{m}_1^2 \approx v M_{\text{Pl}}$ and $\langle \mathfrak{B} \rangle_A = \sqrt{F} \approx \mathbf{m}_1$. The SUSY breaking is communicated to the SM via the gravitational interaction so that the effective theory is cut off at the scale $\Lambda \approx M_{\text{Pl}}$. Then, take a subset of fields $X, Y \in \mathfrak{B}$, which, together with the field \bar{n} in the visible sector, are charged under \mathbb{G} . Thus, the μ -term itself is forbidden by \mathbb{G} , but can be dynamically generated from the SUSY-breaking operator

$$\frac{1}{\Lambda} [X^2 H_d H_u]_F, \quad (5.108)$$

leading to the dynamical μ -parameter,

$$\mu \approx \frac{\langle X \rangle_A^2}{\Lambda} \approx \frac{\mathbf{m}_1^2}{\Lambda} \approx \frac{\mathbf{m}_1^2}{M_{\text{Pl}}} \approx v. \quad (5.109)$$

Similarly, there are additional operators associated with \bar{n} , which contribute the following Lagrangian terms,

$$\Delta \mathcal{L} = -\frac{c_1}{\Lambda} [Y^\dagger \bar{n} \bar{n}]_D - \frac{c_2}{\Lambda} [Y H_u L \bar{n}]_F + \text{H.c.} \quad (5.110)$$

The operators (5.108) and (5.110) can be justified from the R -symmetry under which (X, Y, \bar{n}) have charges $(1, \frac{4}{3}, \frac{2}{3})$ and L and H_u are R -singlets. In (5.110) we could have additional operators involving the X fields but they are suppressed by higher powers of $1/\Lambda$. A proper superpotential in the hidden sector will ensure that (X, Y) develop VEVs for their F and A components, i.e., $\langle X \rangle_F = \langle Y \rangle_F = F \approx v M_{\text{Pl}} \approx (10^{10} \text{ GeV})^2$ and $\langle X \rangle_A = \langle Y \rangle_A = \sqrt{F}$. Now, the first term in

(5.110) generates a weak-scale Majorana mass for \bar{n} , $M_R \approx F/\Lambda \approx F/M_{\text{Pl}} \approx v$, while its second term gives the Dirac mass term $m_D \approx v\sqrt{F}/\Lambda \approx v\sqrt{vM_{\text{Pl}}}/M_{\text{Pl}} \approx \sqrt{v^3/M_{\text{Pl}}} = \mathcal{O}(\text{keV})$. Hence, a non-canonical seesaw mechanism occurs at tree-level,

$$\mathcal{M}_\nu \approx \begin{pmatrix} 0 & \frac{v\sqrt{F}}{\Lambda} \\ \frac{v\sqrt{F}}{\Lambda} & \frac{F}{\Lambda} \end{pmatrix}, \quad \Rightarrow \quad \mathcal{M}_\nu^{\text{diag}} = \begin{pmatrix} \mathcal{O}\left(\frac{v^2}{\Lambda}\right) & 0 \\ 0 & \mathcal{O}(v) \end{pmatrix}, \quad (5.111)$$

which predicts a right-handed singlet neutrino ν_R at the weak-scale in addition to the conventional seesaw Majorana masses of $\mathcal{O}\left(\frac{v^2}{\Lambda}\right)$ for the active neutrinos. The light seesaw mass is retained in a nontrivial way: the global symmetry \mathbb{G} properly suppresses both the Dirac mass m_D and Majorana mass M_R simultaneously. Now, we can re-analyze the unitarity violation limit from Majorana neutrino scattering $\bar{\chi}\chi \rightarrow V_L^a V_L^a$ in the effective theory with \bar{n} “integrated out”. Since the effective Lagrangian remains the same as Eq. (5.100) in Sec. 5.2.2A, we find the unitarity violation scale to be still as high as the GUT scale, despite the fact that the right-handed ν_R mass is actually at the weak scale. Indeed, such a SUSY induced neutrino mass mechanism has a “screening” feature that *hides* the real neutrino mass generation scale to well below that revealed from the unitarity violation of high energy neutrino-neutrino scattering²⁹. However, since the ν_R is so light, the most effective way to probe the scale of neutrino mass generation in this scenario is by the *direct production* of ν_R and its scalar-partner $\tilde{\nu}_R$, which can be the LSP (lightest supersymmetric particle), and has unconventional predictions for cold dark matter³⁰ and for the collider signatures of Higgs bosons [77].

²⁹This “seesaw screening” occurs at tree level rather than loop level, unlike Veltman’s screening theorem [87] for the SM Higgs sector.

³⁰Ref. [88] also analyzed a model similar to [77] for TeV-scale resonant leptogenesis.

6. On the Scale of Electroweak Symmetry Breaking

The weak gauge bosons V_L^a ($= W^\pm, Z^0$) have the bare mass term, $M_W^2 W^{+\mu} W_\mu^- + \frac{1}{2} M_Z^2 Z^\mu Z_\mu$, which can be made gauge-invariant by the dimension-2 nonlinear operator of the Goldstone kinetic term in Eq. (2.8) and is necessarily nonrenormalizable. The unitarity violation in the high energy scattering $V_L^{a_1} V_L^{a_2} \rightarrow n V_L^a$ ($n \geq 2$) can be conveniently analyzed in the corresponding Goldstone boson scattering $\pi^{a_1} \pi^{a_2} \rightarrow n \pi^a$ according to the equivalence theorem (ET). The power counting method in Sec. 2.2 shows that the amplitude for this $2 \rightarrow n$ scattering behaves as $\mathcal{O}\left(\frac{E^2}{v^n}\right)$, where the E -power dependence is independent of the number of external lines [cf. Eq. (2.17)].

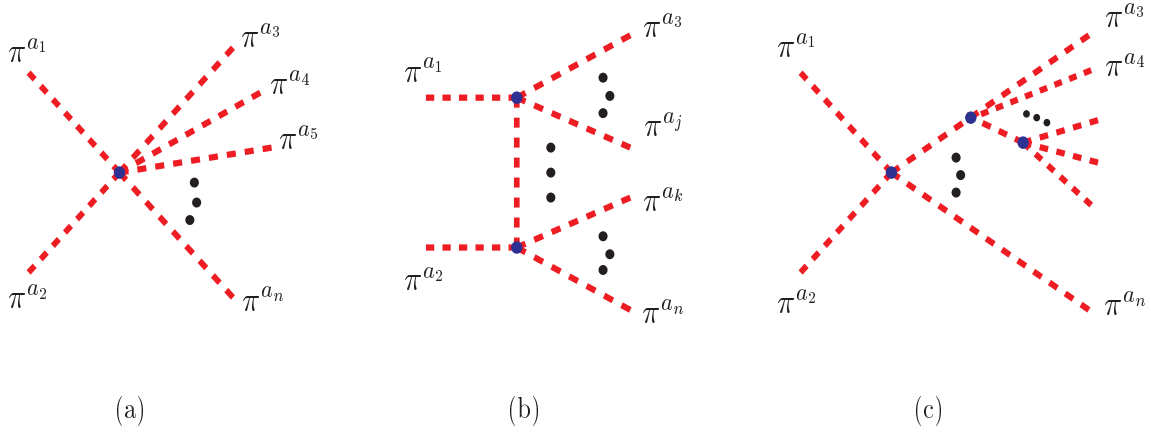


Figure 8: Illustration of the relevant Feynman diagrams for the scattering amplitudes of $\pi^{a_1} \pi^{a_2} \rightarrow n \pi^a$ ($n \geq 4$) which are of $\mathcal{O}(E^2/v^n)$. (a) The “contact” diagrams; (b) the “ $t(u)$ -channel” type diagrams; (c) the “jet-like” diagrams.

For a quantitative analysis, we derive the pure Goldstone Lagrangian from Eq. (2.8) and arrive at

$$\mathcal{L}_\pi = \frac{1}{2} \partial^\mu \vec{\pi} \cdot \partial_\mu \vec{\pi} + \sum_{n(\text{even})=4}^{\infty} \frac{(-)^{\frac{n}{2}} 2^{n-2}}{n! v^{n-2}} (\vec{\pi} \cdot \vec{\pi})^{\frac{n}{2}-2} \left[(\vec{\pi} \cdot \partial_\mu \vec{\pi})^2 - (\vec{\pi} \cdot \vec{\pi}) (\partial^\mu \vec{\pi} \cdot \partial_\mu \vec{\pi}) \right], \quad (6.112)$$

where

$$\begin{aligned} \vec{\pi} \cdot \vec{\pi} &= 2\pi^+ \pi^- + \pi^0 \pi^0, \\ (\vec{\pi} \cdot \partial_\mu \vec{\pi})^2 - (\vec{\pi} \cdot \vec{\pi}) (\partial^\mu \vec{\pi} \cdot \partial_\mu \vec{\pi}) &= (\pi^+ \partial_\mu \pi^- + \pi^- \partial_\mu \pi^+ + \pi^0 \partial_\mu \pi^0)^2 - (2\pi^+ \pi^- + \pi^0 \pi^0) (2\partial^\mu \pi^+ \partial_\mu \pi^- + \partial^\mu \pi^0 \partial_\mu \pi^0). \end{aligned} \quad (6.113)$$

The cancellation of $(\pi^0)^4$ terms in the second equation of (6.113) explicitly shows that all vertices of type $(\pi^0)^n$ ($n \geq 4$) in (6.112) are absent, implying that the scattering process $\pi^0\pi^0 \rightarrow n\pi^0$ ($n \geq 2$) is forbidden at the tree-level. Note that in Eq.(6.112) each interaction vertex contains an even number of Goldstone fields³¹. In contrast to the $2 \rightarrow 2$ scattering discussed earlier in Sec.2.3.2A, the scattering $\pi^{a_1}\pi^{a_2} \rightarrow n\pi^a$ ($n \geq 4$) contains additional non-contact Feynman diagrams as shown in Fig.8(b)-(c), which all have the same leading E^2 power dependence. This greatly complicates the calculation of the cross sections so that a numerical evaluation becomes necessary. Other contributions with internal gauge boson exchanges are at most of $\mathcal{O}(g^2/v^{n-2})$ so that they do not threaten unitarity and thus are not shown in Fig.8.

To study the $2 \rightarrow 4$ scattering, the relevant Goldstone interaction Lagrangian is,

$$\mathcal{L}_\pi^{\text{Int}}[n \leq 6] = \left[\frac{1}{6v^2} - \frac{1}{45v^4} (\vec{\pi} \cdot \vec{\pi}) \right] \left[(\vec{\pi} \cdot \partial_\mu \vec{\pi})^2 - (\vec{\pi} \cdot \vec{\pi}) (\partial^\mu \vec{\pi} \cdot \partial_\mu \vec{\pi}) \right]. \quad (6.114)$$

From (6.114), we consider all possible $2 \rightarrow 4$ scatterings, classified into four types according to their initial states:

$$\begin{aligned} \pi^0\pi^0 &\rightarrow \pi^0\pi^0\pi^0\pi^0 && \text{(absent at tree level),} \\ &\rightarrow \pi^0\pi^0\pi^+\pi^-, \\ &\rightarrow \pi^+\pi^+\pi^-\pi^- && (\checkmark); \\ \pi^+\pi^- &\rightarrow \pi^0\pi^0\pi^0\pi^0, \\ &\rightarrow \pi^+\pi^-\pi^0\pi^0 && (\checkmark), \\ &\rightarrow \pi^+\pi^+\pi^-\pi^-; && (6.115) \\ \pi^\pm\pi^0 &\rightarrow \pi^\pm\pi^0\pi^0\pi^0, \\ &\rightarrow \pi^\pm\pi^+\pi^-\pi^0 && (\checkmark); \\ \pi^\pm\pi^\pm &\rightarrow \pi^\pm\pi^\pm\pi^0\pi^0, \\ &\rightarrow \pi^\pm\pi^\pm\pi^+\pi^- && (\checkmark); \end{aligned}$$

where among each type of processes, the one which has the largest cross section is marked by \checkmark and accordingly, shown in Fig.9(a). In our numerical calculation, each incoming/outgoing Goldstone boson field π^a is put on the mass-shell of its corresponding longitudinal weak boson V_L^a . In Fig.9(a), we also depict the corresponding unitarity bound based on Eq.(2.26). We see that among all processes the channel $\pi^0\pi^0 \rightarrow \pi^+\pi^+\pi^-\pi^-$ gives the largest cross section and thus the best unitarity bound,

$$E^* = 3.9 \text{ TeV}. \quad (6.116)$$

In this channel, we observe that the contribution from the contact graph is about a factor of $1/(2-3)$ of that from the non-contact graphs, and their interference is negative so that the total cross section

³¹This is why in our early estimate of Fig.2 only the even n values are marked for the unitarity bound on the scattering $V_L^{a_1}V_L^{a_2} \rightarrow nV_L^a$.

is smaller than the contact contribution by about a factor of 2–3. But, from Fig. 9(b) we see that the inclusion of all non-contact graphs only weakens the unitarity bound slightly, from $E^* = 3.6$ TeV to $E^* = 3.9$ TeV. This shows that using contact graphs alone can provide a good estimate of the unitarity bound even when the non-contact contributions have the same energy-power dependence. This is due to the fact that an $\mathcal{O}(1)$ correction to the cross section of the $\pi^{a_1}\pi^{a_2} \rightarrow n\pi^a$ scattering only affects the unitarity bound by a factor of $[\mathcal{O}(1)]^{\frac{1}{2n}}$ [cf. Eq.(3.46)], which approaches unity as n becomes much larger than 2. Finally, we may expect to derive a stronger bound by considering the isospin singlet channel, $I = 0$. For the initial state, the $I = 0$ combination is given by $|0_i\rangle = \frac{1}{\sqrt{3}} \sum_a |\pi^a \pi^a\rangle$. For the $4\pi^a$ final state, using the Clebsch-Gordan algebra we derive the following $I = 0$ combination,

$$|0_f\rangle = \frac{1}{\sqrt{120}} [4|\pi^+\pi^+\pi^-\pi^-\rangle + 4|\pi^+\pi^-\pi^0\pi^0\rangle + |\pi^0\pi^0\pi^0\pi^0\rangle]. \quad (6.117)$$

Thus the scattering amplitude $\mathcal{T}[0]$ for the $I = 0$ channel is given by

$$\begin{aligned} \mathcal{T}[0] = \langle 0_f | \mathcal{T} | 0_i \rangle = \frac{1}{6\sqrt{10}} (8\mathcal{T}[+-, ++--] + 8\mathcal{T}[+-, +-00] + 2\mathcal{T}[+-, 0000] \\ + 4\mathcal{T}[00, ++--] + 4\mathcal{T}[00, +-00] + \mathcal{T}[00, 0000]), \end{aligned} \quad (6.118)$$

where $\mathcal{T}[00, 0000] = 0$ at tree-level. The corresponding cross section of the $I = 0$ channel is given by, for $s \gg M_{W,Z}^2$,

$$\sigma[0] = \frac{1}{2s} \int_{\text{PS}_4} |\mathcal{T}[0]|^2. \quad (6.119)$$

A rough estimate would be to simply take the first five individual amplitudes in Eq.(6.118) to be equal, say to the one with the largest value, $\pi^0\pi^0 \rightarrow \pi^+\pi^+\pi^-\pi^-$. Then, we would have $\mathcal{T}[0] \sim \frac{13}{3\sqrt{10}} \mathcal{T}[00, ++--] \simeq 1.37 \mathcal{T}[00, ++--]$, which implies

$$\begin{aligned} \sigma[0] &\sim \frac{1}{2s} \int_{\text{PS}_4} |1.37 \mathcal{T}[00, ++--]|^2 \\ &= 1.37^2 \times 2!^2 \times \sigma[00, ++--] \simeq 7.5 \sigma[00, ++--], \end{aligned} \quad (6.120)$$

where the factor $2!^2$ is due to the conversion of the phase space integration into the channel $\pi^0\pi^0 \rightarrow \pi^+\pi^+\pi^-\pi^-$ which contains two pairs of identical particle in the final state. Hence, the above estimated enhancement factor 7.5 indicates a reduction of the unitarity bound of $\pi^0\pi^0 \rightarrow \pi^+\pi^+\pi^-\pi^-$ channel by factor of $(1/7.5)^{\frac{1}{2n}} = (1/7.5)^{\frac{1}{8}} \simeq 0.78$. We see that the estimated unitarity bound for the singlet $I = 0$ channel is about $3.9 \times 0.78 \simeq 3.0$ TeV which, as expected, is only slightly stronger than that of the best individual channel $\pi^0\pi^0 \rightarrow \pi^+\pi^+\pi^-\pi^-$ shown in Fig. 9(a).

Thus, a further precise numerical calculation of the cross section $\sigma[0]$ is expected not to change the conclusion.

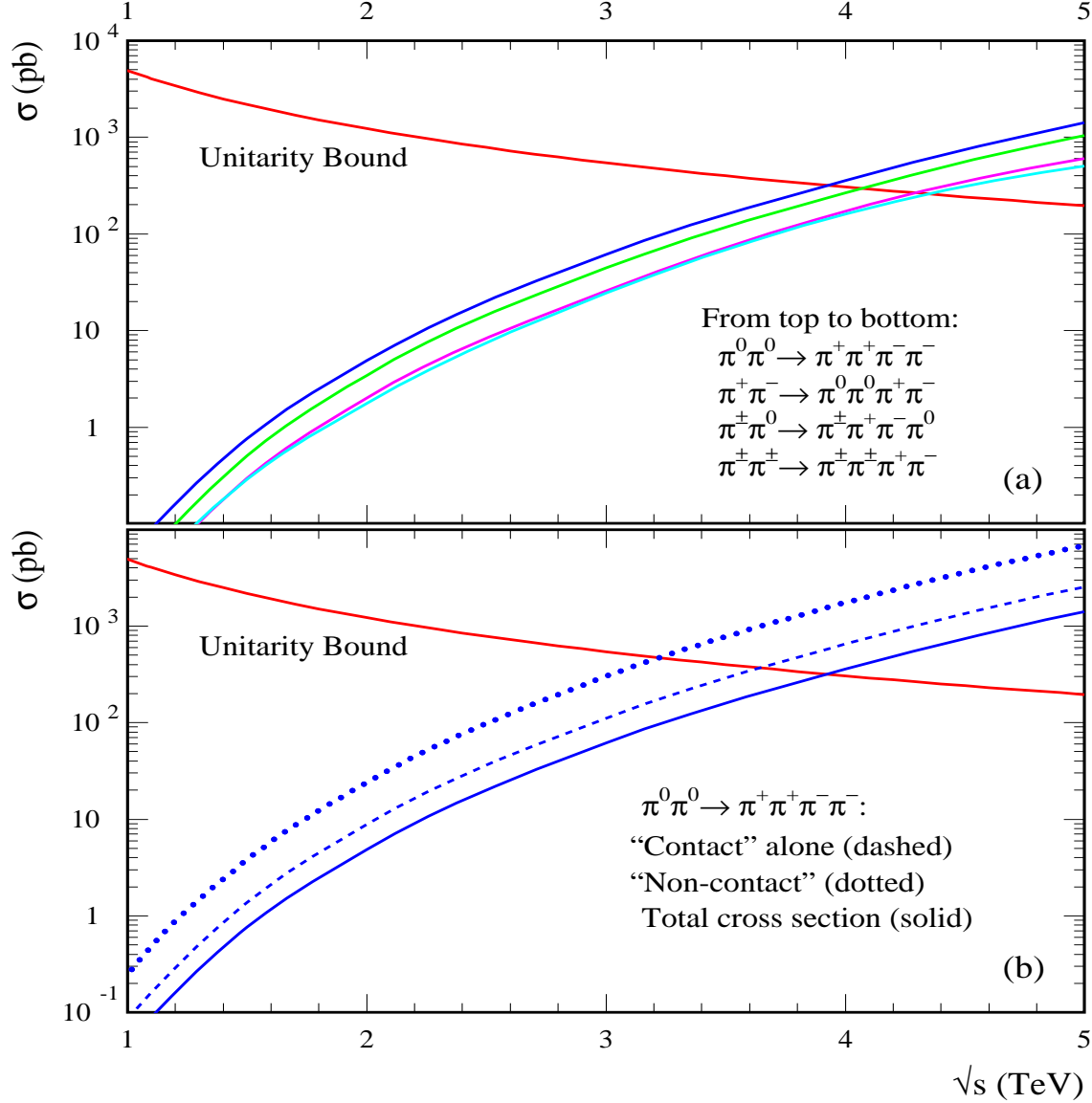


Figure 9: (a) Total cross sections of the scattering processes $\pi^0 \pi^0 \rightarrow \pi^+ \pi^+ \pi^- \pi^-$, $\pi^+ \pi^- \rightarrow \pi^0 \pi^0 \pi^+ \pi^-$, $\pi^+ \pi^0 \rightarrow \pi^+ \pi^+ \pi^- \pi^0$, and $\pi^+ \pi^+ \rightarrow \pi^+ \pi^+ \pi^+ \pi^-$. (b) For $\pi^0 \pi^0 \rightarrow \pi^+ \pi^+ \pi^- \pi^-$, we show the individual contributions from the contact graph alone (dashed curve) and from the non-contact graphs (dotted curve). The total cross section is depicted by the solid curve.

In summary, Fig. 9(a), together with the above estimates, shows that the unitarity bound from $2 \rightarrow 4$ scattering is about 3.0 – 3.9 TeV, significantly weaker than that from the $2 \rightarrow 2$ scattering

[which is about 1.2 TeV, cf. Eq. (2.33)]. This further supports our earlier estimate for $V_L^{a_1} V_L^{a_2} \rightarrow n V_L^a$ ($n \geq 2$) in Fig. 2 (Sec. 3.2), i.e., the strongest unitarity bound for the EWSB scale occurs at $n = 2$, in contrast to the case for the scales of fermion mass generation (cf. Sec. 4-5).

7. Conclusions

The requirement from unitarity that the partial wave amplitudes for $2 \rightarrow 2$ scattering, $V_L^{a_1} V_L^{a_2} \rightarrow V_L^{a_3} V_L^{a_4}$ and $f \bar{f}, \nu_L \nu_L \rightarrow V_L^{a_1} V_L^{a_2}$, be bounded for all energy has imposed nontrivial upper limits on the energy scales at which the new physics responsible for the mass-generations of the weak gauge bosons ($V^a = W^\pm, Z^0$) and fermions (f, ν_L) must become evident. The limit on the mass-generation scale for V_L^a is about 1 TeV [cf. Eq. (1.1)] while the limits for the fermions are proportional to $v^2/m_{f,\nu}$ [cf. Eqs. (1.2) and (2.38)] which is substantially above 1 TeV except for the top-quark (cf. Table 2), indicating that the scales of mass generation for all the light SM fermions might not be directly accessible by current or foreseeable high energy accelerators. More recently it was pointed out [44] that the scattering $f \bar{f} \rightarrow n V_L^a$, with $n > 2$, could impose much stronger unitarity bounds for the light fermions when n becomes sufficiently large; these bounds are so severe that they approach the weak scale $v = (\sqrt{2}G_F)^{-\frac{1}{2}} \simeq 246$ GeV as n becomes large [cf. Eq. (1.3)]. This leads to the conclusion that the scattering $f \bar{f} \rightarrow n V_L^a$ does not reveal an independent new scale for fermion mass generation [44]. We further observe that such a bound would unavoidably contradict the kinematics [cf. Eq. (1.4)]. We have resolved this contradiction by treating the n -body phase space exactly. The present analysis shows that *the scattering $f \bar{f} \rightarrow n V_L^a$ ($n \geq 2$) does reveal a separate scale for fermion mass generation*. Our bounds from $2 \rightarrow n$ scattering with $n > 2$ establish a *new scale of mass generation for all light fermions (including Majorana neutrinos)* and are *substantially stronger* than the conventional $2 \rightarrow 2$ limits.

In the SM, the arbitrary Yukawa interactions of fermions with a single Higgs boson are assumed to be the mechanism for the mass generation of all fermions; this is, however, not experimentally verified so far. Even if a SM-like light Higgs boson is found to generate the electroweak symmetry breaking (EWSB) in forthcoming collider experiments, it could still be completely irrelevant to fermion mass generation because such a Higgs scalar is *not* required to couple to the SM fermions via Yukawa interactions by any known fundamental principle. This makes probing the scale of fermion mass generation an *independent* task. The crucial point is to note that all the known fermions must join the SM gauge interactions and must also be chiral rather than vector-like under

the electroweak gauge group. Therefore, a bare mass term for a SM fermion can be made gauge-invariant only in the nonlinear realization of the electroweak gauge symmetry [cf. Eqs.(2.9) and (2.10)], so it is necessarily nonrenormalizable and thus will cause unitarity violation in high energy fermion-antifermion scattering. The energy where such a unitarity violation happens provides a *model independent upper bound* on the scale at which the new physics responsible for fermion mass generation must be manifest. The gauge-invariant, nonlinear formulation of the bare fermion mass terms also allows us to efficiently compute the high energy scattering amplitude of $f\bar{f} \rightarrow nV_L^a$ from that with the corresponding final-state Goldstone bosons, $f\bar{f} \rightarrow n\pi^a$, by using the equivalence theorem. This is extremely valuable when the final state involves multiple longitudinal weak bosons.

For quarks and charged leptons, the scale of unitarity violation is shown, as a function of the number of final state weak bosons, n , in Fig. 3. These results depend on two opposing factors, one of which causes the cross section of $2 \rightarrow n$ scattering to increase as n becomes large, similar to Eq.(1.3), and one of which causes the cross section to decrease with n until it eventually overcomes the first factor completely. Strikingly, the *competition* between these two opposing factors makes the strongest energy bounds occur at a proper value of $n > 2$ (except, perhaps, for the top quark). The values of n (called n_s) which give the strongest upper bounds are summarized in Table 3. These new limits depend on the fermion mass and range from about 3.5 TeV ($n_s = 2$) for top quarks to 84 TeV ($n_s = 10$) for up quarks, and from 34 TeV ($n_s = 6$) for tau leptons to 107 TeV ($n_s = 12$) for electrons.³² Hence, while the masses of the involved fermions decrease by a factor up to $\sim 3 \times 10^5$, the bounds weaken by only a factor of ~ 30 in contrast to the customary $2 \rightarrow 2$ limits which are weakened by a factor of $\sim 6 \times 10^5$ (cf. Table 2). These unitarity bounds could be affected somewhat by model-dependent effects from the EWSB mechanism through self-interactions among the V_L^a 's (π^a 's), but such changes are shown to be small, to decrease rapidly with the increase of n , and furthermore, to be in the direction of lowering the above limits for a SM or SM-like EWSB sector. Such effects indicate that even for the *top quark* the best bound becomes stronger than the customary $2 \rightarrow 2$ limit and occurs at $n_s = 3$ rather than $n_s = 2$ [cf. Eq.(4.79)].

The bounds for the Majorana neutrinos depend on the neutrino mass m_ν . With the typical values of m_ν between 1 eV and 0.01 eV (as suggested by the current experiments on neutrino oscillations, neutrinoless double-beta decays and astrophysics observations), the strongest bound varies from 136 TeV to 170 TeV with $n = n_s = 20 - 24$. Thus the scale of neutrino mass generation is only a factor of 1.3 – 1.6 higher than that for the electron despite the tiny mass ratio of $m_\nu/m_e \simeq 2 \times (10^{-6} - 10^{-8})$. These bounds are universal, independent of the details of the

³²These are the energies which, for instance, could be within the reach of a Very Large Hadron Collider (VLHC) [89].

Table 4: Summary of the *strongest* unitarity bound $E_{2 \rightarrow n}^{\star \min}$ (in TeV) for each scattering $\xi_1 \xi_2 \rightarrow n V_L^a$ ($\xi_{1,2} = V_L, f, \bar{f}, \nu_L$) and the corresponding number of final state particles $n = n_s$, in comparison with the classic $2 \rightarrow 2$ limit $E_{2 \rightarrow 2}^{\star}$ (in TeV). For Majorana neutrinos, $m_\nu = 0.05$ eV is chosen.

$\xi_1 \xi_2$	$V_L^{a1} V_L^{a2}$	$t\bar{t}$	$b\bar{b}$	$c\bar{c}$	$s\bar{s}$	$d\bar{d}$	$u\bar{u}$	$\tau^- \tau^+$	$\mu^- \mu^+$	$e^- e^+$	$\nu_L \nu_L$
n_s	2	2	4	6	8	10	10	6	8	12	22
$E_{2 \rightarrow n}^{\star(\min)}$	1.2	3.49	23.4	30.8	52.1	77.4	83.6	33.9	56.3	107	158
$E_{2 \rightarrow 2}^{\star}$	1.2	3.49	128	377	6×10^3	10^5	2×10^5	606	10^4	2×10^6	1.1×10^{13}

mechanism for the neutrino mass generation, even though the underlying dynamics may invoke mass parameters of a very different scale such as the right-handed singlet neutrino mass M_R in the traditional seesaw mechanism (where $M_R \sim M_{\text{GUT}}$) or in the SUSY-breaking induced seesaw mechanism (where $M_R \sim \mathcal{O}(\text{TeV})$), or the charged scalar masses $M_{X,Y}$ in the radiative mechanism (where $M_{X,Y} \sim \mathcal{O}(\text{TeV})$). For all these models, our universal new bounds essentially constrain the new physics scale of the Higgs-fermion Yukawa interaction, which must invoke extra new fields (such as right-handed neutrinos or charged Zee-scalars or triplet-Higgs) as needed for ensuring renormalizability and generating lepton number violation (although our new bounds do not directly constrain the masses M_R and $M_{X,Y}$ of these new fields as they obey the decoupling theorem [82]). Thus, for all known fermions including Majorana neutrinos, the new physics of mass generation must manifest itself at a scale below about 170 TeV.

We see that these bounds are very insensitive to the variation of the fermion masses and when the mass value decreases from that of the bottom quark (~ 4 GeV) down to that of the Majorana neutrinos ($\sim 1 - 0.01$ eV), by about 9 – 11 orders of magnitude, the corresponding unitarity limits are only weakened by about a factor of 7 or less. This strong non-decoupling feature for the scale of new physics associated with light fermion mass generation is essentially due to the *chiral structure* of the fermion bare mass terms, i.e., the fact that all the left-handed SM fermions are weak-doublets but their right-handed chiral partners are weak-singlets or, possibly absent for Majorana neutrinos with radiative mass generation. It is this feature that makes the coupling strength of fermions to multiple Goldstones (or effectively, multiple longitudinal gauge bosons) *proportional to the fermion mass*, so the decoupling theorem [82] no longer applies. A systematic discussion of this is given in Sec. 5.2.1.

The summary Table 4 shows that the established *new scales of mass generation* for all fermions (including Majorana neutrinos) fall in a narrow range, $3 \sim 160$ TeV. This not only provides an important guideline for model-building, but also motivate and quantify where to look for definitive *experimental tests*, such as the proposed VLHC experiment [89] and the relevant astrophysical processes [78], etc.

Finally, for pure gauge boson scattering, $V_L^{a_1} V_L^{a_2} \rightarrow n V_L^a$ ($\pi^{a_1} \pi^{a_2} \rightarrow n \pi^a$) with $n \geq 4$, the quantitative calculations are much more difficult due to nontrivial angular dependences in the leading energy terms of the S -matrix elements, but a comparison of $2 \rightarrow 4$ scattering with $2 \rightarrow 2$ scattering indicates that the rapidly decreasing phase space factor dominates and the best bound remains the customary $2 \rightarrow 2$ bound of ~ 1 TeV. This picture is further supported by our general estimates for the $2 \rightarrow n$ gauge boson scattering with an arbitrary value of n as shown in Fig. 2 and Table 1, where our similar estimates for the upper bounds on the scales of mass generation of the quarks, leptons and Majorana neutrinos are consistent with the quantitative calculations within a factor 2 or so (cf. Sec. 4-5). Also, the current study of $f \bar{f} \rightarrow n V_L^a$ ($n \pi^a$) scattering assumes V_L^a (π^a) to be a local field or remain local up to the limit E_f^* . If V_L^a (π^a) becomes composite much below E_f^* , the pure fermion process $f \bar{f} \rightarrow (f \bar{f})^n$ may be useful for a model-independent analysis.

In conclusion, Table 4 summarizes all the optimal $2 \rightarrow n$ unitarity bounds on the scales of mass-generation, as compared to the classic $2 \rightarrow 2$ limits. A short summary of these key results is given in [90].

Acknowledgments

We thank S. Willenbrock for valuable discussions and a careful reading of the manuscript. We also thank R. S. Chivukula, A. de Gouvêa, E. Ma, M. E. Peskin and W. W. Repko for discussing the unitarity issue, and U. Varadarajan and N. Weiner for discussing aspects of SUSY breaking induced neutrino mass. HJH thanks the SLAC Theory Group for hospitality during the completion of this work. This research was supported by U.S. Department of Energy under grant No. DE-FG03-93ER40757.

Appendices

A. Derivation of n-Body Phase Space

For completeness, we summarize a derivation of the n -body phase space formula (3.43) which is used in our analyses in Sec. 3-5. The phase space integral for n particles is

$$\mathcal{J}_n = \int \frac{d^3 k_1 \cdots d^3 k_n}{2E_1 \cdots 2E_n} \delta^{(4)}(P - k_1 - \cdots - k_n), \quad (\text{A.121})$$

where $P = p_1 + p_2$. For the current purpose, it is safe to ignore the masses of the final state particles, i.e., $m_j^2/E_j^2 \ll 1$ ($j = 1, 2, \dots, n$). Then we obtain the final formula,

$$\mathcal{J}_n = \left(\frac{\pi}{2}\right)^{n-1} \frac{s^{n-2}}{(n-1)!(n-2)!}, \quad (\text{A.122})$$

where $s = P^2$.

To derive Eq.(A.122), we carry out the following steps:

(i). Replace the delta function in (A.121) with

$$\int d^4 Q_{n-2} \delta^{(4)}(Q_{n-2} - k_{n-1} - k_n) \delta^{(4)}(P - k_1 - \cdots - k_{n-2} - Q_{n-2}), \quad (\text{A.123})$$

and multiply by

$$1 = \int ds_{n-2} \delta(s_{n-2} - Q_{n-2}^2). \quad (\text{A.124})$$

(ii). Use the first delta function in (A.123) to do the integration over k_{n-1} and k_n in their center of mass frame, i.e.,

$$\int \frac{d^3 k_{n-1} d^3 k_n}{2E_{n-1} 2E_n} \delta^{(4)}(Q_{n-2} - k_{n-1} - k_n) = \frac{\pi}{2}. \quad (\text{A.125})$$

(iii). Repeat step-(i) by replacing the second delta function in (A.123) by

$$\int d^4 Q_{n-3} \delta^{(4)}(Q_{n-3} - k_{n-2} - Q_{n-2}) \delta^{(4)}(P - k_1 - \cdots - k_{n-3} - Q_{n-3}) \quad (\text{A.126})$$

and multiplying by

$$1 = \int ds_{n-3} \delta(s_{n-3} - Q_{n-3}^2). \quad (\text{A.127})$$

(iv). Repeat step-(ii) by performing the integration over k_{n-2} and Q_{n-2} in their center of mass frame using the delta function in (A.124) and the first delta function in (A.126),

$$\int \frac{d^3 k_{n-2}}{2E_{n-2}} d^4 Q_{n-2} \delta^{(4)}(Q_{n-3} - k_{n-2} - Q_{n-2}) \delta(s_{n-2} - Q_{n-2}^2) = \frac{\pi}{2} \frac{s_{n-3} - s_{n-2}}{s_{n-3}}. \quad (\text{A.128})$$

(v). Continue to repeat the steps **(iii)** and **(iv)**.

The result of steps (i)-(v) is the integral

$$J_n = \left(\frac{\pi}{2}\right)^{n-1} \int_0^s ds_1 \frac{s-s_1}{s} \int_0^{s_1} ds_2 \frac{s_1-s_2}{s_1} \int_0^{s_2} ds_3 \frac{s_2-s_3}{s_2} \cdots \int_0^{s_{n-3}} ds_{n-2} \frac{s_{n-3}-s_{n-2}}{s_{n-3}}, \quad (\text{A.129})$$

which can be directly evaluated to give (A.122).

As an alternate derivation, if we assume the validity of (A.122) for an arbitrary $n (\geq 2)$, then we deduce

$$\begin{aligned} J_{n+1} &= \left(\frac{\pi}{2}\right)^n \int_0^s ds_{n+1} \frac{s-s_{n+1}}{s} \frac{(s_{n+1})^{n-2}}{(n-1)!(n-2)!} \\ &= \left(\frac{\pi}{2}\right)^n \frac{s^{n-1}}{n!(n-1)!}, \end{aligned} \quad (\text{A.130})$$

which proves Eq. (A.122) by induction.

B. Refined Unitarity Conditions

For completeness we improve the unitarity conditions in Sec. 2.3.1 by keeping the masses of initial/final state particles. We first recompute the two-body phase space in Eq. (2.21) without approximation and obtain

$$\int_{\text{PS}_2} |\mathcal{T}_{\text{el}}[2 \rightarrow 2]|^2 = \frac{32\pi\eta_{\text{f}}^{\text{el}}}{\varrho_e} \sum_j (2j+1) |a_j^{\text{el}}|^2, \quad (\text{B.131})$$

where $\eta_{\text{f}}^{\text{el}} = \eta(s, m_3^2, m_4^2)$ with (m_3, m_4) the masses of final state particles, and

$$\eta(x, y, z) \equiv \frac{1}{x} [x^2 + y^2 + z^2 - 2(xy + yz + zx)]^{\frac{1}{2}}. \quad (\text{B.132})$$

For $s \gg m_i^2, m_j^2$, $\eta(s, m_i^2, m_j^2) \simeq 1$ holds well. In the special case $m_3 = m_4 \equiv m$, Eq. (B.132) gives $\eta(s, m^2, m^2) = [1 - 4m^2/s]^{1/2}$. For the elastic scattering $m_1 + m_2 \rightarrow m_3 + m_4$, we have $\eta_{\text{in}} \equiv \eta(s, m_1^2, m_2^2) = \eta(s, m_3^2, m_4^2) \equiv \eta_{\text{f}}^{\text{el}}$. Thus we can derive a refined form of (2.22),

$$\sum_j (2j+1) \frac{1}{\varrho_e} \left[\frac{\varrho_e^2}{4} - (\Re \widehat{a}_j^{\text{el}})^2 - \left(\Im \widehat{a}_j^{\text{el}} - \frac{\varrho_e}{2} \right)^2 \right] = \frac{\eta_{\text{in}}}{32\pi} \sum_n \int_{\text{PS}_n} |\mathcal{T}_{\text{inel}}[2 \rightarrow n]|^2 \geq 0, \quad (\text{B.133})$$

where $\widehat{a}_j^{\text{el}} \equiv \eta_{\text{in}} a_j^{\text{el}} = \sqrt{\eta_{\text{in}} \eta_{\text{f}}^{\text{el}}} a_j^{\text{el}}$ and $\eta_{\text{in}} = \eta_{\text{f}}^{\text{el}} = \eta(s, m_1^2, m_2^2)$. Accordingly, the unitarity conditions (2.24) and (2.26) become,

$$\left| \Re \widehat{a}_j^{\text{el}} \right| \leq \frac{\varrho_e}{2}, \quad \left| \widehat{a}_j^{\text{el}} \right| \leq \varrho_e, \quad (\text{B.134})$$

and

$$\eta_{\text{in}}^2 \sigma_{\text{inel}}[2 \rightarrow n] \leq \frac{4\pi\varrho_e}{s}, \quad (\text{B.135})$$

where the total inelastic cross section is given by $\sigma_{\text{inel}}[2 \rightarrow n] = \frac{1}{2s\eta_{\text{in}}} \int_{\text{PS}_n} |\mathcal{T}_{\text{inel}}[2 \rightarrow n]|^2$. Similarly we rederive Eq. (2.28) as

$$\sum_j (2j+1) \left\{ \frac{\varrho_e}{4} - \frac{1}{\varrho_e} \left[\left(\Re \widehat{a}_j^{\text{el}} \right)^2 + \left(\Im \widehat{a}_j^{\text{el}} - \frac{\varrho_e}{2} \right)^2 \right] \right\} > \sum_j (2j+1) \frac{1}{\varrho_i} |\widehat{a}_j^{\text{inel}}|^2, \quad (\text{B.136})$$

where $\widehat{a}_j^{\text{inel}} \equiv \sqrt{\eta_{\text{in}} \eta_{\text{f}}^{\text{inel}}} a_j^{\text{inel}}$ and $\eta_{\text{f}}^{\text{inel}} \equiv \eta(s, m_3^2, m_4^2)$. Thus, for $2 \rightarrow 2$ inelastic scattering, we find that the unitarity condition (2.29) becomes

$$|\widehat{a}_j^{\text{inel}}| < \frac{\sqrt{\varrho_i \varrho_e}}{2}. \quad (\text{B.137})$$

For the present study in Sec. 3-6, we have $s \gg m_j^2$ ($j = 1, 2, \dots, n+2$), so that $\eta_{\text{in}}, \eta_{\text{f}} \rightarrow 1$, under which all the formulas above reduce back to Sec. 2.3.1. In the traditional case of $2 \rightarrow 2$ scattering, a similar effect of $\eta_{\text{in},\text{f}}$ due to the finite masses of the initial/final state was noted before [91].

References

- [1] S. L. Glashow, Nucl. Phys. **22**, 579 (1961); S. Weinberg, Phys. Rev. Lett. **19**, 1264 (1967); A. Salam, in *Elementary Particle Theory*, Nobel Symposium No. 8, ed. N. Svartholm, pp. 367 (Almqvist and Wiksell, Stockholm, 1968).
- [2] H. Fritzsch and M. Gell-Mann, in *Proceedings of XVI International Conference on High Energy Physics*, eds. J. D. Jackson and A. Roberts (Fermilab, Batavia, IL, 1972); D. J. Gross and F. Wilczek, Phys. Rev. Lett. **30**, 1343 (1973); H. D. Politzer, Phys. Rev. Lett. **30**, 1346 (1973).
- [3] N. Cabibbo, Phys. Rev. Lett. **10**, 531 (1963); M. Kobayashi and T. Maskawa, Prog. Theor. Phys. **49**, 652 (1973).
- [4] S. Fukuda, *et al.*, [Super-Kamiokande Collaboration], Phys. Rev. Lett. **85**, 3999 (2000); **86**, 5656 (2001); **82**, 1810 (1999); **81**, 1562 (1998); **81**, 1158 (1998); and Y. Ashie, *et al.*, [Super-Kamiokande Collaboration], Phys. Rev. Lett. **93**, 101801 (2004) [[hep-ex/0404034](#)]; M. Ishitsuka, [hep-ex/0406076](#).
- [5] S. Fukuda, *et al.*, [Super-Kamiokande Collaboration], Phys. Rev. Lett. **86**, 5656 (2001); Q. R. Ahmad, *et al.*, [SNO collaboration], Phys. Rev. Lett. **87**, 071301 (2001). Q. R. Ahmad, *et al.*, [SNO Collaboration], Phys. Rev. Lett. **89**, 011301 (2002) [[nucl-ex/0204008](#)] and Phys. Rev. Lett. **89**, 011302 (2002) [[nucl-ex/0204009](#)]; B. Aharmim, *et al.*, [SNO collaboration], [hep-ex/0407029](#); A. Bellerive, [hep-ex/0401018](#).
- [6] S. H. Ahn, *et al.* [K2K Collaboration], Phys. Rev. Lett. **93**, 051801 (2004) [[hep-ex/0402017](#)] Phys. Rev. Lett. **90**, 041801 (2003); Phys. Lett. B **511**, 178 (2001).
- [7] M. Apolloni, *et al.*, [CHOOZ Collaboration], Phys. Lett. B **466**, 415 (1999); Phys. Lett. B **420**, 397 (1998); F. Boehm, *et al.*, [Palo Verde Collaboration], Phys. Rev. D **64**, 112001 (2001); Phys. Rev. Lett. **84**, 3764 (2000).
- [8] K. Eguchi, *et al.*, [KamLAND Collaboration], Phys. Rev. Lett. **90**, 021802 (2003) [[hep-ex/0212021](#)]; T. Araki, *et al.*, [KamLAND Collaboration], Phys. Rev. Lett. **94**, 081801 (2005) [[hep-ex/0406035](#)].
- [9] B. Pontecorvo, Sov. Phys. JETP **6**, 429 (1957); Z. Maki, M. Nakagawa, and S. Sakata, Prog. Theor. Phys. **28**, 870 (1962).
- [10] For recent reviews, *e.g.*, J. W. F. Valle, [hep-ph/0410103](#); G. Altarelli and F. Feruglio, New J. Phys. **6**, 106 (2004) [[hep-ph/0405048](#)] and [[hep-ph/0206077](#)]; R. N. Mohapatra, New J. Phys. **6**, 82 (2004) [[hep-ph/0411131](#)]; V. Barger, *et al.*, Int. J. Mod. Phys. E **12**, 569 (2003) [[hep-ph/0308123](#)]; M. C. Gonzalez-Garcia and Y. Nir, Rev. Mod. Phys. **75**, 345 (2003) [[hep-ph/0202058](#)].
- [11] M. Maltoni, T. Schwetz, M. A. Tortola and J.W.F. Valle, New J. Phys. **6**, 122 (2004) [[hep-ph/0405172](#)]; [hep-ph/0305312](#); Nucl. Phys. B **643**, 321 (2002) [[hep-ph/0207157](#)]; and references therein.

- [12] J. Monroe, [MiniBooNE Collaboration], [[hep-ex/0406048](#)], in proceedings of the Moriond Electroweak 2004 Conference; M. H. Shaevitz, [MiniBooNE Collaboration], [hep-ex/0407027](#); A. Bazarko, *et al.*, [MiniBooNE Collaboration], Nucl. Phys. Proc. Suppl. **91**, 210 (2001).
- [13] C. Athanassopoulos, *et al.*, [LSND Collaboration], Phys. Rev. Lett. **81**, 1774 (1998); and A. Aguilar *et al.*, Phys. Rev. **D63**, 112001 (2001) [[hep-ex/0101039](#)].
- [14] D. N. Spergel, *et al.*, [WMAP Collaboration], Astrophys. J. Suppl. **148**, 175 (2003) [[astro-ph/0302209](#)].
- [15] O. Elgaroy, *et al.*, Phys. Rev. Lett. **89**, 061301 (2002) [[astro-ph/0204152](#)]; S. Hannestad, [astro-ph/0205223](#); O. Elgaroy and O. Lahav, JCAP **04**, 004 (2003) [[astro-ph/0303089](#)].
- [16] S. Hannestad, New J. Phys. **6**, 108 (2004) [[hep-ph/0404239](#)]; JCAP **05**, 004 (2003) [[astro-ph/0303076](#)]; and references therein.
- [17] S. Hannestad, [hep-ph/0409108](#) and [hep-ph/0412181](#); O. Elgaroy and O. Lahav, New J. Phys. **7**, 61 (2005) [[hep-ph/0412075](#)].
- [18] P. W. Higgs, Phys. Lett. **12**, 132 (1964); Phys. Rev. Lett. **13**, 508 (1964); Phys. Rev. **145**, 1156 (1966); F. Englert and R. Brout, Phys. Rev. Lett. **13**, 321 (1964); G. S. Guralnik, C. R. Hagen, and T. W. Kibble, Phys. Rev. Lett. **13**, 585 (1964).
- [19] S. Weinberg, Phys. Rev. Lett. **43**, 1566 (1979).
- [20] P. Minkowski, Phys. Lett. **B67**, 421 (1977); M. Gell-Mann, P. Ramond and R. Slansky, in *Proceedings of the Workshop on Supergravity*, eds. F. van Nieuwenhuizen and D. Freedman, Amsterdam, p.315, 1979; T. Yanagida, *Proceedings of the Workshop on Unified Theories and Baryon Number in the Universe*, eds. O. Sawada and A. Sugamoto, KEK, Tsukuba, p.95, 1979; R. N. Mohapatra and G. Senjanovic, Phys. Rev. Lett. **44**, 912 (1980).
- [21] A. Zee, Phys. Lett. **B93**, 389 (1980); Phys. Lett. **B161**, 141 (1985); L. Wolfenstein, Nucl. Phys. **B175**, 93 (1980); S. T. Petcov, Phys. Lett. **B115**, 401 (1982).
- [22] For an updated overview of dynamical symmetry breaking and compositeness, C. T. Hill and E. H. Simmons, Phys. Rept. **381**, 235 (2003) [[hep-ph/0203079](#)]; and references therein.
- [23] E.g., B. A. Dobrescu and C. T. Hill, Phys. Rev. Lett. **81**, 2634 (1998) [[hep-ph/9712319](#)]; R. S. Chivukula, B. A. Dobrescu, H. Georgi, C. T. Hill, Phys. Rev. **D59**, 075003 (1999) [[hep-ph/9809470](#)]; H.-J. He, C. T. Hill, T. Tait, Phys. Rev. **D65**, 055006 (2002) [[hep-ph/0108041](#)].
- [24] E.g., N. Arkani-Hamed, A. G. Cohen and H. Georgi, Phys. Lett. B **513**, 232 (2001); N. Arkani-Hamed, A. G. Cohen, T. Gregoire and J. G. Wacker, JHEP **08**, 020 (2002); N. Arkani-Hamed, A. G. Cohen, E. Katz, A. E. Nelson, T. Gregoire and J. G. Wacker, JHEP **08**, 021 (2002); N. Arkani-Hamed, A. G. Cohen, E. Katz, A. E. Nelson, JHEP **07**, 034 (2002); I. Low, W. Skiba, D. Smith, Phys. Rev. **D66**, 072001 (2002); D. E. Kaplan and M. Schmaltz, JHEP **10**, 039 (2003); S. Chang and J. G. Wacker, Phys. Rev. **D69**, 035002 (2004); S. Chang, JHEP **12**, 057 (2003); S. Chang and H.-J. He, Phys. Lett. B **586**, 95 (2004); and references therein.

- [25] For reviews, *e.g.*, P. Fayet and S. Ferrara, Phys. Rept. **32**, 249 (1977); H. P. Nilles, Phys. Rept. **110**, 1 (1984); H. E. Haber and G. L. Kane, Phys. Rept. **117**, 75 (1985); and more recently, H. E. Haber, [hep-ph/0409008](#) and [hep-ph/0212136](#), and references therein.
- [26] N. Arkani-Hamed and S. Dimopoulos, [hep-th/0405159](#).
- [27] H. Georgi and S. L. Glashow, Phys. Rev. Lett. **32**, 438 (1974); H. Georgi, H. R. Quinn, and S. Weinberg, Phys. Rev. Lett. **33**, 451 (1974); S. Dimopoulos and H. Georgi, Nucl. Phys. B**193**, 150 (1981); S. Dimopoulos, S. Raby, and F. Wilczek, Phys. Rev. D**24**, 1681 (1981).
- [28] N. Arkani-Hamed, S. Dimopoulos, G. R. Dvali, Phys. Lett. B**429** (1998) 263; I. Antoniadis, N. Arkani-Hamed, S. Dimopoulos, G. R. Dvali, Phys. Lett. B**436** (1998) 257; K. R. Dienes, E. Dudas, T. Gherghetta, Phys. Lett. B**436**, 55 (1998); Nucl. Phys. B**537**, 47 (1999); L. Randall and R. Sundrum, Phys. Rev. Lett. **83** (1999) 3370.
- [29] N. Arkani-Hamed, A. G. Cohen, and H. Georgi, Phys. Rev. Lett. **86**, 4757 (2001); C. T. Hill, S. Pokorski, and J. Wang, Phys. Rev. D**64**, 105005 (2001).
- [30] See: L. Susskind, [hep-th/0302219](#) and [hep-th/0405189](#); J. Polchinski, [[hep-th/0209105](#)], in Heisenberg Centennial Symposium, Munich, 2001; and references therein.
- [31] C. T. Hill, Phys. Lett. B**345**, 483 (1995) [[hep-ph/9411426](#)].
- [32] S. Weinberg, Phys. Rev. D**13**, 974 (1976); L. Susskind, Phys. Rev. D**20**, 2619 (1979). For an early review, E. Farhi and L. Susskind, Phys. Rept. **74**, 277 (1981).
- [33] S. Dimopoulos and L. Susskind, Nucl. Phys. B**155**, 237 (1979); E. Eichten and K. Lane, Phys. Lett. B**90**, 125 (1980). For recent reviews, K. Lane, [hep-ph/0202255](#); E. H. Simmons, [hep-ph/0211335](#).
- [34] C. H. Llewellyn Smith, Phys. Lett. B**46**, 233 (1973).
- [35] D. A. Dicus and V. S. Mathur, Phys. Rev. D**7**, 3111 (1973).
- [36] J. M. Cornwall, D. N. Levin, and G. Tiktopoulos, Phys. Rev. D**10**, 1145 (1974).
- [37] B. W. Lee, C. Quigg, and H. B. Thacker, Phys. Rev. D**16**, 1519 (1977); Phys. Rev. Lett. D**38**, 883 (1977).
- [38] M. Veltman, Acta. Phys. Polon. B**8**, 475 (1977).
- [39] M. S. Chanowitz and M. K. Gaillard, Nuc. Phys. B**261**, 379 (1985).
- [40] M. Lüscher and P. Weisz, Phys. Lett. B**212**, 472 (1988).
- [41] W. Marciano, G. Valencia, and S. Willenbrock, Phys. Rev. D**40**, 1725 (1989).
- [42] S. Dawson and S. Willenbrock, Phys. Rev. Lett. **62**, 1232 (1989); L. Durand, J. M. Johnson, and J. L. Lopez, Phys. Rev. Lett. **64**, 1215 (1990).

- [43] T. Appelquist and M. S. Chanowitz, Phys. Rev. Lett. **59**, 2405 (1987).
- [44] F. Maltoni, J. M. Niczyporuk, and S. Willenbrock, Phys. Rev. D **65**, 033004 (2002) [[hep-ph/0106281](#)].
- [45] T. Appelquist and R. Shrock, Phys. Lett. B **548**, 204 (2002) [[hep-ph/0204141](#)]; Phys. Rev. Lett. **90**, 201801 (2003) [[hep-ph/0301108](#)].
- [46] P. Sikivie, L. Susskind, M. Voloshin, and V. Zakharov, Nucl. Phys. B **173**, 189 (1980); B. Holdom, Phys. Rev. D **23**, 1637 (1981); Phys. Lett. B **246**, 169 (1990); T. Appelquist and J. Terning, Phys. Rev. D **50**, 2116 (1994).
- [47] C. G. Callen, S. Coleman, J. Wess, and B. Zumino, Phys. Rev. **177**, 2247 (1969).
- [48] S. Weinberg, Physica A **96**, 327 (1979).
- [49] T. Appelquist and C. Bernard, Phys. Rev. D **22**, 200 (1980); A. C. Langhitano, Nucl. Phys. B **188**, 118 (1981).
- [50] J. Goldstone, Nuovo Cim. **19**, 154 (1961).
- [51] H.-J. He, Y.-P. Kuang and C.-P. Yuan, Phys. Rev. D **55**, 3038 (1997) [[hep-ph/9611316](#)]; Phys. Lett. B **382**, 149 (1996) [[hep-ph/9604309](#)].
- [52] For comprehensive reviews, H.-J. He, [hep-ph/9804210](#), invited review in the Proceedings of “*Physics at the First Muon Collider*”, pp. 685-700, FermiLab, Batavia, IL, Nov. 6-9, 1997, USA; H.-J. He, Y.-P. Kuang and C.-P. Yuan, DESY-97-056 [[hep-ph/9704276](#)], invited lectures in the Proceedings of the Workshop on “*Physics at the TeV Energy Scale*”, CCAST (World Laboratory), vol. 72, pp. 119-234, July 15-26, 1996.
- [53] R. S. Chivukula, D. A. Dicus, H.-J. He, Phys. Lett. B **525**, 175 (2002) [[hep-ph/0111016](#)]; R. S. Chivukula and H.-J. He, Phys. Lett. B **532**, 121 (2002) [[hep-ph/0201164](#)]; R. S. Chivukula, D. A. Dicus, H.-J. He, S. Nandi, Phys. Lett. B **562**, 109 (2003) [[hep-ph/0302263](#)]; R. S. Chivukula, D. A. Dicus, H.-J. He, S. Nandi, [hep-ph/0402222](#), in the proceedings of the international conference of SUSY-2003, June 5-10, 2003, Arizona, USA.
- [54] H.-J. He, [hep-ph/0412113](#), in the proceedings of DPF-2004: Annual Meeting of the Division of Particles and Fields, American Physical Society, Riverside, CA, USA, August 26-31, 2004.
- [55] C. Csaki, C. Grojean, H. Murayama, L. Pilo and J. Terning, Phys. Rev. D **69**, 055006 (2004) [[hep-ph/0305237](#)].
- [56] C. E. Vayonakis, Lett. Nuovo. Cimento **17**, 383 (1976); G. J. Gounaris, R. Kögerler, H. Neufeld, Phys. Rev. D **34**, 3257 (1986); Y.-P. Yao and C.-P. Yuan, Phys. Rev. D **38**, 2237 (1988); J. Bagger and C. Schmidt, Phys. Rev. D **41**, 264 (1990).
- [57] H.-J. He, Y.-P. Kuang and X. Li, Phys. Rev. Lett. **69**, 2619 (1992); Phys. Rev. D **49**, 4842 (1994); Phys. Lett. B **329**, 278 (1994) [[hep-ph/9403283](#)].

- [58] H.-J. He, Y.-P. Kuang and C.-P. Yuan, Phys. Rev. D**51**, 6463 (1995) [[hep-ph/9410400](#)].
- [59] H.-J. He and W.B. Kilgore, Phys. Rev. D**55**, 1515 (1997) [[hep-ph/9609326](#)].
- [60] For related papers, *e.g.*, H. Veltman, Phys. Rev. D**41**, 2294 (1990); W. B. Kilgore, Phys. Lett. B**294**, 257 (1992); A. Dobado and J. R. Pelaez, Nucl. Phys. B**425**, 110 (1994), Erratum B**434**, 475 (1995); J. F. Donoghue and J. Tandean, Phys. Lett. B**361**, 69 (1995); T. Torma, Phys. Rev. D**54**, 2168 (1996); A. Denner and S. Dittmaier, Phys. Rev. D**54**, 4499 (1996).
- [61] C. Balazs, D. A. Dicus, H.-J. He, W. W. Repko, C.-P. Yuan, Phys. Rev. Lett. **83**, 2112 (1999) [[hep-ph/9904220](#)].
- [62] S. Eidelman, *et al.*, [Particle Data Group], Phys. Lett. B **592**, 1 (2004) [<http://pdg.lbl.gov>].
- [63] M. S. Chanowitz, H. Georgi, and M. Golden, Phys. Rev. Lett. **57**, 2344 (1986); Phys. Rev. D**36**, 1490 (1987).
- [64] J. F. Donoghue, C. Ramirez, and G. Valencia, Phys. Rev. D**38**, 2195 (1988).
- [65] M. S. Chanowitz, M. A. Furman and I. Hinchliffe, Nucl. Phys. B**153**, 402 (1979); Phys. Lett. B**78**, 285 (1978).
- [66] F. Maltoni, J. M. Niczyporuk, and S. Willenbrock, Phys. Rev. Lett. **86**, 212 (2001) [[hep-ph/0006358](#)].
- [67] V. Abazov *et al.*, [D0 Collaboration], Nature **429**, 638 (2004) and [hep-ex/0407005](#); P. A. M. Fernandez [CDF Collaboration], [hep-ex/0409001](#).
- [68] P. Azzi, *et al.*, [Tevatron Electroweak Working Group], [hep-ex/0404010](#); L. Cerrito [CDF & D0 Collaborations], [hep-ex/0405046](#), in the proceedings of XXXIXth Rencontres de Moriond, “QCD and High Energy Hadronic Interactions”, March 2004.
- [69] *E.g.*, H.-J. He, D. A. Dicus and J. N. Ng, Phys. Lett. B **536**, 83 (2002) [[hep-ph/0203237](#)]; H. S. Goh, R. N. Mohapatra and S. P. Ng, Phys. Lett. B **542**, 116 (2002) [[hep-ph/0205131](#)]; and references therein.
- [70] For comprehensive reviews of the neutrinoless double β -decay, S. R. Elliott and P. Vogel, Ann. Rev. Nucl. Part. Sci. **52**, 115 (2002) [[hep-ph/0202264](#)]; S. R. Elliott and J. Engel, J. Phys. G **30**, R183 (2004) [[hep-ph/0405078](#)].
- [71] H. V. Klapdor-Kleingrothaus, Part. Nucl. Lett. **104**, 20 (2001) [[hep-ph/0102319](#)]; H. V. Klapdor-Kleingrothaus, *et al.*, Eur. Phys. J. A**12**, 147 (2001) [[hep-ph/0103062](#)]; Mod. Phys. Lett. A**16**, 2409 (2002) [[hep-ph/0201231](#)] and [[hep-ph/0205228](#)]; C. E. Aalseth, *et al.*, Mod. Phys. Lett. A**17**, 1475 (2002) [[hep-ph/0202018](#)]; H. V. Klapdor-Kleingrothaus, *et al.*, Phys. Lett. B **586**, 198 (2004) [[hep-ph/0404088](#)].
- [72] V. A. Miransky, M. Tanabashi and K. Yamawaki, Mod. Phys. Lett. A**4**, 1043 (1989).
- [73] W. A. Bardeen, C. T. Hill, and M. Lindner, Phys. Rev. D**41**, 1647 (1990).

- [74] For a review, G. Cvetic, Rev. Mod. Phys. **71**, 513 (1999) [[hep-ph/9702381](#)], and references therein.
- [75] S. Antusch, J. Kersten and M. Lindner, Nucl. Phys. B **658**, 203 (2003) [[hep-ph/0211385](#)].
- [76] D. Black, T. Han, H.-J. He, M. Sher, Phys. Rev. D **66**, 053002 (2002) [[hep-ph/0206056](#)]; S. Chen *et al.*, [CLEO Collaboration], Phys. Rev. D **66**, 071101 (2002); [[hep-ex/0208019](#)]; K. K. Gan [CLEO Collaboration], Nucl. Phys. Proc. Suppl. **123**, 121 (2003) [[hep-ex/0211027](#)]; Y. Enari *et al.*, [Belle Collaboration], Phys. Lett. B (2005) [[hep-ex/0503041](#)].
- [77] N. Arkani-Hamed, L. Hall, H. Murayama, D. Smith, N. Weiner, Phys. Rev. D **64**, 115011 (2001) [[hep-ph/0006312](#)].
- [78] D. A. Dicus and H.-J. He, work in progress.
- [79] A. Zee, Nucl. Phys. B **264**, 99 (1986); K. S. Babu, Phys. Lett. B **203**, 132 (1988).
- [80] E. Ma, Phys. Rev. Lett. **86**, 2502 (2001); E. Ma, M. Raidal, U. Sarkar, Nucl. Phys. B **615**, 313 (2001); and references therein.
- [81] F. Borzumati, K. Hamaguchi, Y. Nomura, T. Yanagida, [hep-ph/0012118](#); J. March-Russell and S. West, [hep-ph/0403067](#); and references therein.
- [82] T. Appelquist and J. Carrazzone, Phys. Rev. D **11**, 2856 (1975).
- [83] For a comprehensive analysis, see, *e.g.*, S. Dimopoulos and D. Sutter, Nucl. Phys. B **452**, 496 (1995) [[hep-ph/9504415](#)]; and references therein.
- [84] M. Fukugita and T. Yanagida, Phys. Lett. B **174**, 45 (1986).
- [85] *E.g.*, P. H. Frampton, S. L. Glashow, and T. Yanagida, Phys. Lett. B **548**, 119 (2002) [[hep-ph/0208157](#)]; V. Barger, D. A. Dicus, H.-J. He, and T. Li, Phys. Lett. B **583**, 173 (2004) [[hep-ph/0310278](#)]; and references therein.
- [86] *E.g.*, J. F. Gunion and H. E. Haber, Nucl. Phys. B **272**, 1 (1986); B **278**, 449 (1986).
- [87] M. J. Veltman, Acta. Phys. Polon. B **12**, 437 (1981).
- [88] T. Hambye, J. March-Russel, S. M. West, JHEP **07**, 070 (2004) [[hep-ph/0403183](#)]; S. M. West, Phys. Rev. D **71**, 013004 (2005) [[hep-ph/0408318](#)].
- [89] P. Limon, “VLHC Accelerator”, talk given at International Conference on *Future Hadron Colliders, Physics, Detectors and Machines*, Fermilab, Batavia, IL, USA, Oct. 16-18, 2003.
- [90] D. A. Dicus and H.-J. He, Phys. Rev. Lett. **94**, 221802 (2005) [[hep-ph/0502178](#)]; and see also, H.-J. He and D. A. Dicus, [hep-ph/0411024](#), presentation at the DPF-2004 Meeting of American Physical Society, Riverside, California, USA, Aug. 26-31, 2004.
- [91] *E.g.*, G. Barton, *Introduction to dispersion techniques in field theory*, Lecture Notes and Supplements in Physics series, W. A. Benjamin, Inc., NY, 1965.